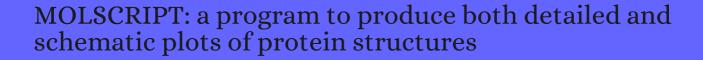
## CITATION REPORT List of articles citing



DOI: 10.1107/s0021889891004399 Journal of Applied Crystallography, 1991, 24, 946-950.

**Source:** https://exaly.com/paper-pdf/22505576/citation-report.pdf

Version: 2024-04-23

This report has been generated based on the citations recorded by exaly.com for the above article. For the latest version of this publication list, visit the link given above.

The third column is the impact factor (IF) of the journal, and the fourth column is the number of citations of the article.

#	Paper	IF	Citations
2306	Nickel-iron hydrogenases: Structural and functional properties. <b>1988</b> , 97-126		42
2305	Novel fold and putative receptor binding site of granulocyte-macrophage colony-stimulating factor. <b>1991</b> , 254, 1779-82		201
2304	Structure of the calcium-dependent lectin domain from a rat mannose-binding protein determined by MAD phasing. <b>1991</b> , 254, 1608-15		518
2303	Backbone dynamics of the Bacillus subtilis glucose permease IIA domain determined from 15N NMR relaxation measurements. <b>1992</b> , 31, 4394-406		223
2302	Response. <b>1992</b> , 258, 1161-2		12
2301	Total chemical synthesis of a D-enzyme: the enantiomers of HIV-1 protease show reciprocal chiral substrate specificity [corrected]. <b>1992</b> , 256, 1445-8		356
2300	Cooperativity induced by a single mutation at the subunit interface of a dimeric enzyme: glutathione reductase. <b>1992</b> , 258, 1140-3		42
2299	Backbone dynamics of calcium-loaded calbindin D9k studied by two-dimensional proton-detected 15N NMR spectroscopy. <b>1992</b> , 31, 4856-66		194
2298	Three-dimensional structure of dimeric human recombinant macrophage colony-stimulating factor. <b>1992</b> , 258, 1358-62		173
2297	The glycophorin A transmembrane domain dimer: sequence-specific propensity for a right-handed supercoil of helices. <b>1992</b> , 31, 12726-32		166
2296	High-resolution solution structure of the double Cys2His2 zinc finger from the human enhancer binding protein MBP-1. <b>1992</b> , 31, 3907-17		54
2295	NMR characterization of a diamagnetic model of unliganded alpha chains from human hemoglobin. <b>1992</b> , 74, 845-51		2
2294	Receptor action and interaction. <b>1992</b> , 2, 852-858		11
2293	The pyruvate dehydrogenase multienzyme complex. <b>1992</b> , 2, 877-887		98
2292	Updating structure-function relationships in the bZip family of transcription factors. <b>1992</b> , 2, 116-123		25
2291	Herbicide binding in the bacterial photosynthetic reaction center. <b>1992</b> , 17, 150-4		50
2290	The three-dimensional structure of the tenth type III module of fibronectin: an insight into RGD-mediated interactions. <b>1992</b> , 71, 671-8		437

2289	ine seven-stranded beta-barrel structure or apo-neocarzinostatin as compared to the immunoglobulin domain. <b>1992</b> , 74, 853-8	16
2288	Macromolecular graphics. <b>1992</b> , 2, 193-201	9
2287	Disulfide exchange folding of insulin-like growth factor I. <b>1992</b> , 31, 1749-56	108
2286	The role of surface-exposed Tyr-83 of plastocyanin in electron transfer from cytochrome c. <b>1992</b> , 1101, 64-68	38
2285	Histidine-aromatic interactions in barnase. Elevation of histidine pKa and contribution to protein stability. <b>1992</b> , 224, 759-70	191
2284	Reactivity of cytochromes c and f with mutant forms of spinach plastocyanin. <b>1992</b> , 1102, 85-90	93
2283	Mechanism of catalysis of Fe(II) oxidation by ferritin H chains. <b>1992</b> , 302, 108-12	70
2282	Three-dimensional structural resemblance between leucine aminopeptidase and carboxypeptidase A revealed by graph-theoretical techniques. <b>1992</b> , 303, 48-52	42
2281	Localization of bound water in the solution structure of the immunoglobulin binding domain of streptococcal protein G. Evidence for solvent-induced helical distortion in solution. <b>1992</b> , 223, 853-6	42
2280	Nuclear magnetic resonance solution structure of hirudin(1-51) and comparison with corresponding three-dimensional structures determined using the complete 65-residue hirudin polypeptide chain. <b>1992</b> , 228, 1193-205	50
2279	Solution structure of the fibrin binding finger domain of tissue-type plasminogen activator determined by 1H nuclear magnetic resonance. <b>1992</b> , 225, 821-33	47
2278	Human interleukin 4. The solution structure of a four-helix bundle protein. <b>1992</b> , 224, 899-904	125
2277	Nuclear magnetic resonance studies of the internal dynamics in Apo, (Cd2+)1 and (Ca2+)2 calbindin D9k. The rates of amide proton exchange with solvent. <b>1992</b> , 227, 1100-17	64
2276	Binding of the dye congo red to the amyloid protein pig insulin reveals a novel homology amongst amyloid-forming peptide sequences. <b>1992</b> , 227, 1205-23	157
2275	Crystal structure of alpha-dendrotoxin from the green mamba venom and its comparison with the structure of bovine pancreatic trypsin inhibitor. <b>1992</b> , 224, 671-83	88
2274	Dissection of an enzyme by protein engineering. The N and C-terminal fragments of barnase form a native-like complex with restored enzymic activity. <b>1992</b> , 224, 741-7	74
2273	Computer simulation of the initial proton transfer step in human carbonic anhydrase I. <b>1992</b> , 224, 7-14	105
2272	Structure of the complex between adenylate kinase from Escherichia coli and the inhibitor Ap5A refined at 1.9 A resolution. A model for a catalytic transition state. <b>1992</b> , 224, 159-77	444

2271	The crystal structure of the Bacillus lentus alkaline protease, subtilisin BL, at 1.4 A resolution. <b>1992</b> , 228, 580-95	35
2270	Structure of oxidized bacteriophage T4 glutaredoxin (thioredoxin). Refinement of native and mutant proteins. <b>1992</b> , 228, 596-618	67
2269	Solution structures of two zinc-finger domains from SWI5 obtained using two-dimensional 1H nuclear magnetic resonance spectroscopy. A zinc-finger structure with a third strand of beta-sheet. <b>1992</b> , 228, 637-51	78
2268	Structural consequences of sequence patterns in the fingerprint region of the nucleotide binding fold. Implications for nucleotide specificity. <b>1992</b> , 228, 662-71	142
2267	Ribose and glucose-galactose receptors. Competitors in bacterial chemotaxis. <b>1992</b> , 227, 418-40	29
2266	1.7 A X-ray structure of the periplasmic ribose receptor from Escherichia coli. <b>1992</b> , 225, 155-75	133
2265	A three-dimensional model of the Photosystem II reaction centre of Pisum sativum. <b>1992</b> , 34, 287-300	167
2264	The roles of serine and threonine sidechains in ion channels: a modelling study. <b>1992</b> , 21, 281-98	16
2263	Functional mapping of the surface of Escherichia coli ribose-binding protein: mutations that affect chemotaxis and transport. <b>1992</b> , 1, 1642-51	45
2262	Structure of the DNA-binding domain of zinc GAL4. <b>1992</b> , 356, 448-50	121
2261	The folding of hen lysozyme involves partially structured intermediates and multiple pathways. <b>1992</b> , 358, 302-7	702
2260	Structure of an SH2 domain of the p85 alpha subunit of phosphatidylinositol-3-OH kinase. <b>1992</b> , 358, 684-7	174
2259	Crystal structure at 1.7 A of the bovine papillomavirus-1 E2 DNA-binding domain bound to its DNA target. <b>1992</b> , 359, 505-12	347
2258	Crystal structure of TFIID TATA-box binding protein. <b>1992</b> , 360, 40-6	391
2257	Structure of a C-type mannose-binding protein complexed with an oligosaccharide. <b>1992</b> , 360, 127-34	879
2256	gyrB mutations which confer coumarin resistance also affect DNA supercoiling and ATP hydrolysis by Escherichia coli DNA gyrase. <b>1992</b> , 6, 1617-24	102
2255	Protein metal-binding sites. <b>1992</b> , 3, 378-87	63
2254	1H and 15N resonance assignments and secondary structure of the human thioredoxin C62A, C69A,	22

2253	Structural relationship between the hexameric and tetrameric family of glutamate dehydrogenases. <b>1992</b> , 209, 851-9	63
2252	On the mechanism of DNA binding by nuclear hormone receptors: a structural and functional perspective. <b>1993</b> , 51, 140-50	108
2251	Crystal Structure Analysis at Normal and Low Temperature Conditions. <b>1993</b> , 28, 767-794	3
2250	15N NMR assignments of (Cd2+,)2-calbindin D9k and comparison with (Ca2+)2-calbindin D9k. Cadmium as a substitute for calcium in calcium-binding proteins. <b>1993</b> , 31, S128-S132	5
2249	Epitope analysis using kinetic measurements of antibody binding to synthetic peptides presenting single amino acid substitutions. <b>1993</b> , 6, 71-9	17
2248	Display and interpretation of solvent electron density distributions in insulin crystals. <b>1993</b> , 11, 218-21, 233	0
2247	Photosynthetic water oxidation: The protein framework. <b>1993</b> , 38, 249-63	70
2246	Pitch diversity in alpha-helical coiled coils. <b>1993</b> , 15, 223-34	55
2245	Prediction of protein folding class from amino acid composition. <b>1993</b> , 16, 79-91	60
2244	Structure determination of feline panleukopenia virus empty particles. <b>1993</b> , 16, 155-71	145
2243	Automated docking in crystallography: analysis of the substrates of aconitase. <b>1993</b> , 17, 1-10	71
2242	Site specific point mutation changes specificity: a molecular modeling study by free energy simulations and enzyme kinetics of the thermodynamics in ribonuclease T1 substrate interactions. 1993, 17, 161-75	8
2241	Crystal structure of TGF-beta 2 refined at 1.8 A resolution. <b>1993</b> , 17, 176-92	49
2240	A calculation strategy for the structure determination of symmetric dimers by 1H NMR. <b>1993</b> , 17, 297-309	301
2239	A comparison of 15N NMR relaxation measurements with a molecular dynamics simulation: backbone dynamics of the glucocorticoid receptor DNA-binding domain. <b>1993</b> , 17, 375-90	51
2238	Mapping the surface properties of macromolecules. <b>1993</b> , 2, 459-69	35
2237	Crystal structure of deoxygenated Limulus polyphemus subunit II hemocyanin at 2.18 A resolution: clues for a mechanism for allosteric regulation. <b>1993</b> , 2, 597-619	259
2236	Prediction of the three-dimensional structures of the biotinylated domain from yeast pyruvate	

2235	Reconstitution of active catalytic trimer of aspartate transcarbamoylase from proteolytically cleaved polypeptide chains. <b>1993</b> , 2, 1001-12	11
2234	Crystal structure of activated tobacco rubisco complexed with the reaction-intermediate analogue 2-carboxy-arabinitol 1,5-bisphosphate. <b>1993</b> , 2, 1136-46	54
2233	Refinement of the structure of human basic fibroblast growth factor at 1.6 A resolution and analysis of presumed heparin binding sites by selenate substitution. <b>1993</b> , 2, 1274-84	70
2232	Identification, classification, and analysis of beta-bulges in proteins. <b>1993</b> , 2, 1574-90	176
2231	Classification of doubly wound nucleotide binding topologies using automated loop searches. <b>1993</b> , 2, 2146-53	34
2230	Asymmetry of calmodulin revealed by peptide binding. <b>1993</b> , 3, 45-9	2
2229	Solution structure of the POU-specific DNA-binding domain of Oct-1. <b>1993</b> , 362, 852-5	152
2228	Recognition by Max of its cognate DNA through a dimeric b/HLH/Z domain. <b>1993</b> , 363, 38-45	658
2227	A novel dimer configuration revealed by the crystal structure at 2.4 A resolution of human interleukin-5. <b>1993</b> , 363, 172-6	241
2226	Crystal structure of cyclin-dependent kinase 2. <b>1993</b> , 363, 595-602	894
2225	Universal nucleic acid-binding domain revealed by crystal structure of the B. subtilis major cold-shock protein. <b>1993</b> , 364, 164-8	319
2224	Co-crystal structure of the HNF-3/fork head DNA-recognition motif resembles histone H5. <b>1993</b> , 364, 412-20	1121
2223	Structure of gelsolin segment 1-actin complex and the mechanism of filament severing. <b>1993</b> , 364, 685-92	529
2222	An SH2-SH3 domain hybrid. <b>1993</b> , 364, 765	24
2221	Crystal structure of active elongation factor Tu reveals major domain rearrangements. <b>1993</b> , 365, 126-32	536
2220	Structure and function of endoglucanase V. <b>1993</b> , 365, 362-4	126
2219	Tandem binding in crystals of a trp repressor/operator half-site complex. <b>1993</b> , 366, 178-82	146
2218	The crystal structure of a two zinc-finger peptide reveals an extension to the rules for zinc-finger/DNA recognition. <b>1993</b> , 366, 483-7	326

2217	Crystal structure of a bacterial non-haem iron hydroxylase that catalyses the biological oxidation of methane. <b>1993</b> , 366, 537-43	838
2216	The interaction between coumarin drugs and DNA gyrase. <b>1993</b> , 9, 681-6	222
2215	Improved bivalent miniantibodies, with identical avidity as whole antibodies, produced by high cell density fermentation of Escherichia coli. <b>1993</b> , 11, 1271-7	34
2214	Molecular modelling of the Norrie disease protein predicts a cystine knot growth factor tertiary structure. <b>1993</b> , 5, 376-80	154
2213	Ordered duplex RNA controls capsid architecture in an icosahedral animal virus. <b>1993</b> , 361, 176-9	220
2212	Globin fold in a bacterial toxin. <b>1993</b> , 361, 309	28
2211	Similarity of active-site structures. <b>1993</b> , 362, 24	12
2210	Yeast tRNA(Asp) recognition by its cognate class II aminoacyl-tRNA synthetase. <b>1993</b> , 362, 181-4	290
2209	Crystal structure of globular domain of histone H5 and its implications for nucleosome binding. <b>1993</b> , 362, 219-23	686
2208	Structure of a major immunogenic site on foot-and-mouth disease virus. <b>1993</b> , 362, 566-8	313
2207	Transcription activation at Class I CAP-dependent promoters. 1993, 8, 797-802	196
2206	Myelin P0-glycoprotein: predicted structure and interactions of extracellular domain. <b>1993</b> , 61, 1987-95	32
2205	Substrate interactions between trypanothione reductase and N1-glutathionylspermidine disulphide at 0.28-nm resolution. <b>1993</b> , 213, 67-75	91
2204	Determination of the nuclear-magnetic-resonance solution structure of cardiotoxin CTX IIb from Naja mossambica mossambica. <b>1993</b> , 213, 891-900	26
2203	Sequential assignment of proton resonances in the NMR spectrum of Zn-substituted alpha chains from human hemoglobin. Ligand-induced tertiary changes in the heme pocket. <b>1993</b> , 214, 383-93	5
2202	1H- and 15N-NMR assignment and solution structure of the chemotactic Escherichia coli Che Y protein. <b>1993</b> , 215, 573-85	29
2201	Solution conformation of an antibacterial peptide, sarcotoxin IA, as determined by 1H-NMR. <b>1993</b> , 217, 639-44	43
2200	Conformations and conformational changes of four Phe>Trp variants of the DNA-binding histone-like protein, HBsu, from Bacillus subtilis studied by circular dichroism and fluorescence spectroscopy. <b>1993</b> , 217, 849-56	11

2199	Site-directed mutagenesis of beta-lactamase TEM-1. Investigating the potential role of specific residues on the activity of Pseudomonas-specific enzymes. <b>1993</b> , 217, 939-46	22
2198	Automatic and accurate method for analysis of proteins that undergo hinge-mediated domain and loop movements. <b>1993</b> , 3, 740-8	12
2197	Myosin-actin motors: the partnership goes atomic. <b>1993</b> , 1, 1-5	19
2196	The crystal structure of elongation factor EF-Tu from Thermus aquaticus in the GTP conformation. <b>1993</b> , 1, 35-50	382
2195	Structure of the glycosylated adhesion domain of human T lymphocyte glycoprotein CD2. <b>1993</b> , 1, 69-81	64
2194	New folds for all-beta proteins. <b>1993</b> , 1, 217-22	67
2193	Unusual structural features in the parallel beta-helix in pectate lyases. 1993, 1, 241-51	139
2192	Crystal structure of the Awd nucleotide diphosphate kinase from Drosophila. <b>1993</b> , 1, 283-93	85
2191	Recognition between a bacterial ribonuclease, barnase, and its natural inhibitor, barstar. <b>1993</b> , 1, 165-76	101
2190	Alpha plus beta folds revisited: some favoured motifs. <b>1993</b> , 1, 105-20	142
2190 2189	Alpha plus beta folds revisited: some favoured motifs. <b>1993</b> , 1, 105-20  Molecular modelling and epitope prediction of gp29 from lymphatic filariae. <b>1993</b> , 58, 145-53	142
2189	Molecular modelling and epitope prediction of gp29 from lymphatic filariae. <b>1993</b> , 58, 145-53  Characterization of yeast EF-1 alpha: non-conservation of post-translational modifications. <b>1993</b> ,	14
2189	Molecular modelling and epitope prediction of gp29 from lymphatic filariae. <b>1993</b> , 58, 145-53  Characterization of yeast EF-1 alpha: non-conservation of post-translational modifications. <b>1993</b> , 1163, 75-80	14 60
2189 2188 2187	Molecular modelling and epitope prediction of gp29 from lymphatic filariae. 1993, 58, 145-53  Characterization of yeast EF-1 alpha: non-conservation of post-translational modifications. 1993, 1163, 75-80  Comparison of transferrin sequences from different species. 1993, 106, 203-18  Review of HIV-1 reverse transcriptase three-dimensional structure: Implications for drug design.	14 60 36
2189 2188 2187 2186	Molecular modelling and epitope prediction of gp29 from lymphatic filariae. 1993, 58, 145-53  Characterization of yeast EF-1 alpha: non-conservation of post-translational modifications. 1993, 1163, 75-80  Comparison of transferrin sequences from different species. 1993, 106, 203-18  Review of HIV-1 reverse transcriptase three-dimensional structure: Implications for drug design. 1993, 1, 129-150	14 60 36 115
2189 2188 2187 2186 2185	Molecular modelling and epitope prediction of gp29 from lymphatic filariae. 1993, 58, 145-53  Characterization of yeast EF-1 alpha: non-conservation of post-translational modifications. 1993, 1163, 75-80  Comparison of transferrin sequences from different species. 1993, 106, 203-18  Review of HIV-1 reverse transcriptase three-dimensional structure: Implications for drug design. 1993, 1, 129-150  Seeing our way to drug design. 1993, 1, 329-344  Modern NMR spectroscopy of proteins and peptides in solution and its relevance to drug design.	14 60 36 115

2181	Identification of the barstar binding site of barnase by NMR spectroscopy and hydrogen-deuterium exchange. <b>1993</b> , 331, 165-72	34
2180	NMR determination of the secondary structure and the three-dimensional polypeptide backbone fold of the human sterol carrier protein 2. <b>1993</b> , 335, 18-26	30
2179	The structure of apo-calmodulin. A 1H NMR examination of the carboxy-terminal domain. <b>1993</b> , 336, 368-74	27
2178	A left-handed crossover involved in amidohydrolase catalysis. Crystal structure of Erwinia chrysanthemi L-asparaginase with bound L-aspartate. <b>1993</b> , 328, 275-9	56
2177	Crystal structure of apo-glycolate oxidase. <b>1993</b> , 327, 361-5	12
2176	Low pH crystal structure of glycosylated lignin peroxidase from Phanerochaete chrysosporium at 2.5 A resolution. <b>1993</b> , 315, 119-24	153
2175	Structural alignment of globins, phycocyanins and colicin A. <b>1993</b> , 315, 301-6	68
2174	Prediction of a novel topology in the N-terminal, 14 kDa fragment of Ada protein. <b>1993</b> , 323, 257-60	3
2173	Three-dimensional structural resemblance between the ribonuclease H and connection domains of HIV reverse transcriptase and the ATPase fold revealed using graph theoretical techniques. <b>1993</b> , 324, 15-21	28
2172	A structural model for the glutamate-specific endopeptidase from Streptomyces griseus that explains substrate specificity. <b>1993</b> , 324, 45-50	4
2171	1H and 15N assignments and secondary structure of the Src SH3 domain. <b>1993</b> , 324, 87-92	45
2170	1H and 15N assignments and secondary structure of the PI3K SH3 domain. <b>1993</b> , 324, 93-8	16
2169	Structure of the thiamine- and flavin-dependent enzyme pyruvate oxidase. <b>1993</b> , 259, 965-7	217
2168	Cytokine structural taxonomy and mechanisms of receptor engagement. <b>1993</b> , 3, 815-827	236
2167	Solution structure of gamma 1-H and gamma 1-P thionins from barley and wheat endosperm determined by 1H-NMR: a structural motif common to toxic arthropod proteins. <b>1993</b> , 32, 715-24	201
2166	Thiamin diphosphate dependent enzymes: transketolase, pyruvate oxidase and pyruvate decarboxylase. <b>1993</b> , 3, 896-901	39
2165	Crystal structure analysis of a mutant Escherichia coli thioredoxin in which lysine 36 is replaced by glutamic acid. <b>1993</b> , 32, 5093-8	17
2164	Crystal structure of cholesterol oxidase complexed with a steroid substrate: Implications for flavin adenine dinucleotide dependent alcohol oxidases. <b>1993</b> , 32, 11507-11515	175

2163	Structure of an interleukin-1 beta mutant with reduced bioactivity shows multiple subtle changes in conformation that affect protein-protein recognition. <b>1993</b> , 32, 8749-57	13
2162	Probing the determinants of disulfide stability in native pancreatic trypsin inhibitor. <b>1993</b> , 32, 2835-44	40
2161	The high-resolution, three-dimensional solution structure of human interleukin-4 determined by multidimensional heteronuclear magnetic resonance spectroscopy. <b>1993</b> , 32, 6744-62	128
2160	Interaction of barnase with its polypeptide inhibitor barstar studied by protein engineering. <b>1993</b> , 32, 5145-50	244
2159	The Asp-His-iron triad of cytochrome c peroxidase controls the reduction potential electronic structure, and coupling of the tryptophan free radical to the heme. <b>1993</b> , 32, 3313-3324	284
2158	1H-NMR resonance assignments, secondary structure, and global fold of the TR1C fragment of turkey skeletal troponin C in the calcium-free state. <b>1993</b> , 32, 3461-7	15
2157	Effects of ion binding on the backbone dynamics of calbindin D9k determined by 15N NMR relaxation. <b>1993</b> , 32, 9832-44	172
2156	Designed replacement of an internal hydration water molecule in BPTI: structural and functional implications of a glycine-to-serine mutation. <b>1993</b> , 32, 4564-70	50
2155	Hydrogen exchange in unligated and ligated staphylococcal nuclease. <b>1993</b> , 32, 11022-8	87
2154	Solution conformation of the (+)-trans-anti-[BPh]dA adduct opposite dT in a DNA duplex: intercalation of the covalently attached benzo[c]phenanthrene to the 5'-side of the adduct site without disruption of the modified base pair. <b>1993</b> , 32, 12488-97	85
2153	Refined solution structure of the glucocorticoid receptor DNA-binding domain. 1993, 32, 13463-71	91
2152	Effects of amino acid substitutions on the pressure denaturation of staphylococcal nuclease as monitored by fluorescence and nuclear magnetic resonance spectroscopy. <b>1993</b> , 32, 5222-32	136
2151	The energetics and cooperativity of protein folding: a simple experimental analysis based upon the solvation of internal residues. <b>1993</b> , 32, 3842-51	65
2150	Mutagenesis of the conserved lysine 14 of cytochrome c-550 from Thiobacillus versutus affects the protein structure and the electron self-exchange rate. <b>1993</b> , 32, 13893-901	25
2149	Molecular structure of the oxidized, recombinant, heterocyst [2Fe-2S] ferredoxin from Anabaena 7120 determined to 1.7-A resolution. <b>1993</b> , 32, 6788-93	89
2148	A noncovalent peptide complex as a model for an early folding intermediate of cytochrome c. <b>1993</b> , 32, 10271-6	102
2147	Glutathione proteins. <b>1993</b> , 3, 875-884	15
2146	Rendering a membrane protein soluble in water: a common packing motif in bacterial protein toxins. <b>1993</b> , 18, 391-5	117

2145	Dinitrogen reduction by nitrogenase: if N2 isn't broken, it can't be fixed. <b>1993</b> , 3, 921-928	20
2144	Progress in protein structure prediction?. <b>1993</b> , 18, 120-3	76
2143	Bacterial porins: lessons from three high-resolution structures. <b>1993</b> , 3, 501-507	61
2142	Myosin subfragment-1: structure and function of a molecular motor. <b>1993</b> , 3, 944-952	20
2141	DNA repair enzymes. <b>1993</b> , 3, 17-23	10
2140	Software for macromolecular crystallography: a user's overview. <b>1993</b> , 3, 741-747	12
2139	Methionine as translation start signal: a review of the enzymes of the pathway in Escherichia coli. <b>1993</b> , 75, 1061-75	211
2138	Yeast aspartyl-tRNA synthetase: a structural view of the aminoacylation reaction. <b>1993</b> , 75, 1117-23	18
2137	Crystal structure of the Hhal DNA methyltransferase complexed with S-adenosyl-L-methionine. <b>1993</b> , 74, 299-307	361
2136	A player of many parts: the spotlight falls on thrombin's structure. <b>1993</b> , 69, 1-58	416
2135	Evolutionary relationships among the serpins. <b>1993</b> , 342, 101-19	54
2134	A partially folded state of hen egg white lysozyme in trifluoroethanol: structural characterization and implications for protein folding. <b>1993</b> , 32, 669-78	264
2133	Kinetics of folding of the all-beta sheet protein interleukin-1 beta. <b>1993</b> , 260, 1110-3	161
2132	The segment identity functions of Ultrabithorax are contained within its homeo domain and carboxy-terminal sequences. <b>1993</b> , 7, 796-811	100
2131	The nonhelical structure of antifreeze protein type III. <b>1993</b> , 259, 1154-7	100
2130	Crystal structure of domains 3 and 4 of rat CD4: relation to the NH2-terminal domains. <b>1993</b> , 260, 979-83	129
2129	•	2
2128	Molecular orbital calculations on (MgO)n and (MgO)n+ clusters (n=1🛮 3). <b>1993</b> , 98, 4783-4792	78

2127 Rat annexin V crystal structure: Ca(2+)-induced conformational changes. <b>1993</b> , 261, 1321-4	185
2126 Structure and function of channel-forming peptaibols. <b>1993</b> , 26, 365-421	148
Computational challenges for macromolecular structure determination by X-ray crystallogram and solution NMR-spectroscopy. <b>1993</b> , 26, 49-125	phy 143
NMR structure of a specific DNA complex of Zn-containing DNA binding domain of GATA-1. $^{2124}$ 261, 438-46	<b>1993,</b> 420
Conformational stability of the DNA-binding histone-like protein, HBsu, from Bacillus subtilis of the four HBsu variants [F29W], [F47W], [F50W] and [F79W]. <b>1993</b> , 11, 381-94	s, and 4
Structure of the Mg(2+)-bound form of CheY and mechanism of phosphoryl transfer in bacte chemotaxis. <b>1993</b> , 32, 13375-80	rial 206
Subunit specificity of mutations that confer resistance to nonnucleoside inhibitors in human immunodeficiency virus type 1 reverse transcriptase. <b>1994</b> , 38, 1909-14	75
Toxic shock syndrome toxin-1 complexed with a class II major histocompatibility molecule HL <b>1994</b> , 266, 1870-4	_A-DR1266
2119 The structural basis of sequence-independent peptide binding by OppA protein. <b>1994</b> , 264, 1	578-81 206
2118 Rubredoxin in crystalline state. <b>1994</b> , 243, 203-16	64
2118 Rubredoxin in crystalline state. <b>1994</b> , 243, 203-16  2117 Structural Elements Involved in the Assembly and Mechanism of Action of Rubisco. <b>1994</b> , 287	, in the second second
	, in the second second
2117 Structural Elements Involved in the Assembly and Mechanism of Action of Rubisco. <b>1994</b> , 287	7-335 1
2117 Structural Elements Involved in the Assembly and Mechanism of Action of Rubisco. <b>1994</b> , 287 2116 Structure of the allosteric regulatory enzyme of purine biosynthesis. <b>1994</b> , 264, 1427-33	7-335 1 239 214
2117 Structural Elements Involved in the Assembly and Mechanism of Action of Rubisco. <b>1994</b> , 287 2116 Structure of the allosteric regulatory enzyme of purine biosynthesis. <b>1994</b> , 264, 1427-33 2115 Structure-function relationships for the EGF/TGF-alpha family of mitogens. <b>1994</b> , 11, 235-57 Structure of the RGD protein decorsin: conserved motif and distinct function in leech protein	7-335 1 239 214
2117 Structural Elements Involved in the Assembly and Mechanism of Action of Rubisco. 1994, 287 2116 Structure of the allosteric regulatory enzyme of purine biosynthesis. 1994, 264, 1427-33 2115 Structure-function relationships for the EGF/TGF-alpha family of mitogens. 1994, 11, 235-57 2114 Structure of the RGD protein decorsin: conserved motif and distinct function in leech protein affect blood clotting. 1994, 264, 1944-7	7-335 1 239 214 ans that 138 90
2117 Structural Elements Involved in the Assembly and Mechanism of Action of Rubisco. 1994, 287 2116 Structure of the allosteric regulatory enzyme of purine biosynthesis. 1994, 264, 1427-33 2115 Structure-function relationships for the EGF/TGF-alpha family of mitogens. 1994, 11, 235-57 2114 Structure of the RGD protein decorsin: conserved motif and distinct function in leech protein affect blood clotting. 1994, 264, 1944-7 2113 Folding pattern diversity of integral membrane proteins. 1994, 264, 914-6 Structures of ternary complexes of rat DNA polymerase beta, a DNA template-primer, and do	7-335 1 239 214 ns that 138 90

2109	Crystal structure of the catalytic domain of HIV-1 integrase: similarity to other polynucleotidyl transferases. <b>1994</b> , 266, 1981-6	718
2108	Subsite preferences of retroviral proteinases. <b>1994</b> , 241, 254-78	59
2107	Complexes between osmium tetraoxide bispyridine and DNA: a molecular mechanics study. <b>1994</b> , 12, 327-42	1
2106	Structure of an electron transfer complex: methylamine dehydrogenase, amicyanin, and cytochrome c551i. <b>1994</b> , 264, 86-90	207
2105	How a protein binds B12: A 3.0 A X-ray structure of B12-binding domains of methionine synthase. <b>1994</b> , 266, 1669-74	571
2104	Crystallographic studies of DNA helix structure. <b>1994</b> , 50, 157-67	30
2103	A comparison of the predicted and X-ray structures of angiogenin. Implications for further studies of model building of homologous proteins. <b>1994</b> , 13, 649-58	12
2102	Determination of the NMR solution structure of the cyclophilin A-cyclosporin A complex. <b>1994</b> , 4, 463-82	55
2101	1H, 15N, 13C and 13CO resonance assignments and secondary structure of villin 14T, a domain conserved among actin-severing proteins. <b>1994</b> , 4, 553-74	11
2100	113Cd-1H heteroTOCSY: a method for determining metal-protein connectivities. <b>1994</b> , 4, 761-74	14
2099	SH3 domain-mediated dimerization of an n-terminal fragment of the phosphatidylinositol 3-kinase p85 subunit. <b>1994</b> , 4, 1755-1760	9
2098	Amino acids that specify structure through hydrophobic clustering and histidine-aromatic interactions lead to biologically active peptidomimetics. <b>1994</b> , 2, 999-1006	22
2097	Synthesis of sulfur analogues of methyl and allyl kojibiosides and methyl isomaltoside and conformational analysis of the kojibiosides. <b>1994</b> , 5, 2367-2396	33
2096	Solution structure of villin 14T, a domain conserved among actin-severing proteins. <b>1994</b> , 3, 70-81	48
2095	Crystal structure of cholera toxin B-pentamer bound to receptor GM1 pentasaccharide. <b>1994</b> , 3, 166-75	462
2094	The 2.6-A refined structure of the Escherichia coli recombinant Saccharomyces cerevisiae flavocytochrome b2-sulfite complex. <b>1994</b> , 3, 303-13	28
2093	Young Investigator Award Lecture. Structures of larger proteins, protein-ligand and protein-DNA complexes by multidimensional heteronuclear NMR. <b>1994</b> , 3, 372-90	102
2092	De novo protein design using pairwise potentials and a genetic algorithm. <b>1994</b> , 3, 567-74	95

2091	A structural basis for the interaction of urea with lysozyme. <b>1994</b> , 3, 706-10	62
2090	Modeling studies of the change in conformation required for cleavage of limited proteolytic sites. <b>1994</b> , 3, 757-68	174
2089	Crystal structures of pheasant and guinea fowl egg-white lysozymes. <b>1994</b> , 3, 788-98	14
2088	Crystal structure of recombinant human triosephosphate isomerase at 2.8 A resolution. Triosephosphate isomerase-related human genetic disorders and comparison with the trypanosomal enzyme. <b>1994</b> , 3, 810-21	101
2087	Biological meaning, statistical significance, and classification of local spatial similarities in nonhomologous proteins. <b>1994</b> , 3, 866-75	58
2086	Receptor binding properties of four-helix-bundle growth factors deduced from electrostatic analysis. <b>1994</b> , 3, 920-35	52
2085	Relative stabilities of synthetic peptide homo- and heterodimeric troponin-C domains. <b>1994</b> , 3, 1010-9	17
2084	Phosphopeptide binding to the N-terminal SH2 domain of the p85 alpha subunit of PI 3'-kinase: a heteronuclear NMR study. <b>1994</b> , 3, 1020-30	46
2083	Crystal structure of inorganic pyrophosphatase from Thermus thermophilus. <b>1994</b> , 3, 1098-107	67
2082	Transglutaminase factor XIII uses proteinase-like catalytic triad to crosslink macromolecules. <b>1994</b> , 3, 1131-5	132
2081	Equilibrium unfolding of Escherichia coli ribonuclease H: characterization of a partially folded state. <b>1994</b> , 3, 1401-8	77
2080	Refined structure of dimeric diphtheria toxin at 2.0 A resolution. <b>1994</b> , 3, 1444-63	161
2079	Influenza virus neuraminidase: structure, antibodies, and inhibitors. <b>1994</b> , 3, 1687-96	288
2078	Electrostatic effects in the control of glycogen phosphorylase by phosphorylation. <b>1994</b> , 3, 1726-30	34
2077	Structural studies of the engrailed homeodomain. <b>1994</b> , 3, 1779-87	133
2076	A common structural motif incorporating a cystine knot and a triple-stranded beta-sheet in toxic and inhibitory polypeptides. <b>1994</b> , 3, 1833-9	471
2075	A quantitative methodology for the de novo design of proteins. <b>1994</b> , 3, 1871-82	10
2074	On the evolution of alternate core packing in eightfold beta/alpha-barrels. <b>1994</b> , 3, 1889-92	29

2073	Different protein sequences can give rise to highly similar folds through different stabilizing interactions. <b>1994</b> , 3, 1938-44	31
2072	Redesigning the hydrophobic core of a four-helix-bundle protein. <b>1994</b> , 3, 2015-22	120
2071	Engineering the quaternary structure of an enzyme: construction and analysis of a monomeric form of malate dehydrogenase from Escherichia coli. <b>1994</b> , 3, 2023-32	40
2070	Protein structural similarities predicted by a sequence-structure compatibility method. <b>1994</b> , 3, 2055-63	54
2069	Effect of pH and phosphate ions on self-association properties of the major cold-shock protein from Bacillus subtilis. <b>1994</b> , 3, 2144-7	37
2068	A revised set of potentials for beta-turn formation in proteins. <b>1994</b> , 3, 2207-16	845
2067	Three-dimensional structure of Schistosoma japonicum glutathione S-transferase fused with a six-amino acid conserved neutralizing epitope of gp41 from HIV. <b>1994</b> , 3, 2233-44	161
2066	Structure-function analysis of human IL-6: identification of two distinct regions that are important for receptor binding. <b>1994</b> , 3, 2280-93	74
2065	The structures of RNase A complexed with 3'-CMP and d(CpA): active site conformation and conserved water molecules. <b>1994</b> , 3, 2322-39	174
2064	Conservation of polyproline II helices in homologous proteins: implications for structure prediction by model building. <b>1994</b> , 3, 2395-410	50
2063	The structure of Trypanosoma cruzi trypanothione reductase in the oxidized and NADPH reduced state. <b>1994</b> , 18, 161-73	76
2062	Searching protein structure databases has come of age. <b>1994</b> , 19, 165-73	220
2061	The closed conformation of a highly flexible protein: the structure of E. coli adenylate kinase with bound AMP and AMPPNP. <b>1994</b> , 19, 183-98	123
2060	Parser for protein folding units. <b>1994</b> , 19, 256-68	182
2059	Molecular basis of cooperativity in protein folding. V. Thermodynamic and structural conditions for the stabilization of compact denatured states. <b>1994</b> , 19, 291-301	116
2058	Crystallographic analysis of oxygenated and deoxygenated states of arthropod hemocyanin shows unusual differences. <b>1994</b> , 19, 302-9	329
2057	Structural analysis of two crystal forms of lentil lectin at 1.8 A resolution. <b>1994</b> , 20, 330-46	27
2056	Diphtheria toxin-related cytokine fusion proteins: elongation factor 2 as a target for the treatment of neoplastic disease. <b>1994</b> , 138, 151-6	7

2055	The monosaccharide binding site of lentil lectin: an X-ray and molecular modelling study. <b>1994</b> , 11, 507-17	34
2054	Structure and function of the photosynthetic reaction center from Rhodobacter sphaeroides. <b>1994</b> , 26, 5-15	73
2053	Plastocyanin: structural and functional analysis. <b>1994</b> , 26, 49-66	173
2052	Structure-function studies of [2Fe-2S] ferredoxins. <b>1994</b> , 26, 67-88	93
2051	Buried surface analysis of HIV-1 reverse transcriptase p66/p51 heterodimer and its interaction with dsDNA template/primer. <b>1994</b> , 7, 157-61	22
2050	Kringle solution structures via NMR: two-dimensional 1H-NMR analysis of horse plasminogen kringle 4. <b>1994</b> , 67-68, 43-58	9
2049	Hydrating peptides using a sprouting technique. <b>1994</b> , 15, 23-27	3
2048	Gaussian multipoles in practice: Electrostatic energies for intermolecular potentials. <b>1994</b> , 15, 1187-1198	71
2047	alpha/beta barrel evolution and the modular assembly of enzymes: emerging trends in the flavin oxidase/dehydrogenase family. <b>1994</b> , 16, 115-22	41
2046	Taking a long, hard look at calmodulin's warm embrace. <b>1994</b> , 16, 221-4	33
	Taking a long, hard look at calmodulin's warm embrace. <b>1994</b> , 16, 221-4  Structural aspects of biomolecular recognition and self-assembly. <b>1994</b> , 9, 753-60	<ul><li>33</li><li>5</li></ul>
2045		
2045	Structural aspects of biomolecular recognition and self-assembly. <b>1994</b> , 9, 753-60  Racemic macromolecules for use in X-ray crystallography. <b>1994</b> , 5, 343-5	5
2045	Structural aspects of biomolecular recognition and self-assembly. <b>1994</b> , 9, 753-60  Racemic macromolecules for use in X-ray crystallography. <b>1994</b> , 5, 343-5	5
2045	Structural aspects of biomolecular recognition and self-assembly. <b>1994</b> , 9, 753-60  Racemic macromolecules for use in X-ray crystallography. <b>1994</b> , 5, 343-5  Structure prediction of proteinswhere are we now?. <b>1994</b> , 5, 372-80  Engineering proteases with altered specificity. <b>1994</b> , 5, 403-8	5 6 18
2045 2044 2043 2042	Structural aspects of biomolecular recognition and self-assembly. 1994, 9, 753-60  Racemic macromolecules for use in X-ray crystallography. 1994, 5, 343-5  Structure prediction of proteinswhere are we now?. 1994, 5, 372-80  Engineering proteases with altered specificity. 1994, 5, 403-8	5 6 18
2045 2044 2043 2042 2041	Structural aspects of biomolecular recognition and self-assembly. 1994, 9, 753-60  Racemic macromolecules for use in X-ray crystallography. 1994, 5, 343-5  Structure prediction of proteinswhere are we now?. 1994, 5, 372-80  Engineering proteases with altered specificity. 1994, 5, 403-8  DRAWNA: a program for drawing schematic views of nucleic acids. 1994, 12, 201-6, 196  Thermodynamic prediction of structural determinants of the molten globule state of barnase. 1994	5 6 18 11 63

2037	The structure of flavocytochrome c sulfide dehydrogenase from a purple phototrophic bacterium. <b>1994</b> , 266, 430-2	142
2036	Sprouting peptides in unprejudiced conformation space searches. <b>1994</b> , 308, 1-11	2
2035	Structure and function of glutathione S-transferases. <b>1994</b> , 1205, 1-18	455
2034	Substrate and pseudosubstrate interactions with protein kinases: determinants of specificity. <b>1994</b> , 19, 440-4	120
2033	Structural model for the reaction mechanism of glutamine synthetase, based on five crystal structures of enzyme-substrate complexes. <b>1994</b> , 33, 675-81	107
2032	Crystal structure of rat DNA polymerase beta: evidence for a common polymerase mechanism. <b>1994</b> , 264, 1930-5	467
2031	Analysis of tyrosinase mutations associated with tyrosinase-related oculocutaneous albinism (OCA1). <b>1994</b> , 7, 285-90	27
2030	Methionine-321 in the C-terminal alpha-helix of catabolic ornithine carbamoyltransferase from Pseudomonas aeruginosa is important for positive homotropic cooperativity. <b>1994</b> , 124, 411-7	5
2029	Three-dimensional structure of the 67K N-terminal fragment of E. coli DNA topoisomerase I. <b>1994</b> , 367, 138-46	272
2028	Structure of the Aeromonas toxin proaerolysin in its water-soluble and membrane-channel states. <b>1994</b> , 367, 292-5	378
2027	Atomic model of plant light-harvesting complex by electron crystallography. <b>1994</b> , 367, 614-21	1820
2026	Doughnut-shaped structure of a bacterial muramidase revealed by X-ray crystallography. <b>1994</b> , 367, 750-3	151
2025	Crystal structure of the human class II MHC protein HLA-DR1 complexed with an influenza virus peptide. <b>1994</b> , 368, 215-21	1431
2024	Destabilization of the complete protein secondary structure on binding to the chaperone GroEL. <b>1994</b> , 368, 261-5	145
2023	Structure of the regulatory domain of scallop myosin at 2.8 A resolution. <b>1994</b> , 368, 306-12	296
2022	Structure of restriction endonuclease BamHI and its relationship to EcoRI. <b>1994</b> , 368, 660-4	170
2021	Three-dimensional structure of a human class II histocompatibility molecule complexed with superantigen. <b>1994</b> , 368, 711-8	532
2020	Structure of the regulatory domains of the Src-family tyrosine kinase Lck. <b>1994</b> , 368, 764-9	253

Picornaviral 3C cysteine proteinases have a fold similar to chymotrypsin-like serine proteinases.  1994, 369, 72-6	270
Structure of murine polyomavirus complexed with an oligosaccharide receptor fragment. <b>1994</b> , 369, 160-3	279
2017 Insights into autoregulation from the crystal structure of twitchin kinase. <b>1994</b> , 369, 581-4	196
2016 Structure of the pleckstrin homology domain from beta-spectrin. <b>1994</b> , 369, 675-7	239
2015 Three-dimensional structure of beta-galactosidase from E. coli. <b>1994</b> , 369, 761-6	557
2014 Structure of ribonucleotide reductase protein R1. <b>1994</b> , 370, 533-9	520
Crystal structure of Yersinia protein tyrosine phosphatase at 2.5 A and the complex with tungstate. <b>1994</b> , 370, 571-5	396
2012 Structure at 2.8 A resolution of F1-ATPase from bovine heart mitochondria. <b>1994</b> , 370, 621-8	2799
2011 Crystal structure of the extracellular region of human tissue factor. <b>1994</b> , 370, 662-6	205
2010 Structural similarity between the p17 matrix protein of HIV-1 and interferon-gamma. <b>1994</b> , 370, 666-	8 127
2009 Structure of influenza haemagglutinin at the pH of membrane fusion. <b>1994</b> , 371, 37-43	1377
2008 Crystal structure of an isoleucine-zipper trimer. <b>1994</b> , 371, 80-3	433
	338
2007 Crystal structure of an RNA bacteriophage coat protein-operator complex. <b>1994</b> , 371, 623-6	33*
2007 Crystal structure of an RNA bacteriophage coat protein-operator complex. <b>1994</b> , 371, 623-6  2006 Crystal structure at 2.2 A resolution of the MHC-related neonatal Fc receptor. <b>1994</b> , 372, 336-43	281
2006 Crystal structure at 2.2 A resolution of the MHC-related neonatal Fc receptor. <b>1994</b> , 372, 336-43	281
2006 Crystal structure at 2.2 A resolution of the MHC-related neonatal Fc receptor. <b>1994</b> , 372, 336-43  2005 Crystal structure of the complex of rat neonatal Fc receptor with Fc. <b>1994</b> , 372, 379-83	281 4 <sup>0</sup> 7

2001 Crystal structure of the tyrosine kinase domain of the human insulin receptor. <b>1994</b> , 372, 746-54	1009
2000 Structural characterization of a highly-ordered 'molten globule' at low pH. <b>1994</b> , 1, 23-9	128
1999 Crystal structure of the holotoxin from Shigella dysenteriae at 2.5 A resolution. <b>1994</b> , 1, 59-64	242
1998 Coordination of acetate with the di-iron centre of methane monooxygenase. <b>1994</b> , 1, 81-2	1
1997 Three sisters, different names. <b>1994</b> , 1, 146-7	28
T and R states in the crystals of bacterial L-lactate dehydrogenase reveal the mechanism for allosteric control. <b>1994</b> , 1, 176-85	<del>7</del> 6
Structure of and kinetic channelling in bifunctional dihydrofolate reductase-thymidylate synthase.  1995 1994, 1, 186-94	165
1994 Structural dynamics in an electron-transfer complex. <b>1994</b> , 1, 234-8	28
1993 Proteinase inhibitor homologues as potassium channel blockers. <b>1994</b> , 1, 246-50	46
The abetalipoproteinemia gene is a member of the vitellogenin family and encodes an alpha-helical domain. <b>1994</b> , 1, 285-6	47
Comparison of four independently determined structures of human recombinant interleukin-4. <b>1994</b> , 1, 301-10	39
1990 Solution structure of a cysteine rich domain of rat protein kinase C. <b>1994</b> , 1, 383-7	121
1989 Structure of the carboxy-terminal LIM domain from the cysteine rich protein CRP. <b>1994</b> , 1, 388-98	161
1988 Structure of a unique twofold symmetric haem-binding site. <b>1994</b> , 1, 453-60	188
High-resolution crystal structures of tyrosine kinase SH3 domains complexed with proline-rich peptides. <b>1994</b> , 1, 546-51	244
1986 The fine art of pore formation. <b>1994</b> , 1, 563-7	7
1985 Structure of a pertussis toxin-sugar complex as a model for receptor binding. <b>1994</b> , 1, 591-6	94
1984 2.1 A resolution refined structure of a TATA box-binding protein (TBP). <b>1994</b> , 1, 621-37	100

1983	1.9 A resolution refined structure of TBP recognizing the minor groove of TATAAAAG. <b>1994</b> , 1, 638-53	199
1982	Nucleotide binding in beta alpha betabeta alpha beta topologies. <b>1994</b> , 1, 677-8	3
1981	Crystallographic observation of a trapped tetrahedral intermediate in a metalloenzyme. <b>1994</b> , 1, 691-4	13
1980	The structure of Bacillus subtilis pectate lyase in complex with calcium. <b>1994</b> , 1, 717-23	151
1979	The structure of avian eye lens delta-crystallin reveals a new fold for a superfamily of oligomeric enzymes. <b>1994</b> , 1, 724-34	70
1978	A tale of two synthetases. <b>1994</b> , 1, 758-60	72
1977	Evolutionary implications. <b>1994</b> , 1, 760-760	5
1976	Solution structure of the tetrameric minimum transforming domain of p53. <b>1994</b> , 1, 877-90	242
1975	Structure of the N-terminal SH3 domain of GRB2 complexed with a peptide from the guanine nucleotide releasing factor Sos. <b>1994</b> , 1, 891-7	88
1974	Iron, DtxR, and the regulation of diphtheria toxin expression. <b>1994</b> , 14, 191-7	125
1973	Galactose-binding site in Escherichia coli heat-labile enterotoxin (LT) and cholera toxin (CT). <b>1994</b> , 13, 745-53	120
1972	The 24 kDa N-terminal sub-domain of the DNA gyrase B protein binds coumarin drugs. <b>1994</b> , 12, 365-73	70
1971	The crystal structure of pertussis toxin. <b>1994</b> , 2, 45-57	297
1970	Crystal structure of chloroplast cytochrome f reveals a novel cytochrome fold and unexpected heme ligation. <b>1994</b> , 2, 95-105	305
1969	NMR-derived three-dimensional solution structure of protein S complexed with calcium. <b>1994</b> , 2, 107-22	74
1968	Lectins on a roll: the structure of E-selectin. <b>1994</b> , 2, 147-50	20
1967	Structure of a soluble, glycosylated form of the human complement regulatory protein CD59. <b>1994</b> , 2, 185-99	160
1966	Serpins: the uncut version. <b>1994</b> , 2, 241-4	17

1965	Antigenic peptide binding by class I and class II histocompatibility proteins. 1994, 2, 245-51	236
1964	Crystal structure of Aeromonas proteolytica aminopeptidase: a prototypical member of the co-catalytic zinc enzyme family. <b>1994</b> , 2, 283-91	246
1963	Electrostatic activation of Escherichia coli methionine repressor. <b>1994</b> , 2, 309-16	61
1962	The three-dimensional structure of N-acetylneuraminate lyase from Escherichia coli. <b>1994</b> , 2, 361-9	115
1961	The crystal structure of glucose dehydrogenase from Thermoplasma acidophilum. <b>1994</b> , 2, 385-93	62
1960	Crystal structure of an ATP-dependent carboxylase, dethiobiotin synthetase, at 1.65 A resolution. <b>1994</b> , 2, 407-14	40
1959	Crystal structures of peptide complexes of the amino-terminal SH2 domain of the Syp tyrosine phosphatase. <b>1994</b> , 2, 423-38	222
1958	Structure of restriction endonuclease bamhi phased at 1.95 A resolution by MAD analysis. <b>1994</b> , 2, 439-52	60
1957	Crystal structure of an extracellular fragment of the rat CD4 receptor containing domains 3 and 4. <b>1994</b> , 2, 469-81	23
1956	Crystal and molecular structure of r(CGCGAAUUAGCG): an RNA duplex containing two G(anti).A(anti) base pairs. <b>1994</b> , 2, 483-94	70
1955	Structural studies on human muscle fatty acid binding protein at 1.4 A resolution: binding interactions with three C18 fatty acids. <b>1994</b> , 2, 523-34	125
1954	Crystal structure of Vibrio cholerae neuraminidase reveals dual lectin-like domains in addition to the catalytic domain. <b>1994</b> , 2, 535-44	189
1953	Structure of human chorionic gonadotropin at 2.6 A resolution from MAD analysis of the selenomethionyl protein. <b>1994</b> , 2, 545-58	442
1952	Proteins with a ring. <b>1994</b> , 2, 571-3	3
1951	The structure of a neutralized virus: canine parvovirus complexed with neutralizing antibody fragment. <b>1994</b> , 2, 595-607	79
1950	Crystallographic study of coenzyme, coenzyme analogue and substrate binding in 6-phosphogluconate dehydrogenase: implications for NADP specificity and the enzyme mechanism. <b>1994</b> , 2, 651-68	107
1949	High-resolution structure of Ascaris trypsin inhibitor in solution: direct evidence for a pH-induced conformational transition in the reactive site. <b>1994</b> , 2, 669-78	60
1948	The molecular structure of the complex of Ascaris chymotrypsin/elastase inhibitor with porcine elastase. <b>1994</b> , 2, 679-89	74

1947	Crystal structures of influenza virus hemagglutinin in complex with high-affinity receptor analogs. <b>1994</b> , 2, 719-31	108
1946	Crystal structure of the extracellular region of the human cell adhesion molecule CD2 at 2.5 A resolution. <b>1994</b> , 2, 755-66	143
1945	Crystal structure of the FAD-containing fragment of corn nitrate reductase at 2.5 A resolution: relationship to other flavoprotein reductases. <b>1994</b> , 2, 809-21	87
1944	Crystal structure of scytalone dehydratasea disease determinant of the rice pathogen, Magnaporthe grisea. <b>1994</b> , 2, 937-44	127
1943	Stability and function: two constraints in the evolution of barstar and other proteins. <b>1994</b> , 2, 945-51	152
1942	2.2 A resolution structure of the amino-terminal half of HIV-1 reverse transcriptase (fingers and palm subdomains). <b>1994</b> , 2, 953-61	49
1941	Conformational polymorphism of cyclosporin A. <b>1994</b> , 2, 963-72	36
1940	Structure of the Escherichia coli signal transducing protein PII. <b>1994</b> , 2, 981-90	75
1939	Structure of 3-isopropylmalate dehydrogenase in complex with NAD+: ligand-induced loop closing and mechanism for cofactor specificity. <b>1994</b> , 2, 1007-16	88
1938	Solution structure and ligand-binding site of the carboxy-terminal SH3 domain of GRB2. <b>1994</b> , 2, 1029-40	71
1937	A novel class of winged helix-turn-helix protein: the DNA-binding domain of Mu transposase. <b>1994</b> , 2, 1041-8	68
1936	The three-dimensional structure of PNGase F, a glycosylasparaginase from Flavobacterium meningosepticum. <b>1994</b> , 2, 1049-59	38
1935	Mechanistic implications and family relationships from the structure of dethiobiotin synthetase. <b>1994</b> , 2, 1061-72	23
1934	The three-dimensional structure of glucose 6-phosphate dehydrogenase from Leuconostoc mesenteroides refined at 2.0 A resolution. <b>1994</b> , 2, 1073-87	111
1933	Old yellow enzyme at 2 Iresolution: overall structure, ligand binding, and comparison with related flavoproteins. <b>1994</b> , 2, 1089-1105	214
1932	Structure of the catalytic core of the family F xylanase from Pseudomonas fluorescens and identification of the xylopentaose-binding sites. <b>1994</b> , 2, 1107-16	139
1931	The crystal structure of citrate synthase from the thermophilic archaeon, Thermoplasma acidophilum. <b>1994</b> , 2, 1157-67	171
1930	Crystal structure of a bacterial chitinase at 2.3 A resolution. <b>1994</b> , 2, 1169-80	378

1929	Crystal structures of hevamine, a plant defence protein with chitinase and lysozyme activity, and its complex with an inhibitor. <b>1994</b> , 2, 1181-9	217
1928	Crystal structure of a diabody, a bivalent antibody fragment. <b>1994</b> , 2, 1217-26	174
1927	Trimeric structure of a C-type mannose-binding protein. <b>1994</b> , 2, 1227-40	279
1926	Crystal structure of the receptor-binding domain of adenovirus type 5 fiber protein at 1.7 A resolution. <b>1994</b> , 2, 1259-70	252
1925	Two mutations causing vitamin D resistant rickets: modelling on the basis of steroid hormone receptor DNA-binding domain crystal structures. <b>1994</b> , 41, 581-90	58
1924	States and functions of tyrosine residues in Escherichia coli asparaginase II. <b>1994</b> , 224, 533-40	48
1923	NMR assignments and secondary structure of the retinoid X receptor alpha DNA-binding domain. Evidence for the novel C-terminal helix. <b>1994</b> , 224, 639-50	13
1922	Elongation on the amino-terminal part of stefin B decreases inhibition of cathepsin H. <b>1994</b> , 224, 797-802	12
1921	Equilibrium unfolding studies of horse muscle acylphosphatase. <b>1994</b> , 225, 811-7	18
1920	Study of the interaction between salivary proline-rich proteins and a polyphenol by 1H-NMR spectroscopy. <b>1994</b> , 219, 923-35	169
1919	X-ray crystallographic and calorimetric studies of the effects of the mutation Trp59>Tyr in ribonuclease T1. <b>1994</b> , 220, 527-34	12
1918	Escherichia coli elongation-factor-Tu mutants with decreased affinity for aminoacyl-tRNA. <b>1994</b> , 220, 739-44	20
1917	Recombinant anti-sialidase single-chain variable fragment antibody. Characterization, formation of dimer and higher-molecular-mass multimers and the solution of the crystal structure of the single-chain variable fragment/sialidase complex. <b>1994</b> , 221, 151-7	108
1916	Proteins under pressure. The influence of high hydrostatic pressure on structure, function and assembly of proteins and protein complexes. <b>1994</b> , 221, 617-30	558
1915	Solution structure of the epsilon-aminohexanoic acid complex of human plasminogen kringle 1. <b>1994</b> , 221, 939-49	20
1914	Insertion in barnase of a loop sequence from ribonuclease T1. Investigating sequence and structure alignments by protein engineering. <b>1994</b> , 221, 1003-12	7
1913	Cation binding to a Bacillus (1,3-1,4)-beta-glucanase. Geometry, affinity and effect on protein stability. <b>1994</b> , 222, 203-14	42
1912	Homology modelling of the catalytic domain of human furin. A model for the eukaryotic subtilisin-like proprotein convertases. <b>1994</b> , 222, 255-66	83

1911	Kinetics of the reduction of wild-type and mutant cytochrome c-550 by methylamine dehydrogenase and amicyanin from Thiobacillus versutus. <b>1994</b> , 222, 561-71	20
1910	The introduction of a negative charge into the hydrophobic patch of Pseudomonas aeruginosa azurin affects the electron self-exchange rate and the electrochemistry. <b>1994</b> , 222, 583-8	41
1909	Rack-induced bonding in blue-copper proteins. <b>1994</b> , 223, 711-8	195
1908	Probing the structure of hirudin from Hirudinaria manillensis by limited proteolysis. Isolation, characterization and thrombin-inhibitory properties of N-terminal fragments. <b>1994</b> , 226, 323-33	31
1907	The three-dimensional structure of a molecular motor. <b>1994</b> , 19, 129-34	77
1906	Nitrogenase and biological nitrogen fixation. <b>1994</b> , 33, 389-97	306
1905	DNA repair proteins. <b>1994</b> , 4, 51-59	10
1904	Crystal structure of the eukaryotic DNA polymerase processivity factor PCNA. <b>1994</b> , 79, 1233-43	760
1903	The three-dimensional structure of H-2Db at 2.4 A resolution: implications for antigen-determinant selection. <b>1994</b> , 76, 39-50	232
1902	Atomic structure of the RuvC resolvase: a holliday junction-specific endonuclease from E. coli. <b>1994</b> , 78, 1063-72	270
1901	The crystal structure of human hypoxanthine-guanine phosphoribosyltransferase with bound GMP. <b>1994</b> , 78, 325-34	203
1900	Structural basis for the binding of proline-rich peptides to SH3 domains. <b>1994</b> , 76, 933-45	936
1899	Solution structure of a specific DNA complex of the Myb DNA-binding domain with cooperative recognition helices. <b>1994</b> , 79, 639-48	430
1898	Structural studies on recombinant and point mutants of flavocytochrome b2. <b>1994</b> , 76, 501-14	12
1897	A detailed comparison of the refined structures of cytochrome c3 molecules from two strains in Desulfovibrio vulgaris: the relationship between the heme structures and their redox properties. <b>1994</b> , 76, 537-45	5
1896	The blind watchmaker and rational protein engineering. <b>1994</b> , 36, 185-220	23
1895	A putative model of the dopamine transporter. <b>1994</b> , 27, 265-74	44
1894	Three-dimensional solution structure of an immunoglobulin light chain-binding domain of protein L. Comparison with the IgG-binding domains of protein G. <b>1994</b> , 33, 14011-7	110

18	893	Two Crystal Structures of the B1 Immunoglobulin-Binding Domain of Streptococcal Protein G and Comparison with NMR. <b>1994</b> , 33, 4721-4729	371
18	892	The Met repressor-operator complex: DNA recognition by beta-strands. <b>1994</b> , 726, 105-17	10
18	391	Crystal structure of T4 endonuclease V. An excision repair enzyme for a pyrimidine dimer. <b>1994</b> , 726, 198-207	7
18	890	Enhanced in vitro refolding of insulin-like growth factor I using a solubilizing fusion partner. <b>1994</b> , 33, 4207-11	86
18	389	The cytochrome b6f complex. <b>1994</b> , 4, 536-544	42
18	388	Chapter 16 Structures of non-specific diffusion pores from Escherichia coli. <b>1994</b> , 27, 353-362	2
18	887	Three-Dimensional Solution Structure of the Extracellular Region of the Complement Regulatory Protein CD59, a New Cell-Surface Protein Domain Related to Snake Venom Neurotoxins. <b>1994</b> , 33, 4471-4482	135
18	886	Structure of rabbit muscle pyruvate kinase complexed with Mn2+, K+, and pyruvate. <b>1994</b> , 33, 6301-9	205
18	385	Fibronectin structure and assembly. <b>1994</b> , 6, 648-55	184
18	884	DNA-binding motifs from eukaryotic transcription factors. <b>1994</b> , 4, 3-11	35
18	383	Protein-protein recognition mediated by a mini-protein domain: possible evolutionary significance. <b>1994</b> , 19, 360-1	5
18	882	Understanding how proteins fold: the lysozyme story so far. <b>1994</b> , 19, 31-7	325
18	381	Antibody-antigen interactions: new structures and new conformational changes. <b>1994</b> , 4, 857-67	447
18	880	Three-dimensional structure of phosphotriesterase: an enzyme capable of detoxifying organophosphate nerve agents. <b>1994</b> , 33, 15001-7	187
18	379	Pattern recognition and self-correcting distance geometry calculations applied to myohemerythrin. <b>1994</b> , 344, 147-53	29
18	878	Structural similarity of cytochrome c2 from Rhodopseudomonas viridis to mitochondrial cytochromes c revealed by its crystal structure at 2.7 A resolution. <b>1994</b> , 345, 5-8	9
18	377	Prediction of the structural similarity between spermidine/putrescine-binding protein and maltose-binding protein. <b>1994</b> , 345, 23-6	9
18	876	Making a small enzyme smaller; removing the conserved loop structure of hen lysozyme. <b>1994</b> , 347, 199-202	5

1875	Stability and solvation of Thr/Ser to Ala and Gly mutations at the N-cap of alpha-helices. <b>1994</b> , 347, 304-9	5
1874	Solution structure of human interleukin-1 receptor antagonist protein. <b>1994</b> , 349, 79-83	12
1873	Direct observation of the iron binding sites in a ferritin. <b>1994</b> , 350, 258-62	74
1872	Homology modelling and 1H NMR studies of human leukaemia inhibitory factor. <b>1994</b> , 350, 275-80	13
1871	The role of lysine 99 of Thiobacillus versutus cytochrome c-550 in the alkaline transition. <b>1994</b> , 351, 100-4	11
1870	NMR solution structure of the recombinant tick anticoagulant protein (rTAP), a factor Xa inhibitor from the tick Ornithodoros moubata. <b>1994</b> , 352, 251-7	40
1869	Predicted secondary structure of the 20 S proteasome and model structure of the putative peptide channel. <b>1994</b> , 354, 45-9	17
1868	Alteration of the substrate specificity of human lysozyme by site-specific intermolecular cross-linking. <b>1994</b> , 355, 271-4	3
1867	Mapping the binding surface of interleukin-8 complexed with an N-terminal fragment of the type 1 human interleukin-8 receptor. <b>1994</b> , 338, 93-7	82
1866	Structural similarity of plant chitinase and lysozymes from animals and phage. An evolutionary connection. <b>1994</b> , 340, 129-32	76
1865	Elucidation of the poly-L-proline binding site in Acanthamoeba profilin I by NMR spectroscopy. <b>1994</b> , 337, 145-51	54
1864	Structural similarities between chaperone molecules of the HSP60 and HSP70 families deduced from hydrophobic cluster analysis. <b>1994</b> , 342, 242-8	7
1863	Structure of partially-activated E. coli heat-labile enterotoxin (LT) at 2.6 A resolution. <b>1994</b> , 337, 88-92	33
1862	Crystal structure of the tenth type III cell adhesion module of human fibronectin. <b>1994</b> , 236, 1079-92	193
1861	Prediction of the positioning of the seven transmembrane alpha-helices of bacteriorhodopsin. A molecular simulation study. <b>1994</b> , 236, 1105-22	31
1860	Crystal structure of a NAD-dependent D-glycerate dehydrogenase at 2.4 A resolution. <b>1994</b> , 236, 1123-40	99
1859	Refined 1.7 A X-ray crystallographic structure of P-30 protein, an amphibian ribonuclease with anti-tumor activity. <b>1994</b> , 236, 1141-53	132
1858	Refined crystal structure of the 2[4Fe-4S] ferredoxin from Clostridium acidurici at 1.84 A resolution. <b>1994</b> , 243, 683-95	69

1857	Protein three-dimensional structure determination and sequence-specific assignment of 13C and 15N-separated NOE data. A novel real-space ab initio approach. <b>1994</b> , 243, 696-718	54
1856	Modeling protein cores with Markov random fields. <b>1994</b> , 124, 149-79	19
1855	Structure and function of the SH3 domain. <b>1994</b> , 61, 283-97	129
1854	Structures of larger proteins, protein-ligand and protein-DNA complexes by multi-dimensional heteronuclear NMR. <b>1994</b> , 62, 153-84	17
1853	Stability of myoglobin: a model for the folding of heme proteins. <b>1994</b> , 33, 11767-75	129
1852	Snail and spider toxins share a similar tertiary structure and 'cystine motif'. <b>1994</b> , 1, 850-2	86
1851	Getting a grip on DNA recognition: structures of the basic region leucine zipper, and the basic region helix-loop-helix DNA-binding domains. <b>1994</b> , 4, 12-21	107
1850	Structure-activity relationships for the interaction between cyclosporin A derivatives and the Fab fragment of a monoclonal antibody. <b>1994</b> , 31, 913-22	11
1849	Thermodynamic characterization of an equilibrium folding intermediate of staphylococcal nuclease. <b>1994</b> , 3, 2175-84	39
1848	Rigid-body docking with mutant constraints of influenza hemagglutinin with antibody HC19. <b>1994</b> , 18, 8-18	28
1847	Structures of two classes of MHC molecules elucidated: crucial differences and similarities. <b>1994</b> , 4, 852-6	39
1846	Zinc finger diversity. <b>1994</b> , 4, 28-35	33
1845	Classification of protein folds. <b>1994</b> , 4, 429-440	102
1844	Protein engineering and the dissection of protein folding pathways. <b>1994</b> , 4, 107-111	15
1843	Major groove DNA recognition by	70
1842	Coagulation factors and their inhibitors. <b>1994</b> , 4, 823-32	57
1841	Analysis of the functional effects of a mutation in SOD1 associated with familial amyotrophic lateral sclerosis. <b>1994</b> , 13, 727-36	69
1840	New protein folds. <b>1994</b> , 4, 441-449	30

1839	Chronic granulomatous disease. <b>1994</b> , 1227, 1-24	176
1838	Study of structure-activity relationship of fasciculin by acetylation of amino groups. <b>1994</b> , 1199, 1-5	25
1837	Protein kinase superfamily L'omparisons of sequence data with three-dimensional structures. <b>1994</b> , 4, 450-455	16
1836	Chelation of serine 39 to Mg2+ latches a gate at the active site of enolase: structure of the bis(Mg2+) complex of yeast enolase and the intermediate analog phosphonoacetohydroxamate at 2.1-A resolution. <b>1994</b> , 33, 9333-42	106
1835	Structure of the extracellular domain of human tissue factor: location of the factor VIIa binding site. <b>1994</b> , 33, 10864-70	136
1834	X-ray structure of nucleoside diphosphate kinase complexed with thymidine diphosphate and Mg2+at 2-A resolution. <b>1994</b> , 33, 9062-9	75
1833	The refolding of human lysozyme: a comparison with the structurally homologous hen lysozyme. <b>1994</b> , 33, 5867-76	119
1832	NMR solution structure of the isolated N-terminal fragment of protein-G B1 domain. Evidence of trifluoroethanol induced native-like beta-hairpin formation. <b>1994</b> , 33, 6004-14	187
1831	Role of the interdomain hinge of flavocytochrome b2 in intra- and inter-protein electron transfer. <b>1994</b> , 33, 5115-20	40
1830	Adenosine 5'-diphosphate binding and the active site of nucleoside diphosphate kinase. <b>1994</b> , 33, 459-67	91
1829	X-ray crystallographic structures of D-xylose isomerase-substrate complexes position the substrate and provide evidence for metal movement during catalysis. <b>1994</b> , 33, 5469-80	108
1828	Three-dimensional structure of the biotin carboxylase subunit of acetyl-CoA carboxylase. <b>1994</b> , 33, 10249-56	185
1827	Structure of the NADPH-binding motif of glutathione reductase: efficiency determined by evolution. <b>1994</b> , 33, 5721-7	43
1826	Identity switches between tRNAs aminoacylated by class I glutaminyl- and class II aspartyl-tRNA synthetases. <b>1994</b> , 33, 9912-21	37
1825	Kinetic mechanism of cytochrome c folding: involvement of the heme and its ligands. <b>1994</b> , 33, 6925-35	300
1824	The mutant Escherichia coli F112W cyclophilin binds cyclosporin A in nearly identical conformation as human cyclophilin. <b>1994</b> , 33, 5711-20	27
1823	Solution structure of dimeric Mnt repressor (1-76). <b>1994</b> , 33, 15036-45	59
1822	Crystal structure of unmodified tRNA(Gln) complexed with glutaminyl-tRNA synthetase and ATP suggests a possible role for pseudo-uridines in stabilization of RNA structure. <b>1994</b> , 33, 7560-7	185

1821	Solution structure of the active domain of tissue inhibitor of metalloproteinases-2. A new member of the OB fold protein family. <b>1994</b> , 33, 11745-59	97
1820	Crystallographic study of Glu58Ala RNase T1 x 2'-guanosine monophosphate at 1.9-A resolution. <b>1994</b> , 33, 1654-62	13
1819	Subsite binding in an RNase: structure of a barnase-tetranucleotide complex at 1.76-A resolution. <b>1994</b> , 33, 1644-53	80
1818	Synthetic peptides probe folding initiation sites in platelet factor-4: stable chain reversal found within the hydrophobic sequence LIATLKNGRKISL. <b>1994</b> , 33, 13436-44	34
1817	Substrate activation of brewers' yeast pyruvate decarboxylase is abolished by mutation of cysteine 221 to serine. <b>1994</b> , 33, 5630-5	66
1816	Point-mutations affecting the properties of tyrosineD in photosystem II. Characterization by isotopic labeling and spectral simulation. <b>1994</b> , 33, 11805-13	24
1815	Structural analysis of peptide fragment 71-93 of transthyretin by NMR spectroscopy and electron microscopy: insight into amyloid fibril formation. <b>1994</b> , 33, 33-41	26
1814	Crystallographic structure of a phosphonate derivative of the Enterobacter cloacae P99 cephalosporinase: mechanistic interpretation of a beta-lactamase transition-state analog. <b>1994</b> , 33, 6762-72	158
1813	Zinc chelation and structural stability of adenylate kinase from Bacillus subtilis. <b>1994</b> , 33, 9960-7	37
1812	Homeodomain determinants of major groove recognition. <b>1994</b> , 33, 10851-8	57
1811	Transient hydrogen bonds identified on the surface of the NMR solution structure of Hirudin. <b>1994</b> , 33, 9303-10	47
1810	Characterization of mutant Met100Lys of cytochrome c-550 from Thiobacillus versutus with lysine-histidine heme ligation. <b>1994</b> , 33, 10051-9	57
1809	Hydrogen-deuterium exchange in the free and immunoglobulin G-bound protein G B-domain. <b>1994</b> , 33, 5702-10	44
1808	Structural Patterns in Globular Proteins. <b>1994</b> , 635-667	1
1807	The steroid/nuclear receptors: from three-dimensional structure to complex function. <b>1994</b> , 49, 1-47	25
1806	Modeling the Combining Site of the Human Asialoglycoprotein Receptor. <b>1994</b> , 34, 177-184	
1805	Intragenic suppression among CDC34 (UBC3) mutations defines a class of ubiquitin-conjugating catalytic domains. <b>1995</b> , 15, 5635-44	33
1804	Structural studies on fungal endoglucanases from Humicola insolens. <b>1995</b> , 225-237	1

1803	A potent human interleukin-4 antagonist stimulates the proliferation of murine cells expressing the human interleukin-4 binding chain. <b>1995</b> , 12, 69-83	3
1802	X-ray studies of quinoproteins. <b>1995</b> , 258, 191-216	7
1801	X-ray crystallographic studies of cofactors in galactose oxidase. <b>1995</b> , 258, 235-62	11
1800	Solution structure of DNA polymerases and DNA polymerase-substrate complexes. <b>1995</b> , 262, 147-71	1
1799	Electrostatic studies of carbohydrate active enzymes. <b>1995</b> , 10, 181-204	1
1798	Solution structures of horse ferro- and ferricytochrome c using 2D and 3D 1H NMR and restrained simulated annealing. <b>1995</b> , 6, 511-519	
1797	Analysis of the binding site on intercellular adhesion molecule 3 for the leukocyte integrin lymphocyte function-associated antigen 1. <b>1995</b> , 270, 877-84	64
1796	Site-directed mutagenesis confirms the involvement of carboxylate groups in the disassembly of tobacco mosaic virus. <b>1995</b> , 206, 724-30	69
1795	Factor XIIIA Calgary: a candidate missense mutation (Leu667Pro) in the beta barrel 2 domain of the factor XIIIA subunit. <b>1995</b> , 91, 452-7	26
1794	Topology of the CD2-CD48 cell-adhesion molecule complex: implications for antigen recognition by T cells. <b>1995</b> , 5, 74-84	114
1793	Structural characterization of viral fusion proteins. <b>1995</b> , 5, 265-74	102
1792	Ion-channel gating. Twist to open. <b>1995</b> , 5, 373-5	14
1791	Identification of a common fold in the replication terminator protein suggests a possible mode for DNA binding. <b>1995</b> , 20, 300-2	19
	210 (2010ang, 1999) 20, 300 E	
1790	DNA repair in three dimensions. <b>1995</b> , 20, 421-6	15
1790 1789		15
, ,	DNA repair in three dimensions. <b>1995</b> , 20, 421-6  Three-dimensional structure of the diphtheria toxin repressor in complex with divalent cation	
1789	DNA repair in three dimensions. <b>1995</b> , 20, 421-6  Three-dimensional structure of the diphtheria toxin repressor in complex with divalent cation co-repressors. <b>1995</b> , 3, 87-100	120

## (1995-1995)

1785	Structural basis for the specific interaction of lysine-containing proline-rich peptides with the N-terminal SH3 domain of c-Crk. <b>1995</b> , 3, 215-26	223
1784	Annexins: a novel family of calcium- and membrane-binding proteins in search of a function. <b>1995</b> , 3, 233-7	56
1783	Hyperthermophiles: taking the heat and loving it. <b>1995</b> , 3, 251-4	72
1782	Crystal structure of the MS2 coat protein dimer: implications for RNA binding and virus assembly. <b>1995</b> , 3, 255-63	74
1781	Solution structure of human thioredoxin in a mixed disulfide intermediate complex with its target peptide from the transcription factor NF kappa B. <b>1995</b> , 3, 289-97	216
1780	Activity of the MAP kinase ERK2 is controlled by a flexible surface loop. <b>1995</b> , 3, 299-307	105
1779	Self-association of a DNA loop creates a quadruplex: crystal structure of d(GCATGCT) at 1.8 A resolution. <b>1995</b> , 3, 335-40	66
1778	The structural basis for seryl-adenylate and Ap4A synthesis by seryl-tRNA synthetase. <b>1995</b> , 3, 341-52	84
1777	Structure of HIV-1 reverse transcriptase in a complex with the non-nucleoside inhibitor alpha-APA R 95845 at 2.8 A resolution. <b>1995</b> , 3, 365-79	218
1776	Tertiary structure of an immunoglobulin-like domain from the giant muscle protein titin: a new member of the I set. <b>1995</b> , 3, 391-401	101
1775	The avian eye lens protein delta-crystallin shows a novel packing arrangement of tetramers in a supramolecular helix. <b>1995</b> , 3, 403-12	19
1774	Refined three-dimensional solution structure of insect defensin A. <b>1995</b> , 3, 435-48	<b>2</b> 90
1773	Movie of the structural changes during a catalytic cycle of nucleoside monophosphate kinases. <b>1995</b> , 3, 483-90	237
1772	Crystal structure of catalase HPII from Escherichia coli. <b>1995</b> , 3, 491-502	87
1771	Structure of full-length porcine synovial collagenase reveals a C-terminal domain containing a calcium-linked, four-bladed beta-propeller. <b>1995</b> , 3, 541-9	246
1770	1.8 A crystal structure of the C-terminal domain of rabbit serum haemopexin. <b>1995</b> , 3, 551-9	94
1769	Surprising leads for a cholera toxin receptor-binding antagonist: crystallographic studies of CTB mutants. <b>1995</b> , 3, 561-70	25
1768	Structural comparison of two strains of foot-and-mouth disease virus subtype O1 and a laboratory antigenic variant, G67. <b>1995</b> , 3, 571-80	68

1767	Electrostatic analysis of TEM1 beta-lactamase: effect of substrate binding, steep potential gradients and consequences of site-directed mutations. <b>1995</b> , 3, 603-13	56
1766	How Ras works: structure of a Rap-Raf complex. <b>1995</b> , 3, 641-3	15
1765	Viral envelope glycoproteins swing into action. <b>1995</b> , 3, 645-8	4
1764	The crystal structure of the catalytic domain of human urokinase-type plasminogen activator. <b>1995</b> , 3, 681-91	142
1763	A role for quaternary structure in the substrate specificity of leucine dehydrogenase. <b>1995</b> , 3, 693-705	78
1762	Crystal structure of Escherichia coli pyruvate kinase type I: molecular basis of the allosteric transition. <b>1995</b> , 3, 729-41	115
1761	Crystal structure of the superantigen enterotoxin C2 from Staphylococcus aureus reveals a zinc-binding site. <b>1995</b> , 3, 769-79	119
1760	Structural evidence for the evolutionary divergence of mycoplasma from gram-positive bacteria: the histidine-containing phosphocarrier protein. <b>1995</b> , 3, 781-90	20
1759	The solution structure and backbone dynamics of the fibronectin type I and epidermal growth factor-like pair of modules of tissue-type plasminogen activator. <b>1995</b> , 3, 823-33	33
1758	Structures and mechanisms of glycosyl hydrolases. <b>1995</b> , 3, 853-9	1582
1758 1757	Structures and mechanisms of glycosyl hydrolases. <b>1995</b> , 3, 853-9  Modeling of the three-dimensional structure of proteins with the typical leucine-rich repeats. <b>1995</b> , 3, 867-77	1582 216
,,	Modeling of the three-dimensional structure of proteins with the typical leucine-rich repeats. <b>1995</b> ,	
1757	Modeling of the three-dimensional structure of proteins with the typical leucine-rich repeats. <b>1995</b> , 3, 867-77  Mechanistic implications from the structure of a catalytic fragment of Moloney murine leukemia	216
1757 1756	Modeling of the three-dimensional structure of proteins with the typical leucine-rich repeats. 1995, 3, 867-77  Mechanistic implications from the structure of a catalytic fragment of Moloney murine leukemia virus reverse transcriptase. 1995, 3, 879-92	216 152
1757 1756 1755	Modeling of the three-dimensional structure of proteins with the typical leucine-rich repeats. 1995, 3, 867-77  Mechanistic implications from the structure of a catalytic fragment of Moloney murine leukemia virus reverse transcriptase. 1995, 3, 879-92  The prosegment-subtilisin BPN' complex: crystal structure of a specific 'foldase'. 1995, 3, 907-14  The structure of HIV-1 reverse transcriptase complexed with 9-chloro-TIBO: lessons for inhibitor	216 152 170
1757 1756 1755 1754	Modeling of the three-dimensional structure of proteins with the typical leucine-rich repeats. 1995, 3, 867-77  Mechanistic implications from the structure of a catalytic fragment of Moloney murine leukemia virus reverse transcriptase. 1995, 3, 879-92  The prosegment-subtilisin BPN' complex: crystal structure of a specific 'foldase'. 1995, 3, 907-14  The structure of HIV-1 reverse transcriptase complexed with 9-chloro-TIBO: lessons for inhibitor design. 1995, 3, 915-26  Common themes in redox chemistry emerge from the X-ray structure of oilseed rape (Brassica	216 152 170 189
1757 1756 1755 1754 1753	Modeling of the three-dimensional structure of proteins with the typical leucine-rich repeats. 1995, 3, 867-77  Mechanistic implications from the structure of a catalytic fragment of Moloney murine leukemia virus reverse transcriptase. 1995, 3, 879-92  The prosegment-subtilisin BPN' complex: crystal structure of a specific 'foldase'. 1995, 3, 907-14  The structure of HIV-1 reverse transcriptase complexed with 9-chloro-TIBO: lessons for inhibitor design. 1995, 3, 915-26  Common themes in redox chemistry emerge from the X-ray structure of oilseed rape (Brassica napus) enoyl acyl carrier protein reductase. 1995, 3, 927-38	216 152 170 189

1749	plastocyanin. <b>1995</b> , 3, 1159-69	131
1748	Crystal structure of a quinoenzyme: copper amine oxidase of Escherichia coli at 2 A resolution. <b>1995</b> , 3, 1171-84	297
1747	Solution structure of the pleckstrin homology domain of Drosophila beta-spectrin. <b>1995</b> , 3, 1185-95	60
1746	The three domains of a bacterial sialidase: a beta-propeller, an immunoglobulin module and a galactose-binding jelly-roll. <b>1995</b> , 3, 1197-205	183
1745	Substrate binding and carboxylation by dethiobiotin synthetasea kinetic and X-ray study. <b>1995</b> , 3, 1207-15	22
1744	Crystal structure of the di-haem cytochrome c peroxidase from Pseudomonas aeruginosa. <b>1995</b> , 3, 1225-33	120
1743	Three-dimensional structure of the human 'protective protein': structure of the precursor form suggests a complex activation mechanism. <b>1995</b> , 3, 1249-59	97
1742	The crystal structure of a major secreted aspartic proteinase from Candida albicans in complexes with two inhibitors. <b>1995</b> , 3, 1261-71	103
1741	2.0 A structure of indole-3-glycerol phosphate synthase from the hyperthermophile Sulfolobus solfataricus: possible determinants of protein stability. <b>1995</b> , 3, 1295-306	230
1740	X-ray structure of human nucleoside diphosphate kinase B complexed with GDP at 2 A resolution. <b>1995</b> , 3, 1307-14	98
1739	A 26 kDa yeast DNA topoisomerase I fragment: crystallographic structure and mechanistic implications. <b>1995</b> , 3, 1315-22	31
1738	Crystal structure of an acetylcholinesterase-fasciculin complex: interaction of a three-fingered toxin from snake venom with its target. <b>1995</b> , 3, 1355-66	217
1737	The crystal structure of chloroperoxidase: a heme peroxidasecytochrome P450 functional hybrid. <b>1995</b> , 3, 1367-77	402
1736	Crystal structure of human Charcot-Leyden crystal protein, an eosinophil lysophospholipase, identifies it as a new member of the carbohydrate-binding family of galectins. <b>1995</b> , 3, 1379-93	127
1735	Structure of the biotinyl domain of acetyl-coenzyme A carboxylase determined by MAD phasing. <b>1995</b> , 3, 1407-19	160
1734	Investigation of the Energy Requirement and Targeting Signal for the Import of Glycolate Oxidase into Glyoxysomes. <b>1995</b> , 230, 157-163	
1733	Synthesis, Three-Dimensional Structure, and Specific 15N-Labelling of the Streptococcal Protein G B1-Domain. <b>1995</b> , 231, 166-180	5
1732	Identification of Residues Potentially Involved in the Interactions Between Subunits in Yeast Alcohol Dehydrogenases. <b>1995</b> , 231, 214-219	

1731	1H and 15N Resonance Assignments and Structure of the N-Terminal Domain of Escherichia coli Initiation Factor 3. <b>1995</b> , 228, 395-402	3
1730	1H,13C,15N-NMR Resonance Assignments of Oxidized Thioredoxin h from the Eukaryotic Green Alga Chlamydomonas reinhardtii Using New Methods based on Two-Dimensional Triple-Resonance NMR Spectroscopy and Computer-Assisted Backbone Assignment. <b>1995</b> , 229, 473-485	1
1729	Kinetic analysis of Escherichia coli ribonuclease HI using oligomeric DNA/RNA substrates suggests an alternative mechanism for the interaction between the enzyme and the substrate. <b>1995</b> , 231, 557-62	38
1728	The Interaction of Hevein with N-acetylglucosamine-containing Oligosaccharides. <b>1995</b> , 230, 621-633	88
1727	Folding of Protein G B1 Domain Studied by the Conformational Characterization of Fragments Comprising Its Secondary Structure Elements. <b>1995</b> , 230, 634-649	2
1726	X-ray Structures of Human Neutrophil Collagenase Complexed with Peptide Hydroxamate and Peptide Thiol Inhibitors. Implications for Substrate Binding and Rational Drug Design. <b>1995</b> , 228, 830-841	2
1725	Sequential 1H and 15N nuclear magnetic resonance assignments and secondary structure of the lipoyl domain of the 2-oxoglutarate dehydrogenase complex from Azotobacter vinelandii. Evidence for high structural similarity with the lipoyl domain of the pyruvate dehydrogenase complex. <b>1995</b> , 234, 148-59	6
1724	Refined Solution Structure of the Tyr41->His Mutant of the M13 Gene V Protein. <b>1995</b> , 232, 506-514	16
1723	Molecular Cloning and Characterization of Anionic and Cationic Variants of Trypsin from Atlantic Salmon. <b>1995</b> , 232, 677-685	67
1722	Structural Influence of Calcium on the Heme Cavity of Cationic Peanut Peroxidase as Determined by 1H-NMR Spectroscopy. <b>1995</b> , 232, 825-833	
1721	Folding of the squash trypsin inhibitor EETI II. Evidence of native and non-native local structural preferences in a linear analogue. <b>1995</b> , 233, 837-46	20
1720	Crystal and Molecular Structure at 0.16-nm Resolution of the Hybrid Bacillus Endo-1,3-1,4-beta-D-Glucan 4-Glucanohydrolase H(A16-M). <b>1995</b> , 232, 849-858	1
1719	The catalytic subunit of cAMP-dependent protein kinase from Ascaris suum. The cloning and structure of a novel subtype of protein kinase A. <b>1995</b> , 232, 111-7	11
1718	Molecular modelling of the interaction between the catalytic site of pig pancreatic alpha-amylase and amylose fragments. <b>1995</b> , 232, 284-93	22
1717	Kombinatorische Synthese und mehrdimensionale NMR-Spektroskopie: ein Beitrag zum Verstfidnis von Protein-Ligand-Wechselwirkungen. <b>1995</b> , 107, 1041-1058	5
1716	Kinetic analysis of the interaction between protein A domain variants and human Fc using plasmon resonance detection. <b>1995</b> , 8, 270-8	73
1715	Protein structural analysis as a tool for protein design. <b>1995</b> , 37, 377-382	1
1714	Membrane protein assembly: rules of the game. <b>1995</b> , 17, 25-30	49

1713	MDScope 🖪 visual computing environment for structural biology. <b>1995</b> , 91, 111-133	39
1712	Changes in the neuraminidase of neurovirulent influenza virus strains. <b>1995</b> , 10, 253-60	12
1711	Molecular evolution of aphthoviruses. <b>1995</b> , 11, 197-207	25
1710	The importance of Arg40 and 45 in the mitogenic activity and structural stability of basic fibroblast growth factor: effects of acidic amino acid substitutions. <b>1995</b> , 14, 263-74	12
1709	A multiple alignment of the capsid protein sequences of nepoviruses and comoviruses suggests a common structure. <b>1995</b> , 140, 2041-53	21
1708	Matrix metalloproteases: Structure-based drug discovery targets. <b>1995</b> , 2, 343-351	12
1707	Essential degrees of freedom of proteins. <b>1995</b> , 5, 71-79	5
1706	A model of HIV-I reverse transcriptase: Possible mechanisms for AZT resistance. <b>1995</b> , 5, 81-88	1
1705	Dynamic domains: A simple method of analysing structural movements in proteins. <b>1995</b> , 5, 107-119	
1704	Gain-of-function mutations in a human calmodulin-like protein identify residues critical for calmodulin action in yeast. <b>1995</b> , 247, 137-47	7
1703	Evolutionary analysis of aspartate aminotransferases. <b>1995</b> , 40, 455-63	24
1702	The class II aminoacyl-tRNA synthetases and their active site: evolutionary conservation of an ATP binding site. <b>1995</b> , 40, 499-508	37
1701	Structure-based sequence alignment of elongation factors Tu and G with related GTPases involved in translation. <b>1995</b> , 41, 1096	32
1700	Structure and atomic fluctuation patterns of potato carboxypeptidase a inhibitor protein. <b>1995</b> , 24, 1-11	7
1699	Dynamic modelling of a helical peptide in solution using NMR data: multiple conformations and multi-spin effects. <b>1995</b> , 6, 33-40	27
1698	Graph-theoretical assignment of secondary structure in multidimensional protein NMR spectra: application to the lac repressor headpiece. <b>1995</b> , 6, 67-78	10
1697	Modulation of DNA-binding specificity within the nuclear receptor family by substitutions at a single amino acid position. <b>1995</b> , 21, 57-67	10
1696	Three-dimensional structure prediction of the NAD binding site of proton-pumping transhydrogenase from Escherichia coli. <b>1995</b> , 21, 91-104	21

1695	Crystallization, molecular replacement solution, and refinement of tetrameric beta-amylase from sweet potato. <b>1995</b> , 21, 105-17	50
1694	Computational approaches to study protein unfolding: hen egg white lysozyme as a case study. <b>1995</b> , 21, 196-213	89
1693	Long timestep dynamics of peptides by the dynamics driver approach. <b>1995</b> , 21, 282-302	22
1692	LINUS: a hierarchic procedure to predict the fold of a protein. <b>1995</b> , 22, 81-99	230
1691	An analysis of side chain interactions and pair correlations within antiparallel beta-sheets: the differences between backbone hydrogen-bonded and non-hydrogen-bonded residue pairs. <b>1995</b> , 22, 119-31	214
1690	Molecular dynamics simulations of rubredoxin from Clostridium pasteurianum: changes in structure and electrostatic potential during redox reactions. <b>1995</b> , 22, 154-67	48
1689	The catalytic domain of a bacterial lytic transglycosylase defines a novel class of lysozymes. <b>1995</b> , 22, 245-58	61
1688	The cytidylyltransferase superfamily: identification of the nucleotide-binding site and fold prediction. <b>1995</b> , 22, 259-66	81
1687	Size-independent comparison of protein three-dimensional structures. <b>1995</b> , 22, 273-83	101
1686	Local moves: an efficient algorithm for simulation of protein folding. <b>1995</b> , 23, 73-82	58
1685	Three-dimensional model of the alpha-subunit of bacterial luciferase. <b>1995</b> , 23, 241-55	3
1684	Metal search: a computer program that helps design tetrahedral metal-binding sites. <b>1995</b> , 23, 256-63	47
1683	Evaluation of comparative protein modeling by MODELLER. <b>1995</b> , 23, 318-26	930
1682	Protein structure prediction by threading methods: evaluation of current techniques. <b>1995</b> , 23, 337-55	182
1681	Progress in fold recognition. <b>1995</b> , 23, 376-86	86
1680	Successful protein fold recognition by optimal sequence threading validated by rigorous blind testing. <b>1995</b> , 23, 387-97	84
1679	Crystallographic structure of metal-free concanavalin A at 2.5 A resolution. <b>1995</b> , 23, 510-24	50
16 <del>7</del> 8	Hinge-bending motion in citrate synthase arising from normal mode calculations. <b>1995</b> , 23, 557-60	172

1677	Protein-protein interaction at crystal contacts. <b>1995</b> , 23, 580-7	226
1676	Differentiation of peptide molecular recognition by phospholipase C gamma-1 Src homology-2 domain and a mutant Tyr phosphatase PTP1bC215S. <b>1995</b> , 4, 13-20	2
1675	A procedure for detecting structural domains in proteins. <b>1995</b> , 4, 103-12	83
1674	Characterization of the N-terminal half-saturated state of calbindin D9k: NMR studies of the N56A mutant. <b>1995</b> , 4, 1045-55	24
1673	High-resolution structures of adenylate kinase from yeast ligated with inhibitor Ap5A, showing the pathway of phosphoryl transfer. <b>1995</b> , 4, 1262-71	134
1672	Limited proteolysis of native proteins: the interaction between avidin and proteinase K. <b>1995</b> , 4, 1337-45	49
1671	Solution structure of the potassium channel inhibitor agitoxin 2: caliper for probing channel geometry. <b>1995</b> , 4, 1478-89	112
1670	Predicting oligomerization states of coiled coils. <b>1995</b> , 4, 1596-607	200
1669	Predicting the structure of the light-harvesting complex II of Rhodospirillum molischianum. <b>1995</b> , 4, 1670-82	38
1668	A ligand-induced conformational change in the Yersinia protein tyrosine phosphatase. <b>1995</b> , 4, 1904-13	110
1667	Structural analysis of zinc substitutions in the active site of thermolysin. <b>1995</b> , 4, 1955-65	181
1666	Structural similarity between the pleckstrin homology domain and verotoxin: the problem of measuring and evaluating structural similarity. <b>1995</b> , 4, 1977-83	22
1665	Binary patterning of polar and nonpolar amino acids in the sequences and structures of native proteins. <b>1995</b> , 4, 2032-9	116
1664	Thermal stability determinants of chicken egg-white lysozyme core mutants: hydrophobicity, packing volume, and conserved buried water molecules. <b>1995</b> , 4, 2050-62	67
1663	Destabilizing loop swaps in the CDRs of an immunoglobulin VL domain. 1995, 4, 2073-81	41
1662	Molecular modeling of the GM-CSF and IL-3 receptor complexes. <b>1995</b> , 4, 2223-33	22
1661	Covariation of residues in the homeodomain sequence family. <b>1995</b> , 4, 2269-78	89
1660	Discovery of the ammonium substrate site on glutamine synthetase, a third cation binding site. <b>1995</b> , 4, 2358-65	82

1659	Active site model for gamma-aminobutyrate aminotransferase explains substrate specificity and inhibitor reactivities. <b>1995</b> , 4, 2366-74	23
1658	Structural similarities in the noncatalytic domains of phenylalanyl-tRNA and biotin synthetases. <b>1995</b> , 4, 2429-32	21
1657	3D domain swapping: a mechanism for oligomer assembly. <b>1995</b> , 4, 2455-68	678
1656	Solution structure of the catalytic domain of human stromelysin complexed with a hydrophobic inhibitor. <b>1995</b> , 4, 2487-98	74
1655	Crystal structure of recombinant triosephosphate isomerase from Bacillus stearothermophilus. An analysis of potential thermostability factors in six isomerases with known three-dimensional structures points to the importance of hydrophobic interactions. <b>1995</b> , 4, 2594-604	106
1654	Structural and dynamic characterization of the urea denatured state of the immunoglobulin binding domain of streptococcal protein G by multidimensional heteronuclear NMR spectroscopy. <b>1995</b> , 4, 2605-15	129
1653	Protein recognition of ammonium cations using side-chain aromatics: a structural variation for secondary ammonium ligands. <b>1995</b> , 4, 2625-8	28
1652	Structure and function of the porin channel. <b>1995</b> , 48, 930-40	37
1651	Malarial epitopes expressed on the surface of recombinant tobacco mosaic virus. <b>1995</b> , 13, 53-7	175
1650	Calmodulin as a versatile tag for antibody fragments. <b>1995</b> , 13, 373-7	33
1649	The crystal structure of bluetongue virus VP7. <b>1995</b> , 373, 167-70	142
1648	Penicillin acylase has a single-amino-acid catalytic centre. <b>1995</b> , 373, 264-8	420
1647	Structure of the NF-kappa B p50 homodimer bound to DNA. <b>1995</b> , 373, 311-7	480
1646	The structural basis of specific base-excision repair by uracil-DNA glycosylase. <b>1995</b> , 373, 487-93	377
1645	Crystal structure of an integrin-binding fragment of vascular cell adhesion molecule-1 at 1.8 A resolution. <b>1995</b> , 373, 539-44	183
1644	Crystal structure of the nickel-iron hydrogenase from Desulfovibrio gigas. <b>1995</b> , 373, 580-7	1363
1643	A structural basis of the interactions between leucine-rich repeats and protein ligands. <b>1995</b> , 374, 183-6	599
1642	Structural basis of cell-cell adhesion by cadherins. <b>1995</b> , 374, 327-37	1017

1641	Crystal structure of the nuclear Ras-related protein Ran in its GDP-bound form. <b>1995</b> , 374, 378-81	173
1640	The structure of trp RNA-binding attenuation protein. <b>1995</b> , 374, 693-700	176
1639	The envelope glycoprotein from tick-borne encephalitis virus at 2 A resolution. <b>1995</b> , 375, 291-8	1162
1638	Crystal structure of the ligand-binding domain of the human nuclear receptor RXR-alpha. <b>1995</b> , 375, 377-82	1062
1637	The 2.2 A crystal structure of the Ras-binding domain of the serine/threonine kinase c-Raf1 in complex with Rap1A and a GTP analogue. <b>1995</b> , 375, 554-60	581
1636	Crystal structure of isopenicillin N synthase is the first from a new structural family of enzymes. <b>1995</b> , 375, 700-4	396
1635	Structure of influenza virus haemagglutinin complexed with a neutralizing antibody. <b>1995</b> , 376, 92-4	213
1634	Mechanism of CDK activation revealed by the structure of a cyclinA-CDK2 complex. <b>1995</b> , 376, 313-20	1227
1633	Crystal structure of a replication fork single-stranded DNA binding protein (T4 gp32) complexed to DNA. <b>1995</b> , 376, 362-6	223
1632	Sequestration of the membrane-targeting myristoyl group of recoverin in the calcium-free state. <b>1995</b> , 376, 444-7	292
1631	Crystal structure of Thermus aquaticus DNA polymerase. <b>1995</b> , 376, 612-6	332
1630	Structure at 2.8 A resolution of cytochrome c oxidase from Paracoccus denitrificans. <b>1995</b> , 376, 660-9	2027
1629	Three-dimensional structure of the catalytic subunit of protein serine/threonine phosphatase-1. <b>1995</b> , 376, 745-53	751
1628	Crystal structure of a TFIIB-TBP-TATA-element ternary complex. <b>1995</b> , 377, 119-28	495
1627	A potential catalytic site revealed by the 1.7-A crystal structure of the amino-terminal signalling domain of Sonic hedgehog. <b>1995</b> , 378, 212-6	184
1626	Control of protein-ligand recognition using a stimuli-responsive polymer. <b>1995</b> , 378, 472-4	606
1625	Crystal structure of the RAR-gamma ligand-binding domain bound to all-trans retinoic acid. <b>1995</b> , 378, 681-9	1032
1624	Crystal structure of SIV matrix antigen and implications for virus assembly. <b>1995</b> , 378, 743-7	175

1623	A 35-A movement of smooth muscle myosin on ADP release. <b>1995</b> , 378, 748-51	365
1622	A ribosomal protein module in EF-G and DNA gyrase. <b>1995</b> , 2, 25-6	38
1621	The allosteric ligand site in the Vmax-type cooperative enzyme phosphoglycerate dehydrogenase. <b>1995</b> , 2, 69-76	214
1620	Neutron diffraction analysis of the solvent accessible volume in cubic insulin crystals. <b>1995</b> , 2, 77-80	9
1619	Structure of cytochrome P450eryF involved in erythromycin biosynthesis. <b>1995</b> , 2, 144-53	342
1618	What do dysfunctional serpins tell us about molecular mobility and disease?. <b>1995</b> , 2, 96-113	353
1617	Hormone binding site of corticosteroid binding globulin. <b>1995</b> , 2, 196-7	8
1616	A novel variant of the catalytic triad in the Streptomyces scabies esterase. <b>1995</b> , 2, 218-23	115
1615	Implications for viral uncoating from the structure of bovine enterovirus. <b>1995</b> , 2, 224-31	61
1614	Mutation of a buried residue causes loss of activity but no conformational change in the heat-labile enterotoxin of Escherichia coli. <b>1995</b> , 2, 269-72	23
1614		23
	enterotoxin of Escherichia coli. <b>1995</b> , 2, 269-72	
1613	enterotoxin of Escherichia coli. <b>1995</b> , 2, 269-72  Flexibility and function in HIV-1 protease. <b>1995</b> , 2, 274-80  The substrate-binding site in Cu nitrite reductase and its similarity to Zn carbonic anhydrase. <b>1995</b> ,	216
1613 1612 1611	enterotoxin of Escherichia coli. <b>1995</b> , 2, 269-72  Flexibility and function in HIV-1 protease. <b>1995</b> , 2, 274-80  The substrate-binding site in Cu nitrite reductase and its similarity to Zn carbonic anhydrase. <b>1995</b> , 2, 287-92	216 56
1613 1612 1611	Elexibility and function in HIV-1 protease. 1995, 2, 274-80  The substrate-binding site in Cu nitrite reductase and its similarity to Zn carbonic anhydrase. 1995, 2, 287-92  Mechanism of inhibition of HIV-1 reverse transcriptase by non-nucleoside inhibitors. 1995, 2, 303-8  A mosquitocidal toxin with a ricin-like cell-binding domain. 1995, 2, 358-9	<ul><li>216</li><li>56</li><li>381</li></ul>
1613 1612 1611 1610	enterotoxin of Escherichia coli. 1995, 2, 269-72  Flexibility and function in HIV-1 protease. 1995, 2, 274-80  The substrate-binding site in Cu nitrite reductase and its similarity to Zn carbonic anhydrase. 1995, 2, 287-92  Mechanism of inhibition of HIV-1 reverse transcriptase by non-nucleoside inhibitors. 1995, 2, 303-8  A mosquitocidal toxin with a ricin-like cell-binding domain. 1995, 2, 358-9	<ul><li>216</li><li>56</li><li>381</li><li>35</li></ul>
1613 1612 1611 1610	Elexibility and function in HIV-1 protease. 1995, 2, 274-80  The substrate-binding site in Cu nitrite reductase and its similarity to Zn carbonic anhydrase. 1995, 2, 287-92  Mechanism of inhibition of HIV-1 reverse transcriptase by non-nucleoside inhibitors. 1995, 2, 303-8  A mosquitocidal toxin with a ricin-like cell-binding domain. 1995, 2, 358-9  Novel metal-binding proteins by design. 1995, 2, 368-73  NMR structures of phospholipase A2 reveal conformational changes during interfacial activation.	<ul><li>216</li><li>56</li><li>381</li><li>35</li><li>87</li></ul>

1605 A common protein fold and similar active site in two distinct families of beta-glycanases. <b>1995</b> , 2, 569-76	136
Intrinsic phi, psi propensities of amino acids, derived from the coil regions of known structures.  1604 1995, 2, 596-603	202
The structural basis of aspirin activity inferred from the crystal structure of inactivated prostaglandin H2 synthase. <b>1995</b> , 2, 637-43	390
1602 An enzyme-substrate complex involved in bacterial cell wall biosynthesis. <b>1995</b> , 2, 644-53	67
1601 Residues defining V beta specificity in staphylococcal enterotoxins. <b>1995</b> , 2, 680-6	53
1600 One-step evolution of a dimer from a monomeric protein. <b>1995</b> , 2, 746-51	95
Nucleotide mimicry in the crystal structure of the uracil-DNA glycosylase-uracil glycosylase inhibitor protein complex. <b>1995</b> , 2, 752-7	82
1598 Solution structure of calcium-free calmodulin. <b>1995,</b> 2, 768-76	600
1597 The DNA-binding domain of HIV-1 integrase has an SH3-like fold. <b>1995</b> , 2, 807-10	210
1596 Watching protein folding unfold. <b>1995</b> , 2, 817-20	18
1596 Watching protein folding unfold. <b>1995</b> , 2, 817-20  1595 Eleven down and nine to go. <b>1995</b> , 2, 824-31	173
1595 Eleven down and nine to go. <b>1995</b> , 2, 824-31	173
Eleven down and nine to go. <b>1995</b> , 2, 824-31  1594 A disulphide-reinforced structural scaffold shared by small proteins with diverse functions. <b>1995</b> , 2, 835-7  Different enzymes with similar structures involved in Mg(2+)-mediated polynucleotidyl transfer.	173 30
Eleven down and nine to go. <b>1995</b> , 2, 824-31  1594 A disulphide-reinforced structural scaffold shared by small proteins with diverse functions. <b>1995</b> , 2, 835-7  Different enzymes with similar structures involved in Mg(2+)-mediated polynucleotidyl transfer. <b>1593 1995</b> , 2, 838-41	173 30 27
Eleven down and nine to go. <b>1995</b> , 2, 824-31  1594 A disulphide-reinforced structural scaffold shared by small proteins with diverse functions. <b>1995</b> , 2, 835-7  Different enzymes with similar structures involved in Mg(2+)-mediated polynucleotidyl transfer. <b>1995</b> , 2, 838-41  Following protein folding in real time using NMR spectroscopy. <b>1995</b> , 2, 865-70	173 30 27 184
Eleven down and nine to go. 1995, 2, 824-31  1594 A disulphide-reinforced structural scaffold shared by small proteins with diverse functions. 1995, 2, 835-7  Different enzymes with similar structures involved in Mg(2+)-mediated polynucleotidyl transfer. 1995, 2, 838-41  Following protein folding in real time using NMR spectroscopy. 1995, 2, 865-70  Structural basis of the stability of a lysozyme molten globule. 1995, 2, 871-5	173 30 27 184

1587	A plasmid-encoded dihydrofolate reductase from trimethoprim-resistant bacteria has a novel D2-symmetric active site. <b>1995</b> , 2, 1018-25	69
1586	Twixt form and function. <b>1995</b> , 2, 919-22	1
1585	NMR structure of an inhibitory R2 C-terminal peptide bound to mouse ribonucleotide reductase R1 subunit. <b>1995</b> , 2, 951-5	24
1584	Structural features of the epsilon subunit of the Escherichia coli ATP synthase determined by NMR spectroscopy. <b>1995</b> , 2, 961-7	150
1583	Ca(2+)-bridging mechanism and phospholipid head group recognition in the membrane-binding protein annexin V. <b>1995</b> , 2, 968-74	266
1582	Pseudospecific docking surfaces on electron transfer proteins as illustrated by pseudoazurin, cytochrome c550 and cytochrome cd1 nitrite reductase. <b>1995</b> , 2, 975-82	100
1581	Solution structure of a mammalian PCB-binding protein in complex with a PCB. <b>1995</b> , 2, 983-9	35
1580	A short linear peptide derived from the N-terminal sequence of ubiquitin folds into a water-stable non-native beta-hairpin. <b>1995</b> , 2, 999-1006	162
1579	Conformational variability in the refined structure of the chaperonin GroEL at 2.8 A resolution. <b>1995</b> , 2, 1083-94	207
1578	Ligand-induced distortion of an active site in thymidylate synthase upon binding anticancer drug 1843U89. <b>1995</b> , 2, 1095-101	39
1577	Three-dimensional structure of human lysosomal aspartylglucosaminidase. <b>1995</b> , 2, 1102-8	143
1576	Crystal structure of NADH oxidase from Thermus thermophilus. <b>1995</b> , 2, 1109-14	86
1575	Three-dimensional structure of the single-stranded DNA-binding protein encoded by gene V of the filamentous bacteriophage M13 and a model of its complex with single-stranded DNA. <b>1995</b> , 17, 57-72	4
1574	Fibrillin domain folding and calcium binding: significance to Marfan syndrome. <b>1995</b> , 2, 91-7	28
1573	An algorithm for smoothly tessellating beta-sheet structures in proteins. <b>1995</b> , 13, 36-45, 58	
1572	XmMol: an X11 and motif program for macromolecular visualization and modeling. <b>1995</b> , 13, 67-72, 62	26
1571	Methods for displaying macromolecular structural uncertainty: application to the globins. <b>1995</b> , 13, 142-52, 109-2	11
1570	FOLD: integrated analysis and display of protein secondary structure. <b>1995</b> , 13, 377-84	3

1569	Adsorption of lysozyme and Hactalbumin on poly(styrenesulphonate) latices 1. Adsorption and desorption behaviour. <b>1995</b> , 4, 375-387	33
1568	Depletion and replacement of protein metal ligands. <b>1995</b> , 6, 411-8	33
1567	New strategies in protein design. <b>1995</b> , 6, 460-6	32
1566	Active-site conformation of 17-(3-pyridyl)androsta-5,16-dien-3むl, a potent inhibitor of the P450 enzyme C17와droxylase/C17-20 lyase. <b>1995</b> , 5, 1125-1130	11
1565	Protein-protein interactions: a review of protein dimer structures. <b>1995</b> , 63, 31-65	444
1564	Peptidylproline cis/trans isomerases. <b>1995</b> , 63, 67-118	193
1563	Circular permutation of polypeptide chains: implications for protein folding and stability. <b>1995</b> , 64, 121-43	71
1562	Forces and factors that contribute to the structural stability of membrane proteins. <b>1995</b> , 1241, 295-322	86
1561	Sprouting side chain conformations. <b>1995</b> , 332, 183-186	
1560	Complementary roles of mutations at positions 69 and 242 in a class A beta-lactamase. <b>1995</b> , 1247, 113-20	21
1559	beta-Lactamase mutations far from the active site influence inhibitor binding. <b>1995</b> , 1247, 121-5	28
1558	Disruption of the disulfide bridge in azurin from Pseudomonas aeruginosa. <b>1995</b> , 1251, 48-54	20
1557	Crystallographic studies of elongation factor G. <b>1995</b> , 73, 1209-16	19
1556	Switching recognition of two tRNA synthetases with an amino acid swap in a designed peptide. <b>1995</b> , 267, 1994-6	35
1555	Structural analysis of the active site of porcine pancreatic elastase based on the X-ray crystal structures of complexes with trifluoroacetyl-dipeptide-anilide inhibitors. <b>1995</b> , 34, 3193-203	30
1554	Engineering recombinant antibodies for immunotherapy. <b>1995</b> , 27, 47-61	18
1553	Crystal structure and function of the isoniazid target of Mycobacterium tuberculosis. <b>1995</b> , 267, 1638-41	382
1552	Packaging of proteases and proteoglycans in the granules of mast cells and other hematopoietic cells. A cluster of histidines on mouse mast cell protease 7 regulates its binding to heparin serglycin proteoglycans. <b>1995</b> , 270, 19524-31	105

1551	Structural and functional characteristics of partially disulfide-reduced intermediates of ovotransferrin N lobe. Cystine localization by indirect end-labeling approach and implications for the reduction pathway. <b>1995</b> , 270, 29806-12	11
1550	Crystal structure and site-directed mutagenesis of Bacillus macerans endo-1,3-1,4-beta-glucanase. <b>1995</b> , 270, 3081-8	86
1549	Residues important for radical stability in ribonucleotide reductase from Escherichia coli. <b>1995</b> , 270, 6570-6	54
1548	Solvent effects on supercoiled DNA dynamics explored by Langevin dynamics simulations. <b>1995</b> , 51, 6188-620.	329
1547	Influence of constraints on the dynamics of polypeptide chains. <b>1995</b> , 52, 6868-6874	13
1546	Crystal structure of lac repressor core tetramer and its implications for DNA looping. <b>1995</b> , 268, 1721-7	272
1545	The Na+ binding site of thrombin. <b>1995</b> , 270, 22089-92	198
1544	Active site and oligosaccharide recognition residues of peptide-N4-(N-acetyl-beta-D-glucosaminyl)asparagine amidase F. <b>1995</b> , 270, 29493-7	23
1543	Dissociation of hexameric Escherichia coli inorganic pyrophosphatase into trimers on His-136>Gln or His-140>Gln substitution and its effect on enzyme catalytic properties. <b>1995</b> , 270, 30804-12	28
1542	A double mutant of sperm whale myoglobin mimics the structure and function of elephant myoglobin. <b>1995</b> , 270, 20763-74	60
1541	Spectroscopic and electrochemical studies on active-site transitions of the type 1 copper protein pseudoazurin from Achromobacter cycloclastes. <b>1995</b> , 270, 25733-8	67
1540	Stationary phase expression of a novel Escherichia coli outer membrane lipoprotein and its relationship with mammalian apolipoprotein D. Implications for the origin of lipocalins. <b>1995</b> , 270, 23097-103	60
1539	Extended-spectrum and inhibitor-resistant TEM-type beta-lactamases: mutations, specificity, and three-dimensional structure. <b>1995</b> , 39, 2593-601	283
1538	The use of graph theoretical methods for the comparison of the structures of biological macromolecules. <b>1995</b> , 73-103	6
1537	The structure of copper-nitrite reductase from Achromobacter cycloclastes at five pH values, with NO2- bound and with type II copper depleted. <b>1995</b> , 270, 27458-74	189
1536	Structural and functional analysis of the metal-binding sites of Clostridium thermocellum endoglucanase CelD. <b>1995</b> , 270, 9757-62	39
1535	Human hepatic and lipoprotein lipase: the loop covering the catalytic site mediates lipase substrate specificity. <b>1995</b> , 270, 25396-401	95
1534	Protein folding intermediates: native-state hydrogen exchange. <b>1995</b> , 269, 192-7	995

1533	Effects of two mutations detected in medium chain acyl-CoA dehydrogenase (MCAD)-deficient patients on folding, oligomer assembly, and stability of MCAD enzyme. <b>1995</b> , 270, 10284-90	69
1532	A Ca(2+)-binding chimera of human lysozyme and bovine alpha-lactalbumin that can form a molten globule. <b>1995</b> , 270, 10514-24	29
1531	Interleukin-6 (IL-6) antagonism by soluble IL-6 receptor alpha mutated in the predicted gp130-binding interface. <b>1995</b> , 270, 12242-9	31
1530	Protein determinants for specific polysialylation of the neural cell adhesion molecule. <b>1995</b> , 270, 17171-9	99
1529	A stable carbocyclic analog of 5-phosphoribosyl-1-pyrophosphate to probe the mechanism of catalysis and regulation of glutamine phosphoribosylpyrophosphate amidotransferase. <b>1995</b> , 270, 17394-9	11
1528	Reconstitution of Escherichia coli RNase HI from the N-fragment with high helicity and the C-fragment with a disordered structure. <b>1995</b> , 270, 19853-60	12
1527	Development of drug resistance to HIV-1 protease inhibitors. <b>1995</b> , 270, 29621-3	99
1526	Crystal structure of DNA photolyase from Escherichia coli. <b>1995</b> , 268, 1866-72	466
1525	Architectures of class-defining and specific domains of glutamyl-tRNA synthetase. <b>1995</b> , 267, 1958-65	130
1524	Crystal structure of the T4 regA translational regulator protein at 1.9 A resolution. <b>1995</b> , 268, 1170-3	26
1523	Crystal structure of a conserved protease that binds DNA: the bleomycin hydrolase, Gal6. <b>1995</b> , 269, 945-50	113
1522	The X-ray Crystal Structure of the Sulfonated Azo Dye Congo Red, a Non-Peptidic Inhibitor of HIV-1 Protease which also Binds to Reverse Transcriptase and Amyloid Proteins. <b>1995</b> , 6, 25-33	37
1521	Crystal structure of the mammalian Grb2 adaptor. <b>1995</b> , 268, 291-3	179
1520	Specific DNA-RNA hybrid binding by zinc finger proteins. <b>1995</b> , 268, 282-4	80
1519	Interhelical angles in the solution structure of the oligomerization domain of p53: correction. <b>1995</b> , 267, 1515-6	66
1518	Modeling of a possible conformational change associated with the catalytic mechanism in the hammerhead ribozyme. <b>1995</b> , 13, 515-22	11
1517	Crystal structure of Asian elephant (Elephas maximus) cyano-metmyoglobin at 1.78-A resolution. Phe29(B10) accounts for its unusual ligand binding properties. <b>1995</b> , 270, 20754-62	40
1516	Site-directed Mutagenesis of Human Glutathione Transferase P1-1. <b>1995</b> , 270, 1249-1253	67

1515	Crystallographic evidence for dimerization of unliganded tumor necrosis factor receptor. <b>1995</b> , 270, 13303-7	144
1514	NMR, molecular modeling, and crystallographic studies of lentil lectin-sucrose interaction. <b>1995</b> , 270, 25619-28	59
1513	Intrasteric regulation of myosin light chain kinase. <b>1995</b> , 270, 16848-53	34
1512	Structure of a hyperthermophilic tungstopterin enzyme, aldehyde ferredoxin oxidoreductase. <b>1995</b> , 267, 1463-9	513
1511	Calmodulin binding of a peptide derived from the regulatory domain of Bordetella pertussis adenylate cyclase. <b>1995</b> , 270, 7088-96	20
1510	Combining two mutations of human interleukin-6 that affect gp130 activation results in a potent interleukin-6 receptor antagonist on human myeloma cells. <b>1995</b> , 270, 8158-63	41
1509	An L40C mutation converts the cysteine-sulfenic acid redox center in enterococcal NADH peroxidase to a disulfide. <b>1995</b> , 34, 5180-90	20
1508	The Arg7Lys mutant of heat-labile enterotoxin exhibits great flexibility of active site loop 47-56 of the A subunit. <b>1995</b> , 34, 10996-1004	31
1507	Molecular dynamics simulation of cytochrome b5: implications for protein-protein recognition. <b>1995</b> , 34, 9682-93	65
1506	Mechanism of phosphate transfer by nucleoside diphosphate kinase: X-ray structures of the phosphohistidine intermediate of the enzymes from Drosophila and Dictyostelium. <b>1995</b> , 34, 11062-11070	107
1505	Discontinuous equilibrium titrations of cooperative calcium binding to calmodulin monitored by 1-D 1H-nuclear magnetic resonance spectroscopy. <b>1995</b> , 34, 10676-89	48
1504	Binding of cephalothin and cefotaxime to D-ala-D-ala-peptidase reveals a functional basis of a natural mutation in a low-affinity penicillin-binding protein and in extended-spectrum beta-lactamases. <b>1995</b> , 34, 9532-40	100
1503	Effects of C-terminal deletions on the conformational state and denaturation of phosphoglycerate kinase. <b>1995</b> , 34, 7931-40	14
1502	Nature of the early folding intermediate of ribonuclease A. <b>1995</b> , 34, 4088-96	48
1501	Three-dimensional structure of galactose-1-phosphate uridylyltransferase from Escherichia coli at 1.8 A resolution. <b>1995</b> , 34, 11049-61	86
1501 1500	1.8 A resolution. <b>1995</b> , 34, 11049-61  Core domain of hirudin from the leech Hirudinaria manillensis: chemical synthesis, purification, and	86 36
	1.8 A resolution. <b>1995</b> , 34, 11049-61  Core domain of hirudin from the leech Hirudinaria manillensis: chemical synthesis, purification, and	

## (1995-1995)

1497	Mechanism of an ATP-dependent carboxylase, dethiobiotin synthetase, based on crystallographic studies of complexes with substrates and a reaction intermediate. <b>1995</b> , 34, 10985-95	54
1496	Structure and stability of monomeric lambda repressor: NMR evidence for two-state folding. <b>1995</b> , 34, 3884-92	87
1495	Characterization of metal binding by a designed protein: single ligand substitutions at a tetrahedral Cys2His2 site. <b>1995</b> , 34, 10094-100	67
1494	Episelection: novel Ki approximately nanomolar inhibitors of serine proteases selected by binding or chemistry on an enzyme surface. <b>1995</b> , 34, 8264-80	95
1493	X-ray crystal structure of the soybean agglutinin cross-linked with a biantennary analog of the blood group I carbohydrate antigen. <b>1995</b> , 34, 4933-42	161
1492	FGF binding and FGF receptor activation by synthetic heparan-derived di- and trisaccharides. <b>1995</b> , 268, 432-6	272
1491	Pore loops: an emerging theme in ion channel structure. <b>1995</b> , 14, 889-92	227
1490	Structure and function of titin and nebulin. <b>1995</b> , 7, 32-8	63
1489	Ribosomal proteins and elongation factors. <b>1995</b> , 5, 721-7	49
1488	Protein phosphatases. <b>1995</b> , 5, 728-34	76
1487	Structure and function of restriction endonucleases. <b>1995</b> , 5, 11-9	170
1486	Structures of DNA and RNA polymerases and their interactions with nucleic acid substrates. <b>1995</b> , 5, 27-38	65
1485	Enzymes of nucleotide synthesis. <b>1995</b> , 5, 752-7	35
1484	DNA topoisomerases. <b>1995</b> , 5, 39-47	34
1483	Di-iron-carboxylate proteins. <b>1995</b> , 5, 758-66	240
1482	Cytochrome P450. <b>1995</b> , 5, 767-74	92
1481	Light-harvesting mechanisms in purple photosynthetic bacteria. <b>1995</b> , 5, 794-7	51
1480	Protein-peptide interactions. <b>1995</b> , 5, 103-13	146

1479	Antibody engineering. <b>1995</b> , 5, 450-6	15
1478	Superantigen engineering. <b>1995</b> , 5, 464-70	10
1477	Structures of bacterial immunoglobulin-binding domains and their complexes with immunoglobulins. <b>1995</b> , 5, 471-81	87
1476	Molecular mechanisms of protein-mediated membrane fusion. <b>1995</b> , 5, 507-13	36
1475	AB5 toxins. <b>1995</b> , 5, 165-71	251
1474	Modeling superhelical DNA: recent analytical and dynamic approaches. <b>1995</b> , 5, 245-62	134
1473	Structural features of a superfamily of zinc-endopeptidases: the metzincins. <b>1995</b> , 5, 383-90	182
1472	Pleckstrin homology domains: a fact file. <b>1995</b> , 5, 403-8	88
1471	Proteins with leucine-rich repeats. <b>1995</b> , 5, 409-16	334
1470	Rational drug design: a multidisciplinary approach. <b>1995</b> , 1, 31, 34	7
1470 1469	Rational drug design: a multidisciplinary approach. <b>1995</b> , 1, 31, 34  Major and minor epitopes on the self antigen mouse cytochrome c mapped by site-directed mutagenesis. <b>1995</b> , 32, 795-803	7
1469	Major and minor epitopes on the self antigen mouse cytochrome c mapped by site-directed	
1469	Major and minor epitopes on the self antigen mouse cytochrome c mapped by site-directed mutagenesis. <b>1995</b> , 32, 795-803	11
1469 1468	Major and minor epitopes on the self antigen mouse cytochrome c mapped by site-directed mutagenesis. <b>1995</b> , 32, 795-803  Unraveling the modular design of glutamate-gated ion channels. <b>1995</b> , 18, 161-8	233
1469 1468 1467	Major and minor epitopes on the self antigen mouse cytochrome c mapped by site-directed mutagenesis. 1995, 32, 795-803  Unraveling the modular design of glutamate-gated ion channels. 1995, 18, 161-8  Conformation of the propeptide domain of factor IX. 1995, 1245, 227-31  Structural evidence that the activation peptide is not released upon thrombin cleavage of factor	11 233 3
1469 1468 1467 1466	Major and minor epitopes on the self antigen mouse cytochrome c mapped by site-directed mutagenesis. 1995, 32, 795-803  Unraveling the modular design of glutamate-gated ion channels. 1995, 18, 161-8  Conformation of the propeptide domain of factor IX. 1995, 1245, 227-31  Structural evidence that the activation peptide is not released upon thrombin cleavage of factor XIII. 1995, 78, 389-97  Crystal structure of the cys2 activator-binding domain of protein kinase C delta in complex with	111 233 3 79
1469 1468 1467 1466	Major and minor epitopes on the self antigen mouse cytochrome c mapped by site-directed mutagenesis. 1995, 32, 795-803  Unraveling the modular design of glutamate-gated ion channels. 1995, 18, 161-8  Conformation of the propeptide domain of factor IX. 1995, 1245, 227-31  Structural evidence that the activation peptide is not released upon thrombin cleavage of factor XIII. 1995, 78, 389-97  Crystal structure of the cys2 activator-binding domain of protein kinase C delta in complex with phorbol ester. 1995, 81, 917-24  The structure of a Ca(2+)-binding epidermal growth factor-like domain: its role in protein-protein	111 233 3 79 606

## (1995-1995)

1461	Structure of the high affinity complex of inositol trisphosphate with a phospholipase C pleckstrin homology domain. <b>1995</b> , 83, 1037-46	557
1460	Mechanism of corepressor-mediated specific DNA binding by the purine repressor. <b>1995</b> , 83, 147-55	95
1459	Structure of the first C2 domain of synaptotagmin I: a novel Ca2+/phospholipid-binding fold. <b>1995</b> , 80, 929-38	613
1458	Crystal structure of the site-specific recombinase gamma delta resolvase complexed with a 34 bp cleavage site. <b>1995</b> , 82, 193-207	240
1457	Structure of the bacteriophage Mu transposase core: a common structural motif for DNA transposition and retroviral integration. <b>1995</b> , 82, 209-20	208
1456	Dissecting RNA-protein interactions: RNA-RNA recognition by Rop. <b>1995</b> , 80, 41-50	90
1455	Solution structure of the C-terminal core domain of human TFIIB: similarity to cyclin A and interaction with TATA-binding protein. <b>1995</b> , 82, 857-67	122
1454	Crystal structure of the replication terminator protein from B. subtilis at 2.6 A. <b>1995</b> , 80, 651-60	83
1453	Crystal structure of a purple acid phosphatase containing a dinuclear Fe(III)-Zn(II) active site. <b>1995</b> , 268, 1489-92	398
1452	Forces and factors that contribute to the structural stability of membrane proteins. <b>1995</b> , 1228, 1-27	127
1451	Molecular biology of nicotinamide nucleotide transhydrogenasea unique proton pump. <b>1995</b> , 1231, 1-19	65
1450	Modelling packing interactions in parallel helix bundles: pentameric bundles of nicotinic receptor M2 helices. <b>1995</b> , 1239, 122-32	11
1449	Conserved structural features on protein surfaces: small exterior hydrophobic clusters. <b>1995</b> , 249, 251-8	31
1448	A molecular model for the redox potential difference between thioredoxin and DsbA, based on electrostatics calculations. <b>1995</b> , 249, 376-87	67
1447	Isolation, crystallization, crystal structure analysis and refinement of allophycocyanin from the cyanobacterium Spirulina platensis at 2.3 A resolution. <b>1995</b> , 249, 424-40	201
1446	Angiography contrast agents interact with serine proteinases. The molecular structure of the model system elastase/iohexol. <b>1995</b> , 357, 247-50	6
1445	Secondary structure in solution of two anti-HIV-1 hammerhead ribozymes as investigated by two-dimensional 1H 500 MHz NMR spectroscopy in water. <b>1995</b> , 357, 317-23	7
1444	Specific arrangement of three amino acid residues for flavin-binding barrel structures in NADH-cytochrome b5 reductase and the other flavin-dependent reductases. <b>1995</b> , 361, 97-100	19

1443	Pulmonary surfactant-associated polypeptide SP-C in lipid micelles: CD studies of intact SP-C and NMR secondary structure determination of depalmitoyl-SP-C(1-17). <b>1995</b> , 362, 261-5	52
1442	Beta-glucosidase, beta-galactosidase, family A cellulases, family F xylanases and two barley glycanases form a superfamily of enzymes with 8-fold beta/alpha architecture and with two conserved glutamates near the carboxy-terminal ends of beta-strands four and seven. <b>1995</b> , 362, 281-5	211
1441	Atomic structure at 2.5 A resolution of uridine phosphorylase from E. coli as refined in the monoclinic crystal lattice. <b>1995</b> , 367, 183-7	40
1440	Complement assembly of two fragments of the streptococcal protein G B1 domain in aqueous solution. <b>1995</b> , 366, 99-103	55
1439	Structural relationship between the mammalian Fe(III)-Fe(II) and the Fe(III)-Zn(II) plant purple acid phosphatases. <b>1995</b> , 367, 56-60	76
1438	The Grb2 adaptor. <b>1995</b> , 369, 47-51	100
1437	Alteration in relative activities of phenylalanine dehydrogenase towards different substrates by site-directed mutagenesis. <b>1995</b> , 370, 93-6	23
1436	Characterization of in vitro oxidized barstar. <b>1995</b> , 370, 273-7	10
1435	A particularly labile Asp-Pro bond in the green mamba muscarinic toxin MTX2. Effect of protein conformation on the rate of cleavage. <b>1995</b> , 371, 171-5	19
1434	Trigger factor, one of the Escherichia coli chaperone proteins, is an original member of the FKBP family. <b>1995</b> , 374, 211-5	56
1433	Crystal structure of Bacillus licheniformis 1,3-1,4-beta-D-glucan 4-glucanohydrolase at 1.8 A resolution. <b>1995</b> , 374, 221-4	64
1432	Construction of a divalent cell adhesive lysozyme by introducing the Arg-Gly-Asp sequence at two sites. <b>1995</b> , 374, 262-4	1
1431	An antibody VH domain with a lox-Cre site integrated into its coding region: bacterial recombination within a single polypeptide chain. <b>1995</b> , 377, 92-6	110
1430	Crystal structure of an uncleaved alpha 1-antitrypsin reveals the conformation of its inhibitory reactive loop. <b>1995</b> , 377, 150-4	44
1429	Water-mediated conformational transitions in nicotinic receptor M2 helix bundles: a molecular dynamics study. <b>1995</b> , 377, 377-82	24
1428	Structural aspects of cytokine/receptor interactions. <b>1995</b> , 766, 253-62	7
1427	Structural characterization of the interaction between a pleckstrin homology domain and phosphatidylinositol 4,5-bisphosphate. <b>1995</b> , 34, 9859-64	111
1426	Protein secondary structure prediction. <b>2001</b> , Chapter 2, Unit2.3	1

1425 Structure of the calcium ion-bound gamma-carboxyglutamic acid-rich domain of factor IX. 1995, 34, 12126-37 87 Solution small-angle X-ray scattering study of the molecular chaperone Hsc70 and its 93 subfragments. 1995, 34, 12095-106 1423 Tertiary and quaternary structural changes in Gi alpha 1 induced by GTP hydrolysis. 1995, 270, 954-60 270 Crystal structure of the xanthine oxidase-related aldehyde oxido-reductase from D. gigas. 1995, 1422 435 270, 1170-6 1421 Crystal structure of the ternary complex of Phe-tRNAPhe, EF-Tu, and a GTP analog. 1995, 270, 1464-72 808 1420 Solution structure of the activator contact domain of the RNA polymerase alpha subunit. 1995, 270, 1495-7 161 1419 Structure, function, and inhibition of O6-alkylguanine-DNA alkyltransferase. 1995, 51, 167-223 350 Crystal structure of the biphenyl-cleaving extradiol dioxygenase from a PCB-degrading 1418 300 pseudomonad. 1995, 270, 976-80 Kalicludines and kaliseptine. Two different classes of sea anemone toxins for voltage sensitive K+ 1417 159 channels. 1995, 270, 25121-6 Vibrational Raman optical activity of lysozyme: hydrogen deuterium exchange, unfolding and 1416 22 ligand binding. 1995, 91, 2087-2093 The 1.6 A structure of Kunitz-type domain from the alpha 3 chain of human type VI collagen. 1995, 1415 16 246, 609-17 Three-dimensional structure of chemotactic che Y protein in aqueous solution by nuclear magnetic 1414 11 resonance methods. 1995, 247, 717-725 Three-dimensional structure of a lippyl domain from the dihydrolippyl acetyltransferase 1413 40 component of the pyruvate dehydrogenase multienzyme complex of Escherichia coli. 1995, 248, 328-43 1412 Structure and specificity of the anti-digoxin antibody 40-50. 1995, 248, 344-60 33 The refined crystal structure of an endochitinasefrom Hordeum vulgare L. seeds at 1.8 Desolution. 48 1411 **1995**, 248, 402-413 Energetics of protein-protein interactions: analysis of the barnase-barstar interface by single 1410 345 mutations and double mutant cycles. 1995, 248, 478-86 1409 High resolution structures of HIV-1 RT from four RT-inhibitor complexes. 1995, 2, 293-302 477 Conformation and function of the N-linked glycan in the adhesion domain of human CD2. 1995, 1408 297 269, 1273-8

1407	Comparative protein modeling by satisfaction of spatial restraints. <b>1995</b> , 1, 270-7	179
1406	Structural determinants of protein dynamics: analysis of 15N NMR relaxation measurements for main-chain and side-chain nuclei of hen egg white lysozyme. <b>1995</b> , 34, 4041-55	197
1405	Mapping T cell recognition: the identification of a T cell receptor residue critical to the specific interaction with an influenza hemagglutinin peptide. <b>1995</b> , 25, 1654-62	31
1404	Protein design: a hierarchic approach. <b>1995</b> , 270, 935-41	509
1403	Crystal structure of the 20S proteasome from the archaeon T. acidophilum at 3.4 A resolution. <b>1995</b> , 268, 533-9	1402
1402	Structure of Alcaligenes faecalis nitrite reductase and a copper site mutant, M150E, that contains zinc. <b>1995</b> , 34, 12107-17	92
1401	DNA binding specificity of the basic-helix-loop-helix protein MASH-1. <b>1995</b> , 34, 11026-36	36
1400	Crystal structure of Pseudomonas mevalonii HMG-CoA reductase at 3.0 angstrom resolution. <b>1995</b> , 268, 1758-62	88
1399	Three-dimensional structure of bacterial luciferase from Vibrio harveyi at 2.4 A resolution. <b>1995</b> , 34, 6581-6	102
1398	Transforming growth factor beta 1: three-dimensional structure in solution and comparison with the X-ray structure of transforming growth factor beta 2. <b>1996</b> , 35, 8517-34	149
1397	Toward identification of acid/base catalysts in the active site of enolase: comparison of the properties of K345A, E168Q, and E211Q variants. <b>1996</b> , 35, 1692-9	61
1396	Enzymatic C-C bond formation in asymmetric synthesis. <b>1996</b> , 97-194	102
1395	X-ray crystallographic studies of eukaryotic transcription initiation factors. <b>1996</b> , 351, 483-9	8
1394	A carboxylate oxygen of the substrate bridges the magnesium ions at the active site of enolase: structure of the yeast enzyme complexed with the equilibrium mixture of 2-phosphoglycerate and phosphoenolpyruvate at 1.8 A resolution. <b>1996</b> , 35, 4349-58	136
1393	Looking for residues involved in the muscle acylphosphatase catalytic mechanism and structural stabilization: role of Asn41, Thr42, and Thr46. <b>1996</b> , 35, 7077-83	46
1392	Motion of spin-labeled side chains in T4 lysozyme. Correlation with protein structure and dynamics. <b>1996</b> , 35, 7692-704	534
1391	Three-dimensional solution structure and 13C nuclear magnetic resonance assignments of the colicin E9 immunity protein Im9. <b>1996</b> , 35, 9505-12	50
1390	Crystal structure of diphtheria toxin bound to nicotinamide adenine dinucleotide. <b>1996</b> , 35, 1137-49	194

1389	The metzincin-superfamily of zinc-peptidases. <b>1996</b> , 389, 1-11	62
1388	Structure determination of the N-terminal thioredoxin-like domain of protein disulfide isomerase using multidimensional heteronuclear 13C/15N NMR spectroscopy. <b>1996</b> , 35, 7684-91	172
1387	Bacterial diversity based on type II DNA topoisomerase genes. <b>1996</b> , 30, 79-107	119
1386	Carbontarbon Bond Synthesis: The Impact of rDNA Technology on the Production and Use of E. coli Transketolase. <b>1996</b> , 782, 513-525	24
1385	A study of subunit interface residues of fructose-1,6-bisphosphatase by site-directed mutagenesis: effects on AMP and Mg2+ affinities. <b>1996</b> , 35, 7492-8	5
1384	Importance of two buried salt bridges in the stability and folding pathway of barnase. <b>1996</b> , 35, 6786-94	112
1383	Identification of an epitope in antithrombin appearing on insertion of the reactive-bond loop into the A beta-sheet. <b>1996</b> , 35, 10436-40	7
1382	Three-dimensional structure of meso-diaminopimelic acid dehydrogenase from Corynebacterium glutamicum. <b>1996</b> , 35, 13540-51	49
1381	NMR solution structure of a synthetic troponin C heterodimeric domain. <b>1996</b> , 35, 7429-38	16
1380	Tungstoenzymes. <b>1996</b> , 96, 2817-2840	302
1379	Core packing defects in an engineered Cro monomer corrected by combinatorial mutagenesis. <b>1996</b> , 35, 743-8	22
1378	Effects of mutations in plastocyanin on the kinetics of the protein rearrangement gating the electron-transfer reaction with zinc cytochrome c. Analysis of the rearrangement pathway. <b>1996</b> , 35, 16465-74	47
1377	X-ray crystallographic studies of alanine-65 variants of carbonic anhydrase II reveal the structural basis of compromised proton transfer in catalysis. <b>1996</b> , 35, 16429-34	42
1376	Solution conformation of the N-(deoxyguanosin-8-yl)-1-aminopyrene ([AP]dG) adduct opposite dC in a DNA duplex. <b>1996</b> , 35, 12659-70	50
1376 1375		50
	in a DNA duplex. <b>1996</b> , 35, 12659-70  Folding and functional complementation of engineered fragments from yeast phosphoglycerate	
1375	in a DNA duplex. <b>1996</b> , 35, 12659-70  Folding and functional complementation of engineered fragments from yeast phosphoglycerate kinase. <b>1996</b> , 35, 3465-76  Denaturation of Truncated Staphylococcal Nuclease in Molecular Dynamics Simulation at 300 K.	24

1371	D38 is an essential part of the proton translocation pathway in bacteriorhodopsin. <b>1996</b> , 35, 6635-43	112
1370	Metallopeptide Design: Tuning the Metal Cation Affinities with Unnatural Amino Acids and Peptide Secondary Structure. <b>1996</b> , 118, 11349-11356	83
1369	Three-dimensional structure of the inosine-uridine nucleoside N-ribohydrolase from Crithidia fasciculata. <b>1996</b> , 35, 5971-81	77
1368	Crystal structures of three misacylating mutants of Escherichia coli glutaminyl-tRNA synthetase complexed with tRNA(Gln) and ATP. <b>1996</b> , 35, 14725-33	31
1367	Structure of the N-terminal cellulose-binding domain of Cellulomonas fimi CenC determined by nuclear magnetic resonance spectroscopy. <b>1996</b> , 35, 14381-94	122
1366	Structure of a hydrophobically collapsed intermediate on the conformational folding pathway of ribonuclease A probed by hydrogen-deuterium exchange. <b>1996</b> , 35, 11734-46	56
1365	Intestinal fatty acid-binding protein: the structure and stability of a helix-less variant. <b>1996</b> , 35, 7553-8	59
1364	Solution structure of bovine angiogenin by 1H nuclear magnetic resonance spectroscopy. <b>1996</b> , 35, 8870-80	20
1363	Spectroscopic and mechanistic studies of type-1 and type-2 copper sites in Pseudomonas aeruginosa azurin as obtained by addition of external ligands to mutant His46Gly. <b>1996</b> , 35, 1397-407	52
1362	Influence of N-cap mutations on the structure and stability of Escherichia coli HPr. <b>1996</b> , 35, 11268-77	27
1361	Solution structure of the DNA-binding domain of a human papillomavirus E2 protein: evidence for flexible DNA-binding regions. <b>1996</b> , 35, 2095-103	62
1360	Site-directed mutagenesis of histidine 238 in mouse adenosine deaminase: substitution of histidine 238 does not impede hydroxylate formation. <b>1996</b> , 35, 15019-28	30
1359	Comparison of the functional differences for the homologous residues within the carboxy phosphate and carbamate domains of carbamoyl phosphate synthetase. <b>1996</b> , 35, 14362-9	33
1358	Aluminum fluoride inhibition of nitrogenase: stabilization of a nucleotide.Fe-protein.MoFe-protein complex. <b>1996</b> , 35, 5353-8	72
1357	Solution structure of horse heart ferricytochrome c and detection of redox-related structural changes by high-resolution 1H NMR. <b>1996</b> , 35, 12275-86	123
1356	The pKa of the general acid/base carboxyl group of a glycosidase cycles during catalysis: a 13C-NMR study of bacillus circulans xylanase. <b>1996</b> , 35, 9958-66	247
1355	The active-site histidine-10 of enterococcal NADH peroxidase is not essential for catalytic activity. <b>1996</b> , 35, 2380-7	28
1354	Crystal structure of the complex of UMP/CMP kinase from Dictyostelium discoideum and the bisubstrate inhibitor P1-(5'-adenosyl) P5-(5'-uridyl) pentaphosphate (UP5A) and Mg2+ at 2.2 A: implications for water-mediated specificity. <b>1996</b> , 35, 9716-27	82

1353	Deletions in the interdomain hinge region of flavocytochrome b2: effects on intraprotein electron transfer. <b>1996</b> , 35, 891-9	25
1352	Synthesis and use of iodinated nonsteroidal antiinflammatory drug analogs as crystallographic probes of the prostaglandin H2 synthase cyclooxygenase active site. <b>1996</b> , 35, 7330-40	161
1351	Ionophore 4-BrA23187 transports Zn2+ and Mn2+ with high selectivity over Ca2+. <b>1996</b> , 35, 13817-25	38
1350	Three-dimensional structure of the zinc-containing phosphotriesterase with the bound substrate analog diethyl 4-methylbenzylphosphonate. <b>1996</b> , 35, 6020-5	237
1349	X-ray structure of the magnesium(II).ADP.vanadate complex of the Dictyostelium discoideum myosin motor domain to 1.9 A resolution. <b>1996</b> , 35, 5404-17	504
1348	Backbone dynamics of the c-Jun leucine zipper: 15N NMR relaxation studies. <b>1996</b> , 35, 4867-77	50
1347	Crystal structures of the binary and ternary complexes of 7 alpha-hydroxysteroid dehydrogenase from Escherichia coli. <b>1996</b> , 35, 7715-30	212
1346	Nucleated Antiparallel	60
1345	Structure of chymopapain at 1.7 A resolution. <b>1996</b> , 35, 16292-8	46
1344	Functional and structural roles of the highly conserved Trp120 loop region of glucoamylase from Aspergillus awamori. <b>1996</b> , 35, 3050-8	15
1343	Reversal of the hydrogen bond to zinc ligand histidine-119 dramatically diminishes catalysis and enhances metal equilibration kinetics in carbonic anhydrase II. <b>1996</b> , 35, 3439-46	98
1342	High-resolution structure of the diphtheria toxin repressor complexed with cobalt and manganese reveals an SH3-like third domain and suggests a possible role of phosphate as co-corepressor. <b>1996</b> , 35, 12292-302	79
1341	Structure of Synechococcus elongatus [Fe2S2] ferredoxin in solution. <b>1996</b> , 35, 12831-41	42
1340	The structure of nucleotidylated histidine-166 of galactose-1-phosphate uridylyltransferase provides insight into phosphoryl group transfer. <b>1996</b> , 35, 11560-9	76
1339	Solution structure of prokaryotic ribosomal protein S17 by high-resolution NMR spectroscopy. <b>1996</b> , 35, 2845-53	41
1338	Ligand binding and affinity modulation of integrins. <b>1996</b> , 74, 785-98	37
1337	Three-dimensional models for agonist and antagonist complexes with beta 2 adrenergic receptor. <b>1996</b> , 39, 4406-20	34
1336	Structure of the LexA repressor-DNA complex probed by affinity cleavage and affinity photo-cross-linking. <b>1996</b> , 35, 4279-86	19

1335	Solution structure of reduced plastocyanin from the blue-green alga Anabaena variabilis. <b>1996</b> , 35, 7021-31	73
1334	Hydrophobic interactions control zymogen activation in the trypsin family of serine proteases. <b>1996</b> , 35, 4515-23	96
1333	Effect of the interdomain basic region of cytochrome f on its redox reactions in vivo. <b>1996</b> , 35, 14590-8	78
1332	Crystal structure of the hypoxanthine-guanine-xanthine phosphoribosyltransferase from the protozoan parasite Tritrichomonas foetus. <b>1996</b> , 35, 7032-40	97
1331	The role of Glu 57 in the mechanism of the Escherichia coli MutT enzyme by mutagenesis and heteronuclear NMR. <b>1996</b> , 35, 6715-26	51
1330	Covalent reinforcement of a fragile region in the dimeric enzyme thymidylate synthase stabilizes the protein against chaotrope-induced unfolding. <b>1996</b> , 35, 7150-8	14
1329	Three-dimensional solution structure of mu-conotoxin GIIIB, a specific blocker of skeletal muscle sodium channels. <b>1996</b> , 35, 8824-35	93
1328	Solution structure of the IIB domain of the glucose transporter of Escherichia coli. <b>1996</b> , 35, 11286-92	46
1327	Photoreactivity of platinum(II) in cisplatin-modified DNA affords specific cross-links to HMG domain proteins. <b>1996</b> , 35, 2180-8	55
1326	Bis-methionine ligation to heme iron in mutants of cytochrome b562. 2. Characterization by NMR of heme-ligand interactions. <b>1996</b> , 35, 13627-35	20
1325	Acid-induced molten globule state of a fully active mutant of human interleukin-6. <b>1996</b> , 35, 11503-11	31
1324	Determinants of cofactor specificity in isocitrate dehydrogenase: structure of an engineered NADP+> NAD+ specificity-reversal mutant. <b>1996</b> , 35, 5670-8	79
1323	Testing the correlation between delta A and delta V of protein unfolding using m value mutants of staphylococcal nuclease. <b>1996</b> , 35, 10234-9	53
1322	Structure of the R65Q mutant of yeast 3-phosphoglycerate kinase complexed with Mg-AMP-PNP and 3-phospho-D-glycerate. <b>1996</b> , 35, 4118-27	43
1321	A zinc binding site in viral serine proteinases. <b>1996</b> , 35, 13282-7	90
1320	Structure of 4-chlorobenzoyl coenzyme A dehalogenase determined to 1.8 A resolution: an enzyme catalyst generated via adaptive mutation. <b>1996</b> , 35, 8103-9	156
1319	A model for the photosystem II reaction center core including the structure of the primary donor P680. <b>1996</b> , 35, 14486-502	201
1318	Molecular structure, conformational analysis, and structure-activity studies of Dendrotoxin and its homologues using molecular mechanics and molecular dynamics techniques. <b>1996</b> , 39, 2141-55	17

1317	Crystallographic complexes of glucoamylase with maltooligosaccharide analogs: relationship of stereochemical distortions at the nonreducing end to the catalytic mechanism. <b>1996</b> , 35, 8319-28	94
1316	Nuclear magnetic resonance solution structure of the growth factor receptor-bound protein 2 Src homology 2 domain. <b>1996</b> , 35, 11852-64	24
1315	A pseudo-michaelis quaternary complex in the reverse reaction of a ligase: structure of Escherichia coli B glutathione synthetase complexed with ADP, glutathione, and sulfate at 2.0 A resolution. <b>1996</b> , 35, 11967-74	63
1314	The relative orientation of Gla and EGF domains in coagulation factor X is altered by Ca2+ binding to the first EGF domain. A combined NMR-small angle X-ray scattering study. <b>1996</b> , 35, 11547-59	76
1313	Three-dimensional structure of the immunophilin-like domain of FKBP59 in solution. <b>1996</b> , 35, 11045-52	43
1312	Structural and functional significance of aspartic acid 89 of the troponin C central helix in Ca2+ signaling. <b>1996</b> , 35, 15515-21	12
1311	Heteronuclear (1H, 13C, 15N) NMR assignments and solution structure of the monocyte chemoattractant protein-1 (MCP-1) dimer. <b>1996</b> , 35, 6569-84	155
1310	Understanding the binding of 5-substituted 2'-deoxyuridine substrates to thymidine kinase of herpes simplex virus type-1. <b>1996</b> , 39, 4727-37	34
1309	Structural and energetic responses to cavity-creating mutations in hydrophobic cores: observation of a buried water molecule and the hydrophilic nature of such hydrophobic cavities. <b>1996</b> , 35, 4298-305	145
1308	The high-resolution crystal structure of human annexin III shows subtle differences with annexin V. <b>1996</b> , 35, 1740-4	68
1307	Engineering stabilized ion channels: covalent dimers of alamethicin. <b>1996</b> , 35, 6225-32	74
1306	A flexible loop at the dimer interface is a part of the active site of the adjacent monomer of Escherichia coli orotate phosphoribosyltransferase. <b>1996</b> , 35, 3803-9	72
1305	Structure of the Fusarium oxysporum endoglucanase I with a nonhydrolyzable substrate analogue: substrate distortion gives rise to the preferred axial orientation for the leaving group. <b>1996</b> , 35, 15280-7	227
1304	Real-time refolding studies of 6-19F-tryptophan labeled Escherichia coli dihydrofolate reductase using stopped-flow NMR spectroscopy. <b>1996</b> , 35, 16843-51	57
1303	Solution conformation of the (-)-cis-anti-benzo[a]pyrenyl-dG adduct opposite dC in a DNA duplex: intercalation of the covalently attached BP ring into the helix with base displacement of the modified deoxyguanosine into the major groove. <b>1996</b> , 35, 9850-63	83
1302	Crystal structure of phosphatidylinositol-specific phospholipase C from Bacillus cereus in complex with glucosaminyl(alpha 1>6)-D-myo-inositol, an essential fragment of GPI anchors. <b>1996</b> , 35, 9496-504	52
1301	Characterization of the metal ion binding helix-hairpin-helix motifs in human DNA polymerase beta by X-ray structural analysis. <b>1996</b> , 35, 12778-87	80
1300	Side chain packing of the N- and C-terminal helices plays a critical role in the kinetics of cytochrome c folding. <b>1996</b> , 35, 5538-49	157

1299	The [4Fe-4S] cluster domain of the nitrogenase iron protein facilitates conformational changes required for the cooperative binding of two nucleotides. <b>1996</b> , 35, 15654-62	7
1298	Involvement of the carboxyl groups of glutathione in the catalytic mechanism of human glutathione transferase A1-1. <b>1996</b> , 35, 7731-42	76
1297	Covalent binding of three epoxyalkyl xylosides to the active site of endo-1,4-xylanase II from Trichoderma reesei. <b>1996</b> , 35, 9617-24	81
1296	An essential role for water in an enzyme reaction mechanism: the crystal structure of the thymidylate synthase mutant E58Q. <b>1996</b> , 35, 16270-81	35
1295	Dynamic structure of the calmodulin-binding domain of the plasma membrane Ca-ATPase in native erythrocyte ghost membranes. <b>1996</b> , 35, 12015-28	27
1294	Structural consequences of heme removal: molecular dynamics simulations of rat and bovine apocytochrome b5. <b>1996</b> , 35, 11596-604	31
1293	ATP-binding site of human brain hexokinase as studied by molecular modeling and site-directed mutagenesis. <b>1996</b> , 35, 13157-64	45
1292	A symmetry-driven search for electrostatic interaction partners in charybdotoxin and a voltage-gated K+ channel. <b>1996</b> , 35, 6181-7	32
1291	Synthesis and Conformational Preferences of a Potential beta-Sheet Nucleator Based on the 9,9-Dimethylxanthene Skeleton. <b>1996</b> , 61, 7408-7414	25
1290	Orientation of tryptophan-26 in coat protein subunits of the filamentous virus Ff by polarized Raman microspectroscopy. <b>1996</b> , 35, 10403-10	52
1289	Molecular structure of the NADH/UDP-glucose abortive complex of UDP-galactose 4-epimerase from Escherichia coli: implications for the catalytic mechanism. <b>1996</b> , 35, 5137-44	142
1288	Small molecule interactions with protein-tyrosine phosphatase PTP1B and their use in inhibitor design. <b>1996</b> , 35, 15989-96	126
1287	Crystallographic identification of metal-binding sites in Escherichia coli inorganic pyrophosphatase. <b>1996</b> , 35, 4670-7	58
1286	Towards an understanding of protein-DNA recognition. <b>1996</b> , 351, 501-9	54
1285	Thermodynamic properties of an extremely rapid protein folding reaction. <b>1996</b> , 35, 16833-42	143
1284	Heme-CO binding to tryptophan-containing calmodulin mutants. <b>1996</b> , 1313, 209-16	1
1283	Structural basis of autoimmunity against G protein coupled membrane receptors. <b>1996</b> , 54, 103-11	46
1282	The serum albumin-binding domain of streptococcal protein G is a three-helical bundle: a heteronuclear NMR study. <b>1996</b> , 378, 190-4	54

1281	Tailoring echistatin to possess higher affinity for integrin alpha(IIb)beta(3). <b>1996</b> , 387, 11-15	22
1280	The allosteric regulation of pyruvate kinase. <b>1996</b> , 389, 15-9	92
1279	Crystal structure of macrophage migration inhibitory factor from human lymphocyte at 2.1 A resolution. <b>1996</b> , 389, 145-8	47
1278	Cloning and sequencing of winged bean (Psophocarpus tetragonolobus) basic agglutinin (WBA I): presence of second glycosylation site and its implications in quaternary structure. <b>1996</b> , 389, 289-92	10
1277	The three-dimensional structure of capsule-specific CMP: 2-keto-3-deoxy-manno-octonic acid synthetase from Escherichia coli. <b>1996</b> , 391, 157-61	23
1276	The role of the T-loop of the signal transducing protein PII from Escherichia coli. <b>1996</b> , 391, 223-8	43
1275	Amino acid sequence and crystal structure of buffalo alpha-lactalbumin. <b>1996</b> , 394, 91-5	22
1274	Site-directed mutagenesis of azurin from Pseudomonas aeruginosa enhances the formation of an electron-transfer complex with a copper-containing nitrite reductase from Alcaligenes faecalis S-6. <b>1996</b> , 394, 87-90	23
1273	Structural characterization of a monomeric chemokine: monocyte chemoattractant protein-3. <b>1996</b> , 395, 277-82	57
1272	Three-dimensional structure of glutathione S-transferase from Arabidopsis thaliana at 2.2 A resolution: structural characterization of herbicide-conjugating plant glutathione S-transferases and a novel active site architecture. <b>1996</b> , 255, 289-309	189
1271	Crystal structures of adenylosuccinate synthetase from Escherichia coli complexed with GDP, IMP hadacidin, NO3-, and Mg2+. <b>1996</b> , 264, 1013-27	43
1270	Mechanism of ribonuclease inhibition by ribonuclease inhibitor protein based on the crystal structure of its complex with ribonuclease A. <b>1996</b> , 264, 1028-43	177
1269	Crystal structure of Arabidopsis thaliana NADPH dependent thioredoxin reductase at 2.5 A resolution. <b>1996</b> , 264, 1044-57	90
1268	Ribosomal protein L9: a structure determination by the combined use of X-ray crystallography and NMR spectroscopy. <b>1996</b> , 264, 1058-71	71
1267	Channelling of dioxygen into the respiratory enzyme. <b>1996</b> , 1275, 1-4	91
1266	Functional implications of the structure of the 'Rieske' iron-sulfur protein of bovine heart mitochondrial cytochrome bc1 complex. <b>1996</b> , 1275, 54-60	33
1265	Complexes of HIV-1 reverse transcriptase with inhibitors of the HEPT series reveal conformational changes relevant to the design of potent non-nucleoside inhibitors. <b>1996</b> , 39, 1589-600	326
1264	Local Structure in Spider Dragline Silk Investigated by Two-Dimensional Spin-Diffusion Nuclear Magnetic Resonance <b>1996</b> , 29, 2920-2928	229

1263	Covalent attachment of Arc repressor subunits by a peptide linker enhances affinity for operator DNA. <b>1996</b> , 35, 109-16	54
1262	Equilibrium stability and sub-millisecond refolding of a designed single-chain Arc repressor. <b>1996</b> , 35, 13878-84	59
1261	Fc receptors and their interactions with immunoglobulins. <b>1996</b> , 12, 181-220	246
1260	Inhibition of trypsin and thrombin by amino(4-amidinophenyl)methanephosphonate diphenyl ester derivatives: X-ray structures and molecular models. <b>1996</b> , 35, 3147-55	52
1259	Structural basis of light harvesting by carotenoids: peridinin-chlorophyll-protein from Amphidinium carterae. <b>1996</b> , 272, 1788-91	418
1258	Tumor marker disaccharide D-Gal-beta 1, 3-GalNAc complexed to heat-labile enterotoxin from Escherichia coli. <b>1996</b> , 5, 1184-8	25
1257	Conformational stability of apoflavodoxin. <b>1996</b> , 5, 1376-88	72
1256	Ligand binding: molecular mechanics calculation of the streptavidin-biotin rupture force. <b>1996</b> , 271, 997-9	751
1255	Crystal structures of guinea-pig, goat and bovine alpha-lactalbumin highlight the enhanced conformational flexibility of regions that are significant for its action in lactose synthase. <b>1996</b> , 4, 691-703	186
1254	The catalytic domain of human immunodeficiency virus integrase: ordered active site in the F185H mutant. <b>1996</b> , 398, 175-8	92
1253	Three-dimensional structure of a DNA repair enzyme, 3-methyladenine DNA glycosylase II, from Escherichia coli. <b>1996</b> , 86, 311-9	130
1252	Structure of the FGF receptor tyrosine kinase domain reveals a novel autoinhibitory mechanism. <b>1996</b> , 86, 577-87	347
1251	Solution structure of the link module: a hyaluronan-binding domain involved in extracellular matrix stability and cell migration. <b>1996</b> , 86, 767-75	264
1250	2.0 A crystal structure of a four-domain segment of human fibronectin encompassing the RGD loop and synergy region. <b>1996</b> , 84, 155-64	576
1249	Structural basis for the autoinhibition of calcium/calmodulin-dependent protein kinase I. <b>1996</b> , 84, 875-87	295
1248	The crystal structure of the DNA-binding domain of yeast RAP1 in complex with telomeric DNA. <b>1996</b> , 85, 125-36	269
1247	The 1.85 A structure of vaccinia protein VP39: a bifunctional enzyme that participates in the modification of both mRNA ends. <b>1996</b> , 85, 247-56	156
1246	Anatomy of a flexer-DNA complex inside a higher-order transposition intermediate. <b>1996</b> , 85, 761-71	105

1245	for the Marfan syndrome and other genetic disorders. <b>1996</b> , 85, 597-605	390
1244	Crystal structure of the conserved core of HIV-1 Nef complexed with a Src family SH3 domain. <b>1996</b> , 85, 931-42	399
1243	Tertiary structure of destrin and structural similarity between two actin-regulating protein families. <b>1996</b> , 85, 1047-55	132
1242	Crystal structures of a complexed and peptide-free membrane protein-binding domain: molecular basis of peptide recognition by PDZ. <b>1996</b> , 85, 1067-76	999
1241	A structural model for the HIV-1 Rev-RRE complex deduced from altered-specificity rev variants isolated by a rapid genetic strategy. <b>1996</b> , 87, 115-25	91
1240	Structure of the C-terminal region of p21(WAF1/CIP1) complexed with human PCNA. <b>1996</b> , 87, 297-306	665
1239	Crystal structure of human cyclophilin A bound to the amino-terminal domain of HIV-1 capsid. <b>1996</b> , 87, 1285-94	598
1238	The role of acidic residues of plastocyanin in its interaction with cytochrome []1996, 1277, 115-126	96
1237	Oxidative inactivation of thioredoxin as a cellular growth factor and protection by a Cys73>Ser mutation. <b>1996</b> , 52, 1741-7	58
1236	Structural analysis of ricin and implications for inhibitor design. <b>1996</b> , 34, 1325-34	18
1235	The C-terminal (haemopexin-like) domain structure of human gelatinase A (MMP2): structural implications for its function. <b>1996</b> , 378, 126-30	76
1234	A structure-based model for cytochrome P450cam-putidaredoxin interactions. <b>1996</b> , 78, 723-33	105
1233	The ternary complex of aminoacylated tRNA and EF-Tu-GTP. Recognition of a bond and a fold. <b>1996</b> , 78, 921-33	51
1232	Modulating the immunological properties of a linear B-cell epitope by insertion into permissive sites of the MalE protein. <b>1996</b> , 33, 1345-58	18
1231	The problem of protein folding and dynamics: time-resolved dynamic nonradiative excitation energy transfer measurements. <b>1996</b> , 2, 1088-1106	14
1230	Crystal structure of the lactose operon repressor and its complexes with DNA and inducer. <b>1996</b> , 271, 1247-54	686
1229	Structure of the [NiFe] Hydrogenase Active Site: Evidence for Biologically Uncommon Fe Ligands?. <b>1996</b> , 118, 12989-12996	579
1228	Specificity and kinetics of haloalkane dehalogenase. <b>1996</b> , 271, 14747-53	85

1227	Structure and function of fibronectin modules. <b>1996</b> , 15, 313-20; discussion 321	165
1226	Extracellular calcium-binding proteins. <b>1996</b> , 8, 609-17	80
1225	Structural and mechanistic studies of enolase. <b>1996</b> , 6, 736-43	71
1224	Protein-biotin interactions. <b>1996</b> , 6, 798-803	37
1223	Novel metal sites in protein structures. <b>1996</b> , 6, 804-12	22
1222	Structural classification of proteins: new superfamilies. <b>1996</b> , 6, 386-94	227
1221	Circular assemblies. <b>1996</b> , 6, 142-50	10
1220	Viruses. <b>1996</b> , 6, 151-6	8
1219	RNA-protein complexes. <b>1996</b> , 6, 53-61	163
1218	The TATA box binding protein. <b>1996</b> , 6, 69-75	75
1217	Retroviral integrases and their cousins. <b>1996</b> , 6, 76-83	
	Reciovital filtegrases and their cousins. 1990, 0, 70-03	192
1216	Portrait of a myristoyl switch protein. <b>1996</b> , 6, 432-8	192
1216 1215		
	Portrait of a myristoyl switch protein. <b>1996</b> , 6, 432-8  An altered position of the alpha 2 helix of MHC class I is revealed by the crystal structure of	122
1215	Portrait of a myristoyl switch protein. 1996, 6, 432-8  An altered position of the alpha 2 helix of MHC class I is revealed by the crystal structure of HLA-B*3501. 1996, 4, 203-13  Bound water structure and polymorphic amino acids act together to allow the binding of different	122
1215	Portrait of a myristoyl switch protein. 1996, 6, 432-8  An altered position of the alpha 2 helix of MHC class I is revealed by the crystal structure of HLA-B*3501. 1996, 4, 203-13  Bound water structure and polymorphic amino acids act together to allow the binding of different peptides to MHC class I HLA-B53. 1996, 4, 215-28	122 154 142
1215 1214 1213	Portrait of a myristoyl switch protein. 1996, 6, 432-8  An altered position of the alpha 2 helix of MHC class I is revealed by the crystal structure of HLA-B*3501. 1996, 4, 203-13  Bound water structure and polymorphic amino acids act together to allow the binding of different peptides to MHC class I HLA-B53. 1996, 4, 215-28  The (Greek) key to structures of neural adhesion molecules. 1996, 16, 261-73  Crystal structure of the extracellular domain from P0, the major structural protein of peripheral	122 154 142 96

1209	Oxidative modification of a carboxyl-terminal vicinal methionine in calmodulin by hydrogen peroxide inhibits calmodulin-dependent activation of the plasma membrane Ca-ATPase. <b>1996</b> , 35, 2767-87	133
1208	High-resolution solution structure of the EGF-like domain of heregulin-alpha. <b>1996</b> , 35, 3402-17	61
1207	Calcium-induced interactions of calmodulin domains revealed by quantitative thrombin footprinting of Arg37 and Arg106. <b>1996</b> , 35, 2943-57	56
1206	Phosphorus-31 nuclear magnetic resonance studies on coenzyme binding and specificity in glyceraldehyde-3-phosphate dehydrogenase. <b>1996</b> , 35, 6064-72	13
1205	Carbonic Anhydrase: Evolution of the Zinc Binding Site by Nature and by Design. 1996, 29, 331-339	422
1204	Review. <b>1996</b> , 377, 411-488	3
1203	Structure of the Escherichia coli response regulator NarL. <b>1996</b> , 35, 11053-61	279
1202	Crystal structure of soybean lipoxygenase L-1 at 1.4 A resolution. <b>1996</b> , 35, 10687-701	390
1201	Structural Basis of Biological Nitrogen Fixation. <b>1996</b> , 96, 2965-2982	897
1200	Anion binding by transferrins: importance of second-shell effects revealed by the crystal structure of oxalate-substituted diferric lactoferrin. <b>1996</b> , 35, 9007-13	41
1199	SOME NEW STRUCTURAL ASPECTS AND OLD CONTROVERSIES CONCERNING THE CYTOCHROME b6f COMPLEX OF OXYGENIC PHOTOSYNTHESIS. <b>1996</b> , 47, 477-508	163
1198	Thermodynamic analysis of a designed three-stranded coiled coil. <b>1996</b> , 35, 14480-5	81
1197	The 1.5-A resolution crystal structure of bacterial luciferase in low salt conditions. <b>1996</b> , 271, 21956-68	99
1196	Crystal structure of thermostable family 5 endocellulase E1 from Acidothermus cellulolyticus in complex with cellotetraose. <b>1996</b> , 35, 10648-60	223
1195	Dynamics of ribonuclease H: temperature dependence of motions on multiple time scales. <b>1996</b> , 35, 16009-23	183
1194	Structure of the heat shock protein chaperonin-10 of Mycobacterium leprae. <b>1996</b> , 271, 203-7	136
1193	Catalysis of amide proton exchange by the molecular chaperones GroEL and SecB. <b>1996</b> , 271, 642-5	136
1192	The galvanization of biology: a growing appreciation for the roles of zinc. <b>1996</b> , 271, 1081-5	1612

1191	Structural analysis of substrate binding by the molecular chaperone DnaK. <b>1996</b> , 272, 1606-14	1060
1190	Crystal structure of DMSO reductase: redox-linked changes in molybdopterin coordination. <b>1996</b> , 272, 1615-21	4 <sup>1</sup> 7
1189	Structure of the amino-terminal core domain of the HIV-1 capsid protein. <b>1996</b> , 273, 231-5	400
1188	Functional mimicry of a protein hormone by a peptide agonist: the EPO receptor complex at 2.8 A. <b>1996</b> , 273, 464-71	567
1187	Mapping the protein universe. <b>1996</b> , 273, 595-603	1305
1186	Organization of diphtheria toxin T domain in bilayers: a site-directed spin labeling study. <b>1996</b> , 273, 810-2	119
1185	Crystal structure of DNA recombination protein RuvA and a model for its binding to the Holliday junction. <b>1996</b> , 274, 415-21	151
1184	The crystal structure of a five-stranded coiled coil in COMP: a prototype ion channel?. <b>1996</b> , 274, 761-5	265
1183	Three-dimensional solution structure of Saccharomyces cerevisiae reduced iso-1-cytochrome c. <b>1996</b> , 35, 13788-96	85
1182	Homology modeling of the structure of bacterial acetohydroxy acid synthase and examination of the active site by site-directed mutagenesis. <b>1996</b> , 35, 16282-91	69
1181	Amide hydrogen exchange determined by mass spectrometry: application to rabbit muscle aldolase. <b>1996</b> , 35, 779-91	128
1180	dNTP binding site in rat DNA polymerase beta revealed by controlled proteolysis and azido photoprobe cross-linking. <b>1996</b> , 35, 3728-34	14
1179	Multipole-based calculation of the polarization energy. <b>1996</b> , 94, 287-295	2
1178	Kinetic mechanism of folding and unfolding of Rhodobacter capsulatus cytochrome c2. <b>1996</b> , 35, 16852-62	69
1177	Crystal structures of human DNA polymerase beta complexed with DNA: implications for catalytic mechanism, processivity, and fidelity. <b>1996</b> , 35, 12742-61	256
1176	Structure of 3 alpha-hydroxysteroid/dihydrodiol dehydrogenase complexed with NADP+. <b>1996</b> , 35, 10702-11	101
1175	Crystal structures of an NH2-terminal fragment of T4 DNA polymerase and its complexes with single-stranded DNA and with divalent metal ions. <b>1996</b> , 35, 8110-9	102
1174	Synthesis and structure determination by NMR of a putative vacuolar targeting peptide and model of a proteinase inhibitor from Nicotiana alata. <b>1996</b> , 35, 369-78	28

1173	Biochemical properties of mutant and wild-type fructose-1,6-bisphosphatases are consistent with the coupling of intra- and intersubunit conformational changes in the T- and R-state transition. <b>1996</b> , 271, 33301-7	20
1172	Crystal structure of an antagonist mutant of human growth hormone, G120R, in complex with its receptor at 2.9 A resolution. <b>1996</b> , 271, 32197-203	70
1171	Ferredoxin and ferredoxin-heme maquettes. <b>1996</b> , 93, 15041-6	166
1170	Identification of a binding site for integrin alphaEbeta7 in the N-terminal domain of E-cadherin. <b>1996</b> , 271, 30909-15	70
1169	Altered recognition mutants of the response regulator PhoB: a new genetic strategy for studying protein-protein interactions. <b>1996</b> , 93, 14361-6	53
1168	Systematic mutagenesis of the active site omega loop of TEM-1 beta-lactamase. <b>1996</b> , 178, 1821-8	78
1167	Studies on protein-protein interaction between copper-containing nitrite reductase and pseudoazurin from Alcaligenes faecalis S-6. <b>1996</b> , 271, 13680-3	49
1166	Functional implications of the three-dimensional structures of pectate lyases. <b>1996</b> , 14, 295-308	15
1165	New crystal form of ∉actoglobulin. <b>1996</b> , 63, 575-584	7
1164	Structure and distribution of modules in extracellular proteins. <b>1996</b> , 29, 119-67	266
1164	Structure and distribution of modules in extracellular proteins. <b>1996</b> , 29, 119-67  Molecular cloning of Drosophila mus308, a gene involved in DNA cross-link repair with homology to prokaryotic DNA polymerase I genes. <b>1996</b> , 16, 5764-71	266 113
1163	Molecular cloning of Drosophila mus308, a gene involved in DNA cross-link repair with homology to	
1163	Molecular cloning of Drosophila mus308, a gene involved in DNA cross-link repair with homology to prokaryotic DNA polymerase I genes. <b>1996</b> , 16, 5764-71	113
1163 1162 1161	Molecular cloning of Drosophila mus308, a gene involved in DNA cross-link repair with homology to prokaryotic DNA polymerase I genes. <b>1996</b> , 16, 5764-71  Determinants of DNA-binding specificity of ETS-domain transcription factors. <b>1996</b> , 16, 3338-49  Structure-function relationships among wild-type variants of Staphylococcus aureus	113
1163 1162 1161	Molecular cloning of Drosophila mus308, a gene involved in DNA cross-link repair with homology to prokaryotic DNA polymerase I genes. 1996, 16, 5764-71  Determinants of DNA-binding specificity of ETS-domain transcription factors. 1996, 16, 3338-49  Structure-function relationships among wild-type variants of Staphylococcus aureus beta-lactamase: importance of amino acids 128 and 216. 1996, 178, 7248-53	113 68 23
1163 1162 1161 1160	Molecular cloning of Drosophila mus308, a gene involved in DNA cross-link repair with homology to prokaryotic DNA polymerase I genes. 1996, 16, 5764-71  Determinants of DNA-binding specificity of ETS-domain transcription factors. 1996, 16, 3338-49  Structure-function relationships among wild-type variants of Staphylococcus aureus beta-lactamase: importance of amino acids 128 and 216. 1996, 178, 7248-53  Chaperone activity and structure of monomeric polypeptide binding domains of GroEL. 1996, 93, 15024-9	113 68 23
1163 1162 1161 1160	Molecular cloning of Drosophila mus308, a gene involved in DNA cross-link repair with homology to prokaryotic DNA polymerase I genes. 1996, 16, 5764-71  Determinants of DNA-binding specificity of ETS-domain transcription factors. 1996, 16, 3338-49  Structure-function relationships among wild-type variants of Staphylococcus aureus beta-lactamase: importance of amino acids 128 and 216. 1996, 178, 7248-53  Chaperone activity and structure of monomeric polypeptide binding domains of GroEL. 1996, 93, 15024-9  Crystal structure of the catalytic domain of avian sarcoma virus integrase. 1996, 7, 383-390	113 68 23

1155	The biostructural pathology of the serpins: critical function of sheet opening mechanism. <b>1996</b> , 377, 1-17	52
1154	NMR characterization and solution structure determination of the oxidized cytochrome c7 from Desulfuromonas acetoxidans. <b>1996</b> , 93, 14396-400	49
1153	New compatible solutes related to Di-myo-inositol-phosphate in members of the order Thermotogales. <b>1996</b> , 178, 5644-51	82
1152	Crystal structure of the secretory form of membrane-associated human carbonic anhydrase IV at 2.8-A resolution. <b>1996</b> , 93, 13589-94	134
1151	Crystal structure of the Aequorea victoria green fluorescent protein. <b>1996</b> , 273, 1392-5	1891
1150	Protein engineering studies of dichloromethane dehalogenase/glutathione S-transferase from Methylophilus sp. strain DM11. Ser12 but not Tyr6 is required for enzyme activity. <b>1996</b> , 239, 410-7	47
1149	Structure of the MDM2 oncoprotein bound to the p53 tumor suppressor transactivation domain. <b>1996</b> , 274, 948-53	1806
1148	Structure and function of Escherichia coli met repressor: similarities and contrasts with trp repressor. <b>1996</b> , 351, 527-35	16
1147	Density-Functional and Electrostatic Calculations for a Model of a Manganese Superoxide Dismutase Active Site in Aqueous Solution. <b>1996</b> , 100, 13498-13505	42
1146	A mechanism of drug action revealed by structural studies of enoyl reductase. <b>1996</b> , 274, 2107-10	214
1145	Transient magnetic resonance. Transient spin states in the primary processes of photosynthesis. <b>1996</b> , 100, 2028-2035	4
1144	Partitioning roles of side chains in affinity, orientation, and catalysis with structures for mutant complexes: asparagine-229 in thymidylate synthase. <b>1996</b> , 35, 5125-36	20
1144		20
	complexes: asparagine-229 in thymidylate synthase. <b>1996</b> , 35, 5125-36  Synthesis and structural characterisation of analogues of the potassium channel blocker	
1143	complexes: asparagine-229 in thymidylate synthase. <b>1996</b> , 35, 5125-36  Synthesis and structural characterisation of analogues of the potassium channel blocker charybdotoxin. <b>1996</b> , 1292, 31-8  Conformational analysis of pentapeptide sequences matching a proposed recognition motif for	6
1143 1142 1141	complexes: asparagine-229 in thymidylate synthase. 1996, 35, 5125-36  Synthesis and structural characterisation of analogues of the potassium channel blocker charybdotoxin. 1996, 1292, 31-8  Conformational analysis of pentapeptide sequences matching a proposed recognition motif for lysosomal degradation. 1996, 1293, 243-53  A homology model of the Id-3 helix-loop-helix domain as a basis for structure-function predictions.	6
1143 1142 1141	complexes: asparagine-229 in thymidylate synthase. 1996, 35, 5125-36  Synthesis and structural characterisation of analogues of the potassium channel blocker charybdotoxin. 1996, 1292, 31-8  Conformational analysis of pentapeptide sequences matching a proposed recognition motif for lysosomal degradation. 1996, 1293, 243-53  A homology model of the Id-3 helix-loop-helix domain as a basis for structure-function predictions. 1996, 1294, 138-46	6 3 25

1137	Low frequency motions in phosphoglycerate kinase. A normal mode analysis. <b>1996</b> , 204, 327-336	25
1136	Molecular properties of voltage-gated K+ channels. <b>1996</b> , 28, 231-53	98
1135	Genetically engineered superantigens in experimental tumor therapy. <b>1996</b> , 17, 397-410	2
1134	Peptide inhibitors of melittin action. <b>1996</b> , 15, 395-403	8
1133	Effect of mutations on the sensitivity of human beta-cell glucokinase to liver regulatory protein. <b>1996</b> , 39, 1173-9	38
1132	Viral cysteine proteinases. <b>1996</b> , 6, 64-86	85
1131	Evolutionary analysis of the multigene pregnancy-specific beta 1-glycoprotein family: separation of historical and nonhistorical signals. <b>1996</b> , 42, 273-80	11
1130	Structure and activity of a chimeric interleukin-8-melanoma-growth-stimulatory-activity protein. <b>1996</b> , 235, 26-35	6
1129	Pressure-tuning the conformation of bovine pancreatic trypsin inhibitor studied by Fourier-transform infrared spectroscopy. <b>1996</b> , 236, 254-62	67
1128	Surface location and orientation of the lantibiotic nisin bound to membrane-mimicking micelles of dodecylphosphocholine and of sodium dodecylsulphate. <b>1996</b> , 235, 394-403	70
1127	1H-NMR-derived secondary structure and the overall fold of the potent anti-mammal and anti-insect toxin III from the scorpion Leiurus quinquestriatus quinquestriatus. <b>1996</b> , 236, 395-404	36
1126	Lens crystallins of invertebratesdiversity and recruitment from detoxification enzymes and novel proteins. <b>1996</b> , 235, 449-65	113
1125	X-ray structure of native full-length human fibroblast-growth factor at 0.25-nm resolution. <b>1996</b> , 241, 453-61	19
1124	The crystal structure of transthyretin from chicken. <b>1996</b> , 236, 491-9	47
1123	The role of a trans-proline in the folding mechanism of ribonuclease T1. <b>1996</b> , 241, 516-24	11
1122	Oxygenic photosynthesis. Electron transfer in photosystem I and photosystem II. <b>1996</b> , 237, 519-31	73
1121	Hybrids of chicken cystatin with human kininogen domain 2 sequences exhibit novel inhibition of calpain, improved inhibition of actinidin and impaired inhibition of papain, cathepsin L and cathepsin B. <b>1996</b> , 235, 534-42	11
1120	Backbone dynamics of a domain of protein L which binds to immunoglobulin light chains. <b>1996</b> , 235, 543-8	13

1119	Backbone dynamics of the 269-residue protease Savinase determined from 15N-NMR relaxation measurements. <b>1996</b> , 235, 629-40	14
1118	Phosphate-binding sites in phosphorylating glyceraldehyde-3-phosphate dehydrogenase from Bacillus stearothermophilus. <b>1996</b> , 235, 641-7	21
1117	Solution structure of the DNA-binding domain of the tomato heat-stress transcription factor HSF24. <b>1996</b> , 236, 911-21	49
1116	Crystal structure of the bifunctional soybean Bowman-Birk inhibitor at 0.28-nm resolution. Structural peculiarities in a folded protein conformation. <b>1996</b> , 242, 122-31	77
1115	Analysis of the 1H-NMR chemical shifts of Cu(I)-, Cu(II)- and Cd-substituted pea plastocyanin. Metal-dependent differences in the hydrogen-bond network around the copper site. <b>1996</b> , 242, 132-47	42
1114	A site-directed mutagenesis study of Saccharomyces cerevisiae pyrophosphatase. Functional conservation of the active site of soluble inorganic pyrophosphatases. <b>1996</b> , 239, 138-43	48
1113	Crystal structure of flavodoxin from Desulfovibrio desulfuricans ATCC 27774 in two oxidation states. <b>1996</b> , 239, 190-6	34
1112	Molecular sequencing and modeling of Neobellieria bullata trypsin. Evidence for translational control by Neobellieria trypsin-modulating oostatic factor. <b>1996</b> , 237, 279-87	29
1111	The structure of the Aeromonas proteolytica aminopeptidase complexed with a hydroxamate inhibitor. Involvement in catalysis of Glu151 and two zinc ions of the co-catalytic unit. <b>1996</b> , 237, 393-8	112
1110	4-Hydroxybenzoate hydroxylase from Pseudomonas sp. CBS3. Purification, characterization, gene cloning, sequence analysis and assignment of structural features determining the coenzyme specificity. <b>1996</b> , 239, 469-78	30
1109	Conformational analysis of blood group A trisaccharide in solution and in the binding site of Dolichos biflorus lectin using transient and transferred nuclear Overhauser enhancement (NOE) and rotating-frame NOE experiments. <b>1996</b> , 239, 710-9	33
1108	Participation of two Ser-Ser-Phe-Tyr repeats in interleukin-6 (IL-6)-binding sites of the human IL-6 receptor. <b>1996</b> , 238, 714-23	24
1107	Ras and its effectors. <b>1996</b> , 66, 1-41	49
1106	Principles of membrane protein assembly and structure. <b>1996</b> , 66, 113-39	79
1105	Protein conformational substates from X-ray crystallography. <b>1996</b> , 66, 167-96	34
1104	The structure and activity of membrane receptors: computational simulation of histamine H2-receptor activation. <b>1996</b> , 371, 279-286	2
1103	The dynamics and binding of a Type III antifreeze protein in water and on ice. <b>1996</b> , 388, 65-77	13
1102	Lipoxygenase: a molecular complex with a non-heme iron. <b>1996</b> , 374, 47-52	

1101	Interactions between the components of the human NADPH oxidase: intrigues in the phox family. <b>1996</b> , 128, 461-76	98
1100	Structure-Based Calculations of the Optical Spectra of the LH2 Bacteriochlorophyll-Protein Complex from Rhodopseudomonas acidophila. <b>1996</b> , 64, 564-576	288
1099	Conservative hydrophobic interdomain contacts of IFN-gamma remain in P17 matrix protein of HIV-1. <b>1996</b> , 104, 141-6	1
1098	The Hin dimer interface is critical for Fis-mediated activation of the catalytic steps of site-specific DNA inversion. <b>1996</b> , 6, 163-77	48
1097	The #prism: a new folding motif. <b>1996</b> , 21, 3-6	26
1096	Macromolecular structure information and databases. <b>1996</b> , 21, 251-256	10
1095	Structure and function of the protein tyrosine phosphatases. <b>1996</b> , 21, 413-7	322
1094	Threading thrills and threats. <b>1996</b> , 4, 15-9	43
1093	Crystal structure of the ternary complex of mouse lung carbonyl reductase at 1.8 A resolution: the structural origin of coenzyme specificity in the short-chain dehydrogenase/reductase family. <b>1996</b> , 4, 33-45	203
1092	The structure of the substrate-free form of MurB, an essential enzyme for the synthesis of bacterial cell walls. <b>1996</b> , 4, 47-54	59
1091	The crystal structure of ribosomal protein L14 reveals an important organizational component of the translational apparatus. <b>1996</b> , 4, 55-66	60
1090	The catalytic domain of avian sarcoma virus integrase: conformation of the active-site residues in the presence of divalent cations. <b>1996</b> , 4, 89-96	160
1089	Crystal structures of nucleoside 2-deoxyribosyltransferase in native and ligand-bound forms reveal architecture of the active site. <b>1996</b> , 4, 97-107	44
1088	Crystal structures of various maltooligosaccharides bound to maltoporin reveal a specific sugar translocation pathway. <b>1996</b> , 4, 127-34	151
1087	The structure of simian virus 40 refined at 3.1 A resolution. <b>1996</b> , 4, 165-82	268
1086	The crystal structure of endoglucanase CelA, a family 8 glycosyl hydrolase from Clostridium thermocellum. <b>1996</b> , 4, 265-75	153
1085	Protein-protein interactions in the pyruvate dehydrogenase multienzyme complex: dihydrolipoamide dehydrogenase complexed with the binding domain of dihydrolipoamide acetyltransferase. <b>1996</b> , 4, 277-86	110
1084	Crystal structure of firefly luciferase throws light on a superfamily of adenylate-forming enzymes. <b>1996</b> , 4, 287-98	515

1083	Crystal structure of the yeast cell-cycle control protein, p13suc1, in a strand-exchanged dimer. <b>1996</b> , 4, 299-309	27
1082	Immunoglobulin-like modules from titin I-band: extensible components of muscle elasticity. <b>1996</b> , 4, 323-37	263
1081	How coenzyme B12 radicals are generated: the crystal structure of methylmalonyl-coenzyme A mutase at 2 A resolution. <b>1996</b> , 4, 339-50	450
1080	X-ray structure of a hydroxamate inhibitor complex of stromelysin catalytic domain and its comparison with members of the zinc metalloproteinase superfamily. <b>1996</b> , 4, 375-86	109
1079	Structure of rat procathepsin B: model for inhibition of cysteine protease activity by the proregion. <b>1996</b> , 4, 405-16	162
1078	Insights into substrate binding by D-2-ketoacid dehydrogenases from the structure of Lactobacillus pentosus D-lactate dehydrogenase. <b>1996</b> , 4, 437-47	50
1077	Electrostatic control of GTP and GDP binding in the oncoprotein p21ras. <b>1996</b> , 4, 475-89	57
1076	The crystal structure of bacteriophage Q beta at 3.5 A resolution. <b>1996</b> , 4, 543-54	165
1075	Structure of a water soluble fragment of the 'Rieske' iron-sulfur protein of the bovine heart mitochondrial cytochrome bc1 complex determined by MAD phasing at 1.5 A resolution. <b>1996</b> , 4, 567-79	287
1074	The solution structure of the first zinc finger domain of SWI5: a novel structural extension to a common fold. <b>1996</b> , 4, 599-611	34
1073	Crystal structure of a new heat-labile enterotoxin, LT-IIb. <b>1996</b> , 4, 665-78	63
1072	Crystal structure of a phosphatase-resistant mutant of sporulation response regulator Spo0F from Bacillus subtilis. <b>1996</b> , 4, 679-90	65
1071	Solution structure and peptide binding of the SH3 domain from human Fyn. <b>1996</b> , 4, 705-14	86
1070	Crystal structure of transaldolase B from Escherichia coli suggests a circular permutation of the alpha/beta barrel within the class I aldolase family. <b>1996</b> , 4, 715-24	78
1069	Crystal structures of reduced, oxidized, and mutated human thioredoxins: evidence for a regulatory homodimer. <b>1996</b> , 4, 735-51	325
1068	Flexibility is a likely determinant of binding specificity in the case of ileal lipid binding protein. <b>1996</b> , 4, 785-800	85
1067	Substrate binding is required for assembly of the active conformation of the catalytic site in Ntn amidotransferases: evidence from the 1.8 A crystal structure of the glutaminase domain of glucosamine 6-phosphate synthase. <b>1996</b> , 4, 801-10	126
1066	Mechanism of cyanogenesis: the crystal structure of hydroxynitrile lyase from Hevea brasiliensis. <b>1996</b> , 4, 811-22	100

1065	Crystal structure of the wide-spectrum binuclear zinc beta-lactamase from Bacteroides fragilis. <b>1996</b> , 4, 823-36	359
1064	Insights into specificity of cleavage and mechanism of cell entry from the crystal structure of the highly specific Aspergillus ribotoxin, restrictocin. <b>1996</b> , 4, 837-52	86
1063	The structure of a complex of human 17beta-hydroxysteroid dehydrogenase with estradiol and NADP+ identifies two principal targets for the design of inhibitors. <b>1996</b> , 4, 905-15	189
1062	The structure of an RNA dodecamer shows how tandem U-U base pairs increase the range of stable RNA structures and the diversity of recognition sites. <b>1996</b> , 4, 917-30	82
1061	The role of the divalent cation in the structure of the I domain from the CD11a/CD18 integrin. <b>1996</b> , 4, 931-42	130
1060	Crystal structure of a eukaryotic (pea seedling) copper-containing amine oxidase at 2.2 A resolution. <b>1996</b> , 4, 943-55	233
1059	Conservation within the myosin motor domain: implications for structure and function. <b>1996</b> , 4, 969-87	201
1058	Synchrotron X-ray studies suggest that the core of the transthyretin amyloid fibril is a continuous beta-sheet helix. <b>1996</b> , 4, 989-98	367
1057	A dawning light: the beginnings of an understanding of the photosynthetic reaction center. <b>1996</b> , 4, 1009-12	2
1056	Crystal structure of reduced protein R2 of ribonucleotide reductase: the structural basis for oxygen activation at a dinuclear iron site. <b>1996</b> , 4, 1053-64	258
1055	Crystal structure of UDP-N-acetylglucosamine enolpyruvyltransferase, the target of the antibiotic fosfomycin. <b>1996</b> , 4, 1065-75	82
1054	Structural evidence for specific S8-RNA and S8-protein interactions within the 30S ribosomal subunit: ribosomal protein S8 from Bacillus stearothermophilus at 1.9 A resolution. <b>1996</b> , 4, 1093-104	61
1053	Intramolecular interactions of the regulatory domains of the Bcr-Abl kinase reveal a novel control mechanism. <b>1996</b> , 4, 1105-14	38
1052	Helix unwinding in the effector region of elongation factor EF-Tu-GDP. <b>1996</b> , 4, 1141-51	207
1051	An alpha to beta conformational switch in EF-Tu. <b>1996</b> , 4, 1153-9	182
1050	Crystal structure of the ternary complex of 1,3,8-trihydroxynaphthalene reductase from Magnaporthe grisea with NADPH and an active-site inhibitor. <b>1996</b> , 4, 1161-70	75
1049	The native strains in the hydrophobic core and flexible reactive loop of a serine protease inhibitor: crystal structure of an uncleaved alpha1-antitrypsin at 2.7 A. <b>1996</b> , 4, 1181-92	82
1048	The prosequence of procaricain forms an alpha-helical domain that prevents access to the substrate-binding cleft. <b>1996</b> , 4, 1193-203	100

1047	The structure of the C-terminal domain of methionine synthase: presenting S-adenosylmethionine for reductive methylation of B12. <b>1996</b> , 4, 1263-75	106
1046	The crystal structure of a class II fructose-1,6-bisphosphate aldolase shows a novel binuclear metal-binding active site embedded in a familiar fold. <b>1996</b> , 4, 1303-15	100
1045	The UmuD' protein filament and its potential role in damage induced mutagenesis. <b>1996</b> , 4, 1401-12	40
1044	Crystal structure of a fungal elicitor secreted by Phytophthora cryptogea, a member of a novel class of plant necrotic proteins. <b>1996</b> , 4, 1429-39	84
1043	Structure of UDP-N-acetylglucosamine enolpyruvyl transferase, an enzyme essential for the synthesis of bacterial peptidoglycan, complexed with substrate UDP-N-acetylglucosamine and the drug fosfomycin. <b>1996</b> , 4, 1465-74	214
1042	A model of Ca(2+)-free calmodulin binding to unconventional myosins reveals how calmodulin acts as a regulatory switch. <b>1996</b> , 4, 1475-90	96
1041	The structural basis for pyrophosphatase catalysis. <b>1996</b> , 4, 1491-508	115
1040	Molecular evolution of bacterial beta-lactam resistance. <b>1996</b> , 3, 937-47	130
1039	Redesigning the substrate specificity of the hepatitis C virus NS3 protease. <b>1996</b> , 1, 35-42	25
1038	Unfolded BPTI variants with a single disulfide bond have diminished non-native structure distant from the crosslink. <b>1996</b> , 1, 65-76	19
1037	Optimum superimposition of protein structures: ambiguities and implications. <b>1996</b> , 1, 123-32	112
1036	Towards the complete structural characterization of a protein folding pathway: the structures of the denatured, transition and native states for the association/folding of two complementary fragments of cleaved chymotrypsin inhibitor 2. Direct evidence for a nucleation-condensation	36
1035	A database of globular protein structural domains: clustering of representative family members into similar folds. <b>1996</b> , 1, 209-20	53
1034	An NMR study on the beta-hairpin region of barnase. <b>1996</b> , 1, 231-41	20
1033	High helicity of peptide fragments corresponding to beta-strand regions of beta-lactoglobulin observed by 2D-NMR spectroscopy. <b>1996</b> , 1, 255-63	70
1032	Molecular dynamics simulations of apocytochrome b562the highly ordered limit of molten globules. <b>1996</b> , 1, 335-46	27
1031	Contribution of the intramolecular disulfide bridge to the folding stability of REIv, the variable domain of a human immunoglobulin kappa light chain. <b>1996</b> , 1, 431-40	59
1030	Native-like secondary structure in a peptide from the alpha-domain of hen lysozyme. <b>1996</b> , 1, 473-84	14

1029	Recognition of altered self major histocompatibility complex molecules modulated by specific peptide interactions. <b>1996</b> , 26, 949-52	12
1028	Factor XIII(A) subunit deficiency due to a homozygous 13-base pair deletion in exon 3 of the A subunit gene. <b>1996</b> , 53, 77-80	10
1027	Molecular dynamics study of glucocorticoid receptor-DNA binding. <b>1996</b> , 24, 115-33	24
1026	Secondary structure prediction and unrefined tertiary structure prediction for cyclin A, B, and D. <b>1996</b> , 24, 18-34	5
1025	Modeling of a five-stranded coiled coil structure for the assembly domain of the cartilage oligomeric matrix protein. <b>1996</b> , 24, 218-26	16
1024	Experimental and theoretical study of electrostatic effects on the isoelectric pH and the pKa of the catalytic residue His-102 of the recombinant ribonuclease from Bacillus amyloliquefaciens (barnase). <b>1996</b> , 24, 370-8	10
1023	The role of helix formation in the folding of a fully alpha-helical coiled coil. <b>1996</b> , 24, 427-32	88
1022	Molecular dynamics simulations of N-terminal peptides from a nucleotide binding protein. <b>1996</b> , 24, 450-66	16
1021	Study of global motions in proteins by weighted masses molecular dynamics: adenylate kinase as a test case. <b>1996</b> , 25, 79-88	12
1020	Analysis of topological and nontopological structural similarities in the PDB: new examples with old structures. <b>1996</b> , 25, 354-65	28
1019	Is the binding of	
1018	Refined structures of bobwhite quail lysozyme uncomplexed and complexed with the HyHEL-5 Fab fragment. <b>1996</b> , 26, 55-65	23
1017	Structural stability of disulfide mutants of basic pancreatic trypsin inhibitor: a molecular dynamics study. <b>1996</b> , 26, 66-71	6
1016	A comparative study of dynamic structures between phage 434 Cro and repressor proteins by normal mode analysis. <b>1996</b> , 26, 72-80	5
1015	Improved prediction for the structure of the dimeric transmembrane domain of glycophorin A obtained through global searching. <b>1996</b> , 26, 257-61	141
1014	Refined crystal structure and mutagenesis of human granulocyte-macrophage colony-stimulating factor. <b>1996</b> , 26, 304-13	50
1013	Spectroscopic evidence for preexisting T- and R-state insulin hexamer conformations. <b>1996</b> , 26, 377-90	14
1012	Comparative interaction kinetics of two recombinant Fabs and of the corresponding antibodies directed to the coat protein of tobacco mosaic virus. <b>1996</b> , 9, 39-51	29

1011	Structure and dynamics of the DNA binding protein HU from Bacillus stearothermophilus by NMR spectroscopy. <b>1996</b> , 40, 553-9	23
1010	NMR and protein dynamics. <b>1996</b> , 59, 315-332	9
1009	Protein determinants of metal site reduction potentials: site-directed mutagenesis studies of Clostridium pasteurianum rubredoxin. <b>1996</b> , 242, 245-251	48
1008	Site-specific modification of ⊞helical peptides with electron donors and acceptors. <b>1996</b> , 243, 207-212	12
1007	Conformation and Self-Association of a Hybrid Peptide of Cecropin A and Melittin with Improved Antibiotic Activity. <b>1996</b> , 2, 838-846	5
1006	The structural puzzle of how serpin serine proteinase inhibitors work. <b>1996</b> , 18, 453-64	62
1005	Molecular mechanisms of drug inhibition of DNA gyrase. <b>1996</b> , 18, 661-71	64
1004	Progress towards understanding beta-sheet structure. <b>1996</b> , 4, 739-66	128
1003	Structure and function of the T-cell receptor: insights from X-ray crystallography. <b>1996</b> , 17, 330-6	40
1002	The structure and ligand interactions of CD2: implications for T-cell function. <b>1996</b> , 17, 177-87	348
1001	New approaches in molecular structure prediction. <b>1996</b> , 59, 1-32	54
1000	Time-resolved fluorescence of tryptophan synthase. <b>1996</b> , 61, 9-22	21
999	MOLMOL: a program for display and analysis of macromolecular structures. <b>1996</b> , 14, 51-5, 29-32	6340
998	Lipoxygenase: a molecular complex with a non-heme iron. <b>1996</b> , 374, 47-52	1
997	A Zn(II)-binding site engineered into retinol-binding protein exhibits metal-ion specificity and allows highly efficient affinity purification with a newly designed metal ligand. <b>1996</b> , 3, 645-53	23
996	Protein serine/threonine phosphatases. <b>1996</b> , 7, 397-402	23
995	The collectins in innate immunity. <b>1996</b> , 8, 29-35	242
994	X-CGDbase: a database of X-CGD-causing mutations. <b>1996</b> , 17, 517-521	3

993	Structures of lantibiotics studied by NMR. <b>1996</b> , 69, 99-107	21
992	Molecular dynamics simulations of peptides from BPTI: a closer look at amide-aromatic interactions. <b>1996</b> , 8, 229-38	79
991	An approach to global fold determination using limited NMR data from larger proteins selectively protonated at specific residue types. <b>1996</b> , 8, 360-8	54
990	The purple bacterial photosynthetic unit. <b>1996</b> , 48, 55-63	92
989	Three-dimensional structures of photosynthetic reaction centers. <b>1996</b> , 48, 65-74	33
988	CD studies of peptides that mimic the four helicoidal sequences of the uteroglobin monomer. <b>1996</b> , 2, 353-362	3
987	Molecular dynamics study of an alpha-cyclodextrin-phosphatidylinositol inclusion complex. <b>1996</b> , 24, 300-10	8
986	Polypeptide folding with off-lattice Monte Carlo dynamics: the method. <b>1996</b> , 24, 387-403	41
985	Identification of the Serratia endonuclease dimer: structural basis and implications for catalysis. <b>1996</b> , 5, 24-33	50
984	The crystal structure of trypanothione reductase from the human pathogen Trypanosoma cruzi at 2.3 A resolution. <b>1996</b> , 5, 52-61	78
983	Covalent tethering of the dimer interface annuls aggregation in thymidylate synthase. <b>1996</b> , 5, 270-7	10
982	Second-site suppression of regulatory phosphorylation in Escherichia coli isocitrate dehydrogenase. <b>1996</b> , 5, 287-95	18
981	pH-Dependent self-association of the Src homology 2 (SH2) domain of the Src homologous and collagen-like (SHC) protein. <b>1996</b> , 5, 405-13	9
980	Three-dimensional solution structure of the HIV-1 protease complexed with DMP323, a novel cyclic urea-type inhibitor, determined by nuclear magnetic resonance spectroscopy. <b>1996</b> , 5, 495-506	67
979	A stable intermediate in the thermal unfolding process of a chimeric 3-isopropylmalate dehydrogenase between a thermophilic and a mesophilic enzymes. <b>1996</b> , 5, 511-6	13
978	Thermosensitive mutants of the MPTP and hPTP1B protein tyrosine phosphatases: isolation and structural analysis. <b>1996</b> , 5, 604-13	7
977	Redox-dependent dynamics of putidaredoxin characterized by amide proton exchange. <b>1996</b> , 5, 627-39	38
976	Structural similarity between ornithine and aspartate transcarbamoylases of Escherichia coli: characterization of the active site and evidence for an interdomain carboxy-terminal helix in ornithine transcarbamoylase. <b>1996</b> , 5, 709-18	12

975	Structural similarity between ornithine and aspartate transcarbamoylases of Escherichia coli: implications for domain switching. <b>1996</b> , 5, 719-28	9
974	4-Oxalocrotonate tautomerase, a 41-kDa homohexamer: backbone and side-chain resonance assignments, solution secondary structure, and location of active site residues by heteronuclear NMR spectroscopy. <b>1996</b> , 5, 729-41	17
973	Probing the tertiary structure of proteins by limited proteolysis and mass spectrometry: the case of Minibody. <b>1996</b> , 5, 802-13	60
972	Extremely thermostable L(+)-lactate dehydrogenase from Thermotoga maritima: cloning, characterization, and crystallization of the recombinant enzyme in its tetrameric and octameric state. <b>1996</b> , 5, 862-73	17
971	Energetics of structural domains in alpha-lactalbumin. <b>1996</b> , 5, 923-31	38
970	Derivation of 3D coordinate templates for searching structural databases: application to Ser-His-Asp catalytic triads in the serine proteinases and lipases. <b>1996</b> , 5, 1001-13	189
969	An unusual route to thermostability disclosed by the comparison of Thermus thermophilus and Escherichia coli inorganic pyrophosphatases. <b>1996</b> , 5, 1014-25	60
968	Intrinsic tryptophans of CRABPI as probes of structure and folding. <b>1996</b> , 5, 1108-17	72
967	The lipocalin Xlcpl1 expressed in the neural plate of Xenopus laevis embryos is a secreted retinaldehyde binding protein. <b>1996</b> , 5, 1250-60	20
966	The crystal structure of TGF-beta 3 and comparison to TGF-beta 2: implications for receptor binding. <b>1996</b> , 5, 1261-71	127
965	In vivo formation of allosteric aspartate transcarbamoylase containing circularly permuted catalytic polypeptide chains: implications for protein folding and assembly. <b>1996</b> , 5, 1290-300	43
964	The (QxW)3 domain: a flexible lectin scaffold. <b>1996</b> , 5, 1490-501	174
963	A catalytic function for the structurally conserved residue Phe 100 of ribonuclease T1. <b>1996</b> , 5, 1523-30	14
962	Structural changes in factor VIIa induced by Ca2+ and tissue factor studied using circular dichroism spectroscopy. <b>1996</b> , 5, 1531-40	61
961	What makes a protein a protein? Hydrophobic core designs that specify stability and structural properties. <b>1996</b> , 5, 1584-93	166
960	Ribosome-mediated translational pause and protein domain organization. <b>1996</b> , 5, 1594-612	203
959	Crystal structure of a biologically inactive mutant of toxic shock syndrome toxin-1 at 2.5 A resolution. <b>1996</b> , 5, 1737-41	9
958	Crystal structure of the 2[4Fe-4S] ferredoxin from Chromatium vinosum: evolutionary and mechanistic inferences for [3/4Fe-4S] ferredoxins. <b>1996</b> , 5, 1765-75	61

957	The 1.8-A X-ray structure of the Escherichia coli PotD protein complexed with spermidine and the mechanism of polyamine binding. <b>1996</b> , 5, 1984-90	50
956	Bending of the calmodulin central helix: a theoretical study. <b>1996</b> , 5, 2044-53	66
955	High-resolution X-ray structure of UDP-galactose 4-epimerase complexed with UDP-phenol. <b>1996</b> , 5, 2149-61	83
954	1H NMR assignments of apo calcyclin and comparative structural analysis with calbindin D9k and S100 beta. <b>1996</b> , 5, 2162-74	32
953	Crystal structure analyses of uncomplexed ecotin in two crystal forms: implications for its function and stability. <b>1996</b> , 5, 2236-47	25
952	Individual amino acids in the N-terminal loop region determine the thermostability and unfolding characteristics of bacterial glucanases. <b>1996</b> , 5, 2255-65	13
951	Probing the role of tryptophan residues in a cellulose-binding domain by chemical modification. <b>1996</b> , 5, 2311-8	50
950	Comparison of the NMR and X-ray structures of the HIV-1 matrix protein: evidence for conformational changes during viral assembly. <b>1996</b> , 5, 2391-8	62
949	A distant evolutionary relationship between bacterial sphingomyelinase and mammalian DNase I. <b>1996</b> , 5, 2459-67	58
948	Conformational analysis and clustering of short and medium size loops connecting regular secondary structures: a database for modeling and prediction. <b>1996</b> , 5, 2600-16	94
947	Insights into the molecular basis of thermal stability from the structure determination of Pyrococcus furiosus glutamate dehydrogenase. <b>1996</b> , 18, 105-17	48
946	Structure of the multifunctional loops in the nonclassical ATP-binding fold of glutathione synthetase. <b>1996</b> , 3, 16-8	25
945	The crystal structure of the antifungal protein zeamatin, a member of the thaumatin-like, PR-5 protein family. <b>1996</b> , 3, 19-23	110
944	A canonical structure for the ligand-binding domain of nuclear receptors. <b>1996</b> , 3, 87-94	776
943	Structural transitions during activation and ligand binding in hexadecameric Rubisco inferred from the crystal structure of the activated unliganded spinach enzyme. <b>1996</b> , 3, 95-101	90
942	The N-terminal domain of TFIIB from Pyrococcus furiosus forms a zinc ribbon. <b>1996</b> , 3, 122-4	117
941	Chitinases, chitosanases, and lysozymes can be divided into procaryotic and eucaryotic families sharing a conserved core. <b>1996</b> , 3, 133-40	129
940	X-ray structure of an anti-fungal chitosanase from streptomyces N174. <b>1996</b> , 3, 155-62	111

939	Crystal structure of the neurophysin-oxytocin complex. <b>1996</b> , 3, 163-9	86
938	Comparison of two different DNA-binding modes of the NF-kappa B p50 homodimer. <b>1996</b> , 3, 224-7	21
937	Molecular docking programs successfully predict the binding of a beta-lactamase inhibitory protein to TEM-1 beta-lactamase. <b>1996</b> , 3, 233-9	127
936	Crystal structure of the macrophage migration inhibitory factor from rat liver. <b>1996</b> , 3, 259-66	167
935	X-ray structure of Streptococcus pneumoniae PBP2x, a primary penicillin target enzyme. <b>1996</b> , 3, 284-9	149
934	A potent new mode of beta-lactamase inhibition revealed by the 1.7 A X-ray crystallographic structure of the TEM-1-BLIP complex. <b>1996</b> , 3, 290-7	114
933	Solution structure of ShK toxin, a novel potassium channel inhibitor from a sea anemone. <b>1996</b> , 3, 317-20	161
932	Closure of a tyrosine/tryptophan aromatic gate leads to a compact fold in apo flavodoxin. <b>1996</b> , 3, 329-32	81
931	Three dimensional structure of human C-reactive protein. <b>1996</b> , 3, 346-54	263
930	Crystal structure of the PI 3-kinase p85 amino-terminal SH2 domain and its phosphopeptide complexes. <b>1996</b> , 3, 364-74	116
929	Structure of human beta-glucuronidase reveals candidate lysosomal targeting and active-site motifs. <b>1996</b> , 3, 375-81	195
928	Rapid, electrostatically assisted association of proteins. <b>1996</b> , 3, 427-31	464
927	Packing interactions in the apomyglobin folding intermediate. <b>1996</b> , 3, 439-45	142
926	In vitro evolution of thermodynamically stable turns. <b>1996</b> , 3, 446-51	67
925	Insights into protein adaptation to a saturated salt environment from the crystal structure of a halophilic 2Fe-2S ferredoxin. <b>1996</b> , 3, 452-8	185
924	Retrovirus envelope domain at 1.7 angstrom resolution. <b>1996</b> , 3, 465-9	280
923	The x-ray crystal structure of phosphomannose isomerase from Candida albicans at 1.7 angstrom resolution. <b>1996</b> , 3, 470-9	98
922	The problem with pyrimidines. <b>1996</b> , 3, 485-7	37

### [1996-1996]

921	Pre-formation of the semi-open conformation by the apo-calmodulin C-terminal domain and implications binding IQ-motifs. <b>1996</b> , 3, 501-4	63
920	An engineered allosteric switch in leucine-zipper oligomerization. <b>1996</b> , 3, 510-5	103
919	Hydrogen bonding and equilibrium isotope enrichment in histidine-containing proteins. <b>1996</b> , 3, 522-31	28
918	The structure of Desulfovibrio vulgaris rubrerythrin reveals a unique combination of rubredoxin-like FeS4 and ferritin-like diiron domains. <b>1996</b> , 3, 539-46	118
917	A novel mode of carbohydrate recognition in jacalin, a Moraceae plant lectin with a beta-prism fold. <b>1996</b> , 3, 596-603	195
916	Bacterial chitobiase structure provides insight into catalytic mechanism and the basis of Tay-Sachs disease. <b>1996</b> , 3, 638-48	290
915	A specific structural interaction of Alzheimer's peptide A beta 1-42 with alpha 1-antichymotrypsin. <b>1996</b> , 3, 668-71	38
914	Inhibitory conformation of the reactive loop of alpha 1-antitrypsin. <b>1996</b> , 3, 676-81	208
913	Structural basis of cyclin-dependent kinase activation by phosphorylation. <b>1996</b> , 3, 696-700	501
912	Crystal structure of dimeric HIV-1 capsid protein. <b>1996</b> , 3, 763-70	272
911	Crystal structure of turnip yellow mosaic virus. <b>1996</b> , 3, 771-81	105
910	C2 domain conformational changes in phospholipase C-delta 1. <b>1996</b> , 3, 788-95	100
909	Crystal structure of a camel single-domain VH antibody fragment in complex with lysozyme. <b>1996</b> , 3, 803-11	383
908	Novel zinc-binding centre in thermoacidophilic archaeal ferredoxins. <b>1996</b> , 3, 834-7	46
907	Aromatic hydrogen bond in sequence-specific protein DNA recognition. <b>1996</b> , 3, 837-41	63
906	Three-dimensional structure of human cyclin H, a positive regulator of the CDK-activating kinase. <b>1996</b> , 3, 849-55	57
905	Novel active site in Escherichia coli fructose 1,6-bisphosphate aldolase. <b>1996</b> , 3, 856-62	71
904	Non-native alpha-helical intermediate in the refolding of beta-lactoglobulin, a predominantly beta-sheet protein. <b>1996</b> , 3, 868-73	242

903	Crystal structures of Toxoplasma gondii HGXPRTase reveal the catalytic role of a long flexible loop. <b>1996</b> , 3, 881-7	88
902	Arginine substitutions in the hinge region of antichymotrypsin affect serpin beta-sheet rearrangement. <b>1996</b> , 3, 888-93	33
901	Waiting to inhale. <b>1996</b> , 3, 902-6	5
900	Flexibility of the NSAID binding site in the structure of human cyclooxygenase-2. <b>1996</b> , 3, 927-33	47°
899	Ferryl intermediates of catalase captured by time-resolved Weissenberg crystallography and UV-VIS spectroscopy. <b>1996</b> , 3, 951-6	63
898	Crystal structure of Aplysia ADP ribosyl cyclase, a homologue of the bifunctional ectozyme CD38. <b>1996</b> , 3, 957-64	127
897	Photosystem I at 4 A resolution represents the first structural model of a joint photosynthetic reaction centre and core antenna system. <b>1996</b> , 3, 965-73	296
896	Kinetic intermediates in the formation of the cytochrome c molten globule. <b>1996</b> , 3, 1019-25	88
895	A leucine-rich repeat variant with a novel repetitive protein structural motif. <b>1996</b> , 3, 991-4	42
894	Locating and characterizing binding sites on proteins. <b>1996</b> , 14, 595-9	221
893	Transdermal delivery of peptides by iontophoresis. <b>1996</b> , 14, 1710-3	56
892	Mutations in either the essential or regulatory light chains of myosin are associated with a rare myopathy in human heart and skeletal muscle. <b>1996</b> , 13, 63-9	502
891	Bovine beta-lactoglobulin modified by 3-hydroxyphthalic anhydride blocks the CD4 cell receptor for HIV. <b>1996</b> , 2, 230-4	69
890	The crystal structure of the GroES co-chaperonin at 2.8 A resolution. <b>1996</b> , 379, 37-45	408
889	Structure and mechanism of DNA topoisomerase II. <b>1996</b> , 379, 225-32	723
888	Spatial constraints on the recognition of phosphoproteins by the tandem SH2 domains of the phosphatase SH-PTP2. <b>1996</b> , 379, 277-80	174
887	The structure of the Escherichia coli EF-Tu.EF-Ts complex at 2.5 A resolution. <b>1996</b> , 379, 511-8	275
886	The crystal structure of the complex of blood coagulation factor VIIa with soluble tissue factor. <b>1996</b> , 380, 41-6	668

885	Structural basis of calcium-induced E-cadherin rigidification and dimerization. 1996, 380, 360-4	591
884	Crystal structure of the kinesin motor domain reveals a structural similarity to myosin. <b>1996</b> , 380, 550-5	577
883	Crystal structure of a mammalian phosphoinositide-specific phospholipase C delta. <b>1996</b> , 380, 595-602	532
882	Structure of the UmuD' protein and its regulation in response to DNA damage. <b>1996</b> , 380, 727-30	152
881	Structure and mutational analysis of Rab GDP-dissociation inhibitor. <b>1996</b> , 381, 42-8	153
880	Structure of Bordetella pertussis virulence factor P.69 pertactin. <b>1996</b> , 381, 90-2	259
879	Crystal structure of the p27Kip1 cyclin-dependent-kinase inhibitor bound to the cyclin A-Cdk2 complex. <b>1996</b> , 382, 325-31	804
878	Structure of the WW domain of a kinase-associated protein complexed with a proline-rich peptide. <b>1996</b> , 382, 646-9	379
877	Crystal structure of a PDZ domain. <b>1996</b> , 382, 649-52	298
876	Unique fold and active site in cytomegalovirus protease. <b>1996</b> , 383, 275-9	151
875	Three-dimensional structure of human cytomegalovirus protease. <b>1996</b> , 383, 279-82	146
874	Structure of a unique binuclear manganese cluster in arginase. <b>1996</b> , 383, 554-7	378
873	Structural basis for the binding of a globular antifreeze protein to ice. <b>1996</b> , 384, 285-8	213
872	Crystal structure of the GTPase-activating domain of human p120GAP and implications for the interaction with Ras. <b>1996</b> , 384, 591-6	149
871	Elongation in bacterial protein biosynthesis. <b>1996</b> , 7, 369-75	12
870	Threading your way to protein function. <b>1996</b> , 3, 779-83	7
869	Bacterial resistance to vancomycin: five genes and one missing hydrogen bond tell the story. <b>1996</b> , 3, 21-8	324
868	Interacting residues in the extracellular region of the common beta subunit of the human granulocyte-macrophage colony-stimulating factor, interleukin (IL)-3, and IL-5 receptors involved in constitutive activation. <b>1996</b> , 271, 29707-14	39

867 Epidermal growth factor. **1996**, 1, 85-121

866	Crystallographic evidence that the F2 kringle catalytic domain linker of prothrombin does not cover the fibrinogen recognition exosite. <b>1996</b> , 271, 3413-6	7
865	Induction of helical conformation in all beta-sheet proteins by trifluoroethanol. 1996, 14, 381-5	6
864	Membrane topology of the colicin A pore-forming domain analyzed by disulfide bond engineering. <b>1996</b> , 271, 15401-6	24
863	A Structure-Based Model of Diphtheria Toxin Action. <b>1996</b> , 25-47	O
862	A common structural basis for the inhibition of ribulose 1,5-bisphosphate carboxylase by 4-carboxyarabinitol 1,5-bisphosphate and xylulose 1,5-bisphosphate. <b>1996</b> , 271, 32894-9	26
861	The IgG binding site of human FcgammaRIIIB receptor involves CC' and FG loops of the membrane-proximal domain. <b>1996</b> , 271, 3659-66	53
860	Ligand binding to integrin alphallbbeta3 is dependent on a MIDAS-like domain in the beta3 subunit. <b>1996</b> , 271, 21978-84	141
859	The structural basis of the myosin ATPase activity. <b>1996</b> , 271, 15850-3	104
858	Imparting exquisite specificity to peanut agglutinin for the tumor-associated Thomsen-Friedenreich antigen by redesign of its combining site. <b>1996</b> , 271, 21209-13	36
857	Structural and Functional Characterization of OmpF Porin Mutants Selected for Larger Pore Size. <b>1996</b> , 271, 20669-20675	80
856	Determinants of substrate recognition in the protein-tyrosine phosphatase, PTP1. <b>1996</b> , 271, 5386-92	24
855	Structural Basis of Galactose Recognition by C-type Animal Lectins. <b>1996</b> , 271, 6679-6685	159
854	Characterization of lactogen receptor-binding site 1 of human prolactin. <b>1996</b> , 271, 14353-60	35
853	Lipase activation by nonionic detergents. The crystal structure of the porcine lipase-colipase-tetraethylene glycol monooctyl ether complex. <b>1996</b> , 271, 18007-16	167
852	Retroviral integrase, putting the pieces together. <b>1996</b> , 271, 19633-6	103
851	Nucleoside diphosphate kinase. Investigation of the intersubunit contacts by site-directed mutagenesis and crystallography. <b>1996</b> , 271, 19928-34	37
850	Crystal structure of PotD, the primary receptor of the polyamine transport system in Escherichia coli. <b>1996</b> , 271, 9519-25	73

### [1996-1996]

849	Structural flexibility modulates the activity of human glutathione transferase P1-1. Role of helix 2 flexibility in the catalytic mechanism. <b>1996</b> , 271, 16187-92	78
848	Allosteric activation of L-lactate dehydrogenase analyzed by hybrid enzymes with effector-sensitive and -insensitive subunits. <b>1996</b> , 271, 25611-6	33
847	Sequential structural changes upon zinc and calcium binding to metal-free concanavalin A. <b>1996</b> , 271, 16144-50	52
846	Computational biochemistry of antibodies and T-cell receptors. <b>1996</b> , 49, 149-260	7
845	Folding of a mutant maltose-binding protein of Escherichia coli which forms inclusion bodies. <b>1996</b> , 271, 8046-52	71
844	Protein dynamics with off-lattice Monte Carlo moves. <b>1996</b> , 53, 4221-4224	21
843	Structure-function analysis of the motor domain of myosin. <b>1996</b> , 12, 543-73	77
842	The Bdge strandIhypothesis: Prediction and test of a mutational Bot-spotIbn the transthyretin molecule associated with FAP amyloidogenesis. <b>1996</b> , 3, 75-85	23
841	Characterization of the receptor binding sites of human leukemia inhibitory factor and creation of antagonists. <b>1996</b> , 271, 11971-8	80
840	Programming the Rous sarcoma virus protease to cleave new substrate sequences. <b>1996</b> , 271, 10538-44	21
839	Determinants of helix-loop-helix dimerization affinity. Random mutational analysis of SCL/tal. <b>1996</b> , 271, 2683-8	19
838	A discontinuous eight-amino acid epitope in human interleukin-3 binds the alpha-chain of its receptor. <b>1996</b> , 271, 31922-8	17
837	The crystallographic structure of phytohemagglutinin-L. <b>1996</b> , 271, 20479-85	88
836	Localization of the Putative Sialic Acid-binding Site on the Immunoglobulin Superfamily Cell-surface Molecule CD22. <b>1996</b> , 271, 9273-9280	106
835	The Co-crystal structure of staphylococcal enterotoxin type A with Zn2+ at 2.7 A resolution. Implications for major histocompatibility complex class II binding. <b>1996</b> , 271, 32212-6	41
834	Characterization of the sialic acid-binding site in sialoadhesin by site-directed mutagenesis. <b>1996</b> , 271, 9267-72	114
833	Crystal structure of arcelin-5, a lectin-like defense protein from Phaseolus vulgaris. <b>1996</b> , 271, 32796-802	25
832	Ligand specificity of brain lipid-binding protein. <b>1996</b> , 271, 24711-9	142

831	Changing the structural context of a functional beta-hairpin. Synthesis and characterization of a chimera containing the curaremimetic loop of a snake toxin in the scorpion alpha/beta scaffold. <b>1996</b> , 271, 11979-87	60
830	Two conserved tyrosine residues in protein R1 participate in an intermolecular electron transfer in ribonucleotide reductase. <b>1996</b> , 271, 20655-9	108
829	The Molecular Nature of the F-actin Binding Activity of Aldolase Revealed with Site-directed Mutants. <b>1996</b> , 271, 6861-6865	92
828	Thermal stability of hexameric and tetrameric nucleoside diphosphate kinases. Effect of subunit interaction. <b>1996</b> , 271, 17845-51	36
827	Energetic implications for protein phosphorylation. Conformational stability of HPr variants that mimic phosphorylated forms. <b>1996</b> , 271, 28898-902	16
826	Thermodynamics of monosaccharide and disaccharide binding to Erythrina corallodendron lectin. <b>1996</b> , 271, 17697-703	69
825	An Experimental Approach to Mapping the Binding Surfaces of Crystalline Proteins <b>1996</b> , 100, 2605-2611	167
824	Molecular Dynamics/Free Energy Perturbation Studies of the Thermostable V74I Mutant of Ribonuclease HI. <b>1996</b> , 16, 75-85	11
823	Introduction of selectin-like binding specificity into a homologous mannose-binding protein. <b>1996</b> , 271, 7289-92	33
822	Crystal structures of catalytic subunit of cAMP-dependent protein kinase in complex with isoquinolinesulfonyl protein kinase inhibitors H7, H8, and H89. Structural implications for selectivity. <b>1996</b> , 271, 26157-64	209
821	Purification and kinetic characterization of the mitogen-activated protein kinase phosphatase rVH6. <b>1996</b> , 271, 33486-92	28
820	Enzyme-DNA interactions required for efficient nucleotide incorporation and discrimination in human DNA polymerase beta. <b>1996</b> , 271, 12141-4	146
819	The mechanism of velocity modulated allosteric regulation in D-3-phosphoglycerate dehydrogenase. Site-directed mutagenesis of effector binding site residues. <b>1996</b> , 271, 23235-8	46
818	Structure and function of the glutamine phosphoribosylpyrophosphate amidotransferase glutamine site and communication with the phosphoribosylpyrophosphate site. <b>1996</b> , 271, 15549-57	62
817	Structural analysis of monosaccharide recognition by rat liver mannose-binding protein. <b>1996</b> , 271, 663-74	133
816	Phosphorylation events associated with different states of activation of a hepatic cardiolipin/protease-activated protein kinase. Structural identity to the protein kinase N-type protein kinases. <b>1996</b> , 271, 32233-40	31
815	The X-ray crystal structures of Yersinia tyrosine phosphatase with bound tungstate and nitrate. Mechanistic implications. <b>1996</b> , 271, 18780-8	99
814	The putative substrate recognition loop of Escherichia coli ribonuclease H is not essential for activity. <b>1996</b> , 271, 19883-7	29

813	Histidine Patch Thioredoxins. <b>1996</b> , 271, 5059-5065	48
812	The elongation phase of protein synthesis. <b>1996</b> , 54, 293-332	47
811	A hemoglobin-based blood substitute: transplanting a novel allosteric effect of crocodile Hb. <b>1996</b> , 377, 543-8	4
810	A 1.2 ns Molecular Dynamics Simulation of the Ribonuclease T1BEGuanosine Monophosphate Complex. <b>1996</b> , 100, 2480-2488	6
809	Protein Folding Dynamics: Application of the Diffusion-Collision Model to the Folding of a Four-Helix Bundle. <b>1996</b> , 100, 2498-2509	14
808	Molecular Dynamics Simulations of Cyclic and Linear DPDPE: Influence of the Disulfide Bond on Peptide Flexibility. <b>1996</b> , 100, 2555-2563	12
807	Free Energy Simulation Studies of the Binding Specificity of Mannose-Binding Protein. <b>1996</b> , 100, 2528-2534	22
806	Structure of human C8 protein provides mechanistic insight into membrane pore formation by complement. <b>2011</b> , 286, 17585-92	77
805	ModBase, a database of annotated comparative protein structure models, and associated resources. <b>2011</b> , 39, D465-74	252
804	Metallothioneins. 2011,	
803	Crystal structures of protein glutaminase and its pro forms converted into enzyme-substrate complex. <b>2011</b> , 286, 38691-38702	18
802	Crystal structure of the tandem-type universal stress protein TTHA0350 from Thermus thermophilus HB8. <b>2011</b> , 150, 295-302	7
801	Mapping backbone and side-chain interactions in the transition state of a coupled protein folding and binding reaction. <b>2011</b> , 108, 3952-7	100
800	Nuclear Magnetic Resonance (NMR) Spectroscopy of Metallobiomolecules. <b>2011</b> ,	4
799	Matrix Metalloproteinases. 2011,	1
798	Phospholipase A2. <b>2011</b> ,	
797	Thermolysin. <b>2011</b> ,	
796	The oxidation of tyrosine and tryptophan studied by a molecular dynamics normal hydrogen electrode. <b>2011</b> , 134, 244508	98

795	Structural basis for the sequence-specific recognition of human ISG15 by the NS1 protein of influenza B virus. <b>2011</b> , 108, 13468-73	43
794	Mapping of the disease locus and identification of ADAMTS10 as a candidate gene in a canine model of primary open angle glaucoma. <b>2011</b> , 7, e1001306	76
793	Structural switching of Cu,Zn-superoxide dismutases at loop VI: insights from the crystal structure of 2-mercaptoethanol-modified enzyme. <b>2012</b> , 32, 539-48	9
792	Studies on crenarchaeal tyrosylation accuracy with mutational analyses of tyrosyl-tRNA synthetase and tyrosine tRNA from Aeropyrum pernix. <b>2012</b> , 152, 539-48	2
791	Protein databases on the Internet. <b>2012</b> , Chapter 19, Unit 19.4.	6
790	Theoretical investigation on the binding specificity of sialyldisaccharides with hemagglutinins of influenza A virus by molecular dynamics simulations. <b>2012</b> , 287, 34547-57	23
789	Crystal structure of the N-terminal domain of the yeast general corepressor Tup1p and its functional implications. <b>2012</b> , 287, 26528-38	17
788	Trapping and structure determination of an intermediate in the allosteric transition of aspartate transcarbamoylase. <b>2012</b> , 109, 7741-6	6
787	Characterization of chromoshadow domain-mediated binding of heterochromatin protein 1⊞ (HP1∰to histone H3. <b>2012</b> , 287, 18730-7	23
786	Heparan sulfate dissociates serum amyloid A (SAA) from acute-phase high-density lipoprotein, promoting SAA aggregation. <b>2012</b> , 287, 25669-77	42
785	Dissecting the substrate recognition of 3-O-sulfotransferase for the biosynthesis of anticoagulant heparin. <b>2012</b> , 109, 5265-70	42
784	Structural basis for sequence-specific DNA recognition by an Arabidopsis WRKY transcription factor. <b>2012</b> , 287, 7683-91	62
783	Computer simulations of helix folding in homo- and heteropeptides. <b>2012</b> , 38, 682-694	10
782	Structural mechanisms of the degenerate sequence recognition by Bse634I restriction endonuclease. <b>2012</b> , 40, 6741-51	5
781	Membrane-induced lever arm expansion allows myosin VI to walk with large and variable step sizes. <b>2012</b> , 287, 35021-35035	7
780	Large protein assemblies formed by multivalent interactions between cadherin23 and harmonin suggest a stable anchorage structure at the tip link of stereocilia. <b>2012</b> , 287, 33460-71	22
779	Chimeric glutathione S-transferases containing inserts of kininogen peptides: potential novel protein therapeutics. <b>2012</b> , 287, 22142-50	2
778	NMR structure of Carcinoscorpius rotundicauda thioredoxin-related protein 16 and its role in regulating transcription factor NF-B activity. <b>2012</b> , 287, 29417-28	4

# (2012-2012)

777	Human mitotic chromosomes consist predominantly of irregularly folded nucleosome fibres without a 30-nm chromatin structure. <b>2012</b> , 31, 1644-53	223
776	SCPC: a method to structurally compare protein complexes. <b>2012</b> , 28, 324-30	8
775	HugZ from Helicobacter pylori. <b>2012</b> ,	
774	P2-substituted N-acylprolylpyrrolidine inhibitors of prolyl oligopeptidase: biochemical evaluation, binding mode determination, and assessment in a cellular model of synucleinopathy. <b>2012</b> , 55, 9856-67	21
773	Functional mapping of the A2 domain from human factor VIII. <b>2012</b> , 107, 315-27	7
772	Structural basis for Arf6-MKLP1 complex formation on the Flemming body responsible for cytokinesis. <b>2012</b> , 31, 2590-603	42
771	A propensity scale for type II polyproline helices (PPII): aromatic amino acids in proline-rich sequences strongly disfavor PPII due to proline-aromatic interactions. <b>2012</b> , 51, 5041-51	65
770	Tailoring encodable lanthanide-binding tags as MRI contrast agents. <b>2012</b> , 13, 2567-74	20
769	Engineering a thermostable 即,3-1,4-glucanase from Paecilomyces thermophila to improve catalytic efficiency at acidic pH. <b>2012</b> , 159, 50-5	18
768	Crystal-to-crystal photoinduced reaction of dinitroanthracene to anthraquinone. <b>2012</b> , 134, 17671-9	15
767	A structural element that facilitates proton-coupled electron transfer in oxalate decarboxylase. <b>2012</b> , 51, 2911-20	20
766	Identifying and characterizing the most significant 畇lucosidase of the novel species Aspergillus saccharolyticus. <b>2012</b> , 58, 1035-46	17
765	Molecular differences between a mutase and a phosphatase: investigations of the activation step in Bacillus cereus phosphopentomutase. <b>2012</b> , 51, 1964-75	6
764	Second-contact shell mutation diminishes streptavidin-biotin binding affinity through transmitted effects on equilibrium dynamics. <b>2012</b> , 51, 597-607	7
763	A variable light domain fluorogen activating protein homodimerizes to activate dimethylindole red. <b>2012</b> , 51, 2471-85	19
762	SRLS analysis of 15N spin relaxation from E. coli ribonuclease HI: the tensorial perspective. <b>2012</b> , 116, 886-94	15
761	Influence of heme post-translational modification and distal ligation on the backbone dynamics of a monomeric hemoglobin. <b>2012</b> , 51, 5733-47	16
760	Modeling and computations of the intramolecular electron transfer process in the two-heme protein cytochrome c(4). <b>2012</b> , 14, 5953-65	12

759	An androgen receptor mutation in the MDA-MB-453 cell line model of molecular apocrine breast cancer compromises receptor activity. <b>2012</b> , 19, 599-613	35
758	Allostery and cooperativity in Escherichia coli aspartate transcarbamoylase. <b>2012</b> , 519, 81-90	26
757	Intra-chain 3D segment swapping spawns the evolution of new multidomain protein architectures. <b>2012</b> , 415, 221-35	12
756	Local unfolding of Cu, Zn superoxide dismutase monomer determines the morphology of fibrillar aggregates. <b>2012</b> , 421, 548-60	63
755	Crystal structure of p44, a constitutively active splice variant of visual arrestin. 2012, 416, 611-8	47
754	Structural basis for the slow dark recovery of a full-length LOV protein from Pseudomonas putida. <b>2012</b> , 417, 362-74	42
753	Crystal structure of rice Rubisco and implications for activation induced by positive effectors NADPH and 6-phosphogluconate. <b>2012</b> , 422, 75-86	23
75 <sup>2</sup>	Structure-activity relationship of sphingomyelin analogs with sphingomyelinase from Bacillus cereus. <b>2012</b> , 1818, 474-80	6
751	Chain termini cross-talk in the swapping process of bovine pancreatic ribonuclease. 2012, 94, 1108-18	7
75°	Molecular dynamics, crystallography and mutagenesis studies on the substrate gating mechanism of prolyl oligopeptidase. <b>2012</b> , 94, 1398-411	43
749	Processive steps in the reverse direction require uncoupling of the lead head lever arm of myosin VI. <b>2012</b> , 48, 75-86	16
748	Bacterial and fungal chitinase chiJ orthologs evolve under different selective constraints following horizontal gene transfer. <b>2012</b> , 5, 581	13
747	Protein databases on the internet. <b>2012</b> , Chapter 2, Unit2.6	4
746	Structural analysis of specific metal chelating inhibitor binding to the endonuclease domain of influenza pH1N1 (2009) polymerase. <b>2012</b> , 8, e1002831	123
745	Structure and Behavior of Biomolecules from Raman Optical Activity. <b>2012</b> , 759-793	5
744	Complex of myoglobin with phenol bound in a proximal cavity. <b>2012</b> , 68, 1465-71	3
743	HMGB1-facilitated p53 DNA binding occurs via HMG-Box/p53 transactivation domain interaction, regulated by the acidic tail. <b>2012</b> , 20, 2014-24	89
742	Molecular modeling predicts structural changes in the A subunit of factor XIII caused by two novel mutations identified in a neonate with severe congenital factor XIII deficiency. <b>2012</b> , 130, 506-10	3

# (2012-2012)

741	MEROPS: the database of proteolytic enzymes, their substrates and inhibitors. <b>2012</b> , 40, D343-50	686
740	Metal ion dependency of serine racemase from Dictyostelium discoideum. <b>2012</b> , 43, 1567-76	15
739	Exploring protein dynamics space: the dynasome as the missing link between protein structure and function. <b>2012</b> , 7, e33931	65
738	Crystal structure of the Sema-PSI extracellular domain of human RON receptor tyrosine kinase. <b>2012</b> , 7, e41912	25
737	Structural basis of the substrate specificity of Bacillus cereus adenosine phosphorylase. <b>2012</b> , 68, 239-48	12
736	Mechanism of N10-formyltetrahydrofolate synthetase derived from complexes with intermediates and inhibitors. <b>2012</b> , 21, 219-28	17
735	Crystal structure of bacteriophage ?NIT1 zinc peptidase PghP that hydrolyzes Eglutamyl linkage of bacterial poly-Eglutamate. <b>2012</b> , 80, 722-32	4
734	Peptide and protein-based nanotubes for nanobiotechnology. <b>2012</b> , 4, 575-85	22
733	Analysis of the movements of helices in EF-hands. <b>2012</b> , 80, 2592-600	9
732	Quaternary ammonium oxidative demethylation: X-ray crystallographic, resonance Raman, and UV-visible spectroscopic analysis of a Rieske-type demethylase. <b>2012</b> , 134, 2823-34	39
731	Structure and mechanisms of Escherichia coli aspartate transcarbamoylase. 2012, 45, 444-53	35
730	Molecular and biochemical characterization of a unique mutation in CCS, the human copper chaperone to superoxide dismutase. <b>2012</b> , 33, 1207-15	27
729	Toward a Carbohydrate-Based HIV-1 Vaccine. <b>2012</b> , 187-215	3
728	Biochemical and structural characterization of the GTP-preferring succinyl-CoA synthetase from Thermus aquaticus. <b>2012</b> , 68, 751-62	6
727	Systematic analysis of pyrazinamide-resistant spontaneous mutants and clinical isolates of Mycobacterium tuberculosis. <b>2012</b> , 56, 5186-93	71
726	Design, synthesis, calorimetry, and crystallographic analysis of 2-alkylaminoethyl-1,1-bisphosphonates as inhibitors of Trypanosoma cruzi farnesyl diphosphate synthase. <b>2012</b> , 55, 6445-54	28
725	Sialyldisaccharide conformations: a molecular dynamics perspective. <b>2012</b> , 26, 375-85	7
724	An improved algorithm for MFR fragment assembly. <b>2012</b> , 53, 149-59	5

723	Electron self-exchange and self-amplified posttranslational modification in the hemoglobins from Synechocystis sp. PCC 6803 and Synechococcus sp. PCC 7002. <b>2012</b> , 17, 599-609	18
722	Mechanism for folate-independent aldolase reaction catalyzed by serine hydroxymethyltransferase. <b>2012</b> , 279, 504-14	13
721	Redesign of coenzyme B(12) dependent diol dehydratase to be resistant to the mechanism-based inactivation by glycerol and act on longer chain 1,2-diols. <b>2012</b> , 279, 793-804	30
720	Molecular dynamics simulation and quantum mechanical calculations on ⊞-N-acetylneuraminic acid. <b>2012</b> , 351, 93-7	9
719	Characterization of BshA, bacillithiol glycosyltransferase from Staphylococcus aureus and Bacillus subtilis. <b>2012</b> , 586, 1004-8	17
718	Crystal structures of the state 1 conformations of the GTP-bound H-Ras protein and its oncogenic G12V and Q61L mutants. <b>2012</b> , 586, 1715-8	49
717	Design of [(2-pyrimidinylthio)acetyl]benzenesulfonamides as inhibitors of human carbonic anhydrases. <b>2012</b> , 51, 259-70	30
716	N-(4-Substituted-benzoyl)-N'-(毗-glucopyranosyl)ureas as inhibitors of glycogen phosphorylase: Synthesis and evaluation by kinetic, crystallographic, and molecular modelling methods. <b>2012</b> , 20, 1801-16	13
715	Design and synthesis of novel inhibitors of human kynurenine aminotransferase-I. <b>2012</b> , 22, 1579-81	14
714	3'-axial CH2 OH substitution on glucopyranose does not increase glycogen phosphorylase inhibitory potency. QM/MM-PBSA calculations suggest why. <b>2012</b> , 79, 663-73	19
713	Three-dimensional structure of a schistosome serpin revealing an unusual configuration of the helical subdomain. <b>2012</b> , 68, 686-94	5
712	Structures of the pleckstrin homology domain of Saccharomyces cerevisiae Avo1 and its human orthologue Sin1, an essential subunit of TOR complex 2. <b>2012</b> , 68, 386-92	22
711	Crystal structure analysis of a recombinant predicted acetamidase/formamidase from the thermophile Thermoanaerobacter tengcongensis. <b>2012</b> , 31, 166-74	4
710	Parameterization of the prosthetic redox centers of the bacterial cytochrome bc 1 complex for atomistic molecular dynamics simulations. <b>2013</b> , 132, 1	15
709	Full-length structure of a sensor histidine kinase pinpoints coaxial coiled coils as signal transducers and modulators. <b>2013</b> , 21, 1127-36	140
708	The glyoxylate cycle is involved in pleotropic phenotypes, antagonism and induction of plant defence responses in the fungal biocontrol agent Trichoderma atroviride. <b>2013</b> , 58-59, 33-41	21
707	4-Substituted-2,3,5,6-tetrafluorobenzenesulfonamides as inhibitors of carbonic anhydrases I, II, VII, XII, and XIII. <b>2013</b> , 21, 2093-106	58
706	The presence of outer arm fucose residues on the N-glycans of tissue inhibitor of metalloproteinases-1 reduces its activity. <b>2013</b> , 12, 3547-60	13

# (2013-2013)

705	Effect of the ring size and asymmetry of cyclodextrins on their inclusion ability: a theoretical study. <b>2013</b> , 77, 439-445	7
704	MMGBSA as a tool to understand the binding affinities of filamin-peptide interactions. <b>2013</b> , 53, 2626-33	129
703	Catalytic mechanism of serine racemase from Dictyostelium discoideum. 2013, 44, 1073-84	17
702	An efficient trypsin digestion strategy for improving desB30 productivity from recombinant human insulin precursor fusion protein. <b>2013</b> , 48, 965-971	4
701	The globins of cyanobacteria and algae. <b>2013</b> , 63, 195-272	12
700	Structural basis of preferential binding of fucose-containing saccharide by the Caenorhabditis elegans galectin LEC-6. <b>2013</b> , 23, 797-805	11
699	Essential roles of nucleotide-switch and metal-coordinating residues for chaperone function of diol dehydratase-reactivase. <b>2013</b> , 52, 8677-86	4
698	Protease Families, Evolution and Mechanism of Action. <b>2013</b> , 1-36	5
697	Interaction of profilin with the barbed end of actin filaments. 2013, 52, 6456-66	56
696	3-Phosphoglycerate is an allosteric activator of pyruvate kinase from the hyperthermophilic archaeon Pyrobaculum aerophilum. <b>2013</b> , 52, 5865-75	7
695	Crystal structure of a Na+-bound Na+,K+-ATPase preceding the E1P state. <b>2013</b> , 502, 201-6	202
694	Elastic network models: theoretical and empirical foundations. <b>2013</b> , 924, 601-16	30
693	Diversity and catalytic potential of PAH-specific ring-hydroxylating dioxygenases from a hydrocarbon-contaminated soil. <b>2013</b> , 97, 5125-35	27
692	Effect of antimicrobial preservatives on partial protein unfolding and aggregation. 2013, 102, 365-76	19
691	Structure of the Toxoplasma gondii ROP18 kinase domain reveals a second ligand binding pocket required for acute virulence. <b>2013</b> , 288, 34968-80	14
690	Atomistic simulations indicate cardiolipin to have an integral role in the structure of the cytochrome bc1 complex. <b>2013</b> , 1827, 769-78	46
689	The guanine nucleotide exchange factor Rlf interacts with SH3 domain-containing proteins via a binding site with a preselected conformation. <b>2013</b> , 183, 312-319	1
688	A 2.1-E-esolution crystal structure of unliganded CRM1 reveals the mechanism of autoinhibition. <b>2013</b> , 425, 350-64	25

687	The structure of a novel glucuronoyl esterase from Myceliophthora thermophila gives new insights into its role as a potential biocatalyst. <b>2013</b> , 69, 63-73	29
686	Raman spectroscopy of proteins and nucleoproteins. <b>2013</b> , Chapter 17, Unit17.8	24
685	Crystal structures of the calcium pump and sarcolipin in the Mg2+-bound E1 state. <b>2013</b> , 495, 260-4	171
684	Structure of Vibrio cholerae ribosome hibernation promoting factor. <b>2013</b> , 69, 228-36	8
683	Structure of full-length Toxascaris leonina galectin with two carbohydrate-recognition domains. <b>2013</b> , 69, 168-75	4
682	Incorporation of non-natural amino acids improves cell permeability and potency of specific inhibitors of proteasome trypsin-like sites. <b>2013</b> , 56, 1262-75	66
681	Unanswered questions about the structure of cytochrome bc1 complexes. <b>2013</b> , 1827, 1258-77	38
68o	2NH and 3OH are crucial structural requirements in sphingomyelin for sticholysin II binding and pore formation in bilayer membranes. <b>2013</b> , 1828, 1390-5	39
679	Sourcing the affinity of flavonoids for the glycogen phosphorylase inhibitor site via crystallography, kinetics and QM/MM-PBSA binding studies: comparison of chrysin and flavopiridol. <b>2013</b> , 61, 14-27	23
678	Structural and functional characterization of MppR, an enduracididine biosynthetic enzyme from streptomyces hygroscopicus: functional diversity in the acetoacetate decarboxylase-like superfamily. <b>2013</b> , 52, 4492-506	20
677	Structural consequences of cutting a binding loop: two circularly permuted variants of streptavidin. <b>2013</b> , 69, 968-77	5
676	Selectivity of CDC25 homology domain-containing guanine nucleotide exchange factors. <b>2013</b> , 425, 2782-94	14
675	Introduction. 2013, li-liv	8
674	Eukaryotic GPN-loop GTPases paralogs use a dimeric assembly reminiscent of archeal GPN. <b>2013</b> , 12, 463-72	17
673	Conserved water molecules in family 1 glycosidases: a DXMS and molecular dynamics study. <b>2013</b> , 52, 5900-10	29
672	Mechanism of displacement of a catalytically essential loop from the active site of mammalian fructose-1,6-bisphosphatase. <b>2013</b> , 52, 5206-16	4
671	Crystal structure of peanut (Arachis hypogaea) allergen Ara h 5. <b>2013</b> , 61, 1573-8	19
670	Structural basis for the divergence of substrate specificity and biological function within HAD phosphatases in lipopolysaccharide and sialic acid biosynthesis. <b>2013</b> , 52, 5372-86	17

669	Automatic protein structure solution from weak X-ray data. <b>2013</b> , 4, 2777	177
668	Between-strand disulfides: forbidden disulfides linking adjacent \$\textit{B}\trands. \textit{2013}, 3, 24680	7
667	Cathepsin F mutations cause Type B Kufs disease, an adult-onset neuronal ceroid lipofuscinosis. <b>2013</b> , 22, 1417-23	90
666	Natriuretic peptide receptor-3 gene (NPR3): nonsynonymous polymorphism results in significant reduction in protein expression because of accelerated degradation. <b>2013</b> , 6, 201-10	9
665	Direct metal recognition by guanine nucleotide-exchange factor in the initial step of the exchange reaction. <b>2013</b> , 69, 345-51	2
664	mrtailor: a tool for PDB-file preparation for the generation of external restraints. 2013, 69, 1861-3	4
663	High-resolution structure of a papaya plant-defense barwin-like protein solved by in-house sulfur-SAD phasing. <b>2013</b> , 69, 2017-26	10
662	Structure of a filament of stacked octamers of human DMC1 recombinase. <b>2013</b> , 69, 382-6	3
661	Evolution of vitamin B2 biosynthesis: eubacterial RibG and fungal Rib2 deaminases. 2013, 69, 227-36	4
660	High-resolution crystal structure of human Dim2/TXNL4B. <b>2013</b> , 69, 223-7	3
659	3D Visualization for Life Sciences. <b>2013</b> , 387-404	
658	Crystal structures of carbamate kinase from Giardia lamblia bound with citric acid and AMP-PNP. <b>2013</b> , 8, e64004	4
657	Structural and functional characterisation of TesA - a novel lysophospholipase A from Pseudomonas aeruginosa. <b>2013</b> , 8, e69125	39
656	A remote palm domain residue of RB69 DNA polymerase is critical for enzyme activity and influences the conformation of the active site. <b>2013</b> , 8, e76700	6
655	Two structural motifs within canonical EF-hand calcium-binding domains identify five different classes of calcium buffers and sensors. <b>2014</b> , 9, e109287	39
654	4-amino-substituted benzenesulfonamides as inhibitors of human carbonic anhydrases. <b>2014</b> , 19, 17356-80	16
653	Structural basis for inactivation of Giardia lamblia carbamate kinase by disulfiram. <b>2014</b> , 289, 10502-10509	41
652	Structure and mechanism of the bifunctional CinA enzyme from Thermus thermophilus. <b>2014</b> , 289, 33187-97	8

651	Calcium-dependent energetics of calmodulin domain interactions with regulatory regions of the Ryanodine Receptor Type 1 (RyR1). <b>2014</b> , 193-194, 35-49	7
650	Crystal structure of the R-protein of the multisubunit ATP-dependent restriction endonuclease NgoAVII. <b>2014</b> , 42, 14022-30	7
649	Protein Quaternary Structure: Symmetry Patterns. <b>2014</b> ,	
648	Structural and thermodynamic basis of the inhibition of Leishmania major farnesyl diphosphate synthase by nitrogen-containing bisphosphonates. <b>2014</b> , 70, 802-10	17
647	17⊞hydroxylase deficiency diagnosed in early infancy caused by a novel mutation of the CYP17A1 gene. <b>2014</b> , 81, 350-5	3
646	Structural effect of the Asp345a insertion in penicillin-binding protein 2 from penicillin-resistant strains of Neisseria gonorrhoeae. <b>2014</b> , 53, 7596-603	12
645	Thalidomide mimics uridine binding to an aromatic cage in cereblon. <b>2014</b> , 188, 225-32	35
644	Crystal structure determination of anti-DNA Fab A52. <b>2014</b> , 82, 1674-8	6
643	An activin A/BMP2 chimera, AB204, displays bone-healing properties superior to those of BMP2. <b>2014</b> , 29, 1950-9	25
642	Structural insight into the specificity of the B3 DNA-binding domains provided by the co-crystal structure of the C-terminal fragment of Bfil restriction enzyme. <b>2014</b> , 42, 4113-22	19
641	Crystallographic and molecular dynamics simulation analysis of Escherichia coli dihydroneopterin aldolase. <b>2014</b> , 4, 52	5
640	ModBase, a database of annotated comparative protein structure models and associated resources. <b>2014</b> , 42, D336-46	207
639	The core of allosteric motion in Thermus caldophilus L-lactate dehydrogenase. <b>2014</b> , 289, 31550-64	7
638	The structure of rice weevil pectin methylesterase. <b>2014</b> , 70, 1480-4	11
637	Characterisation of three novel CYP11B1 mutations in classic and non-classic 11即ydroxylase deficiency. <b>2014</b> , 170, 697-706	16
636	Crystal structure of the tetrameric fibrinogen-like recognition domain of fibrinogen C domain containing 1 (FIBCD1) protein. <b>2014</b> , 289, 2880-7	17
635	Structural basis for the binding specificity of human Recepteur d'Origine Nantais (RON) receptor tyrosine kinase to macrophage-stimulating protein. <b>2014</b> , 289, 29948-60	16
634	Reversal of the DNA-binding-induced loop L1 conformational switch in an engineered human p53 protein. <b>2014</b> , 426, 936-44	24

# (2014-2014)

633	Crystallographic snapshot of the Escherichia coli EnvZ histidine kinase in an active conformation. <b>2014</b> , 186, 376-9	40
632	Insights into the binding specificity of wild type and mutated wheat germ agglutinin towards Neu5Ac(2-3)Gal: a study by in silico mutations and molecular dynamics simulations. <b>2014</b> , 27, 482-92	10
631	Congenital adrenal hyperplasia due to 11-beta-hydroxylase deficiency: functional consequences of four CYP11B1 mutations. <b>2014</b> , 22, 610-6	33
630	Cobalamin-dependent dehydratases and a deaminase: radical catalysis and reactivating chaperones. <b>2014</b> , 544, 40-57	45
629	A widespread glutamine-sensing mechanism in the plant kingdom. <b>2014</b> , 159, 1188-1199	86
628	Structural studies of cinnamoyl-CoA reductase and cinnamyl-alcohol dehydrogenase, key enzymes of monolignol biosynthesis. <b>2014</b> , 26, 3709-27	48
627	Discovery and characterization of novel selective inhibitors of carbonic anhydrase IX. <b>2014</b> , 57, 9435-46	65
626	Chromatin structure revealed by X-ray scattering analysis and computational modeling. <b>2014</b> , 70, 154-61	22
625	Rice cytochrome P450 MAX1 homologs catalyze distinct steps in strigolactone biosynthesis. <b>2014</b> , 10, 1028-33	230
624	Protein Stability. <b>2014</b> ,	5
624	Protein Stability. 2014,  Crystal structure of Korean pine (Pinus koraiensis) 7S seed storage protein with copper ligands. 2014, 62, 222-8	5
	Crystal structure of Korean pine (Pinus koraiensis) 7S seed storage protein with copper ligands.	
623	Crystal structure of Korean pine (Pinus koraiensis) 7S seed storage protein with copper ligands. <b>2014</b> , 62, 222-8	17
623	Crystal structure of Korean pine (Pinus koraiensis) 7S seed storage protein with copper ligands.  2014, 62, 222-8  Thermal adaptation of Emylases: a review. 2014, 18, 937-44  Molecular phylogeny and intricate evolutionary history of the three isofunctional enzymes involved	17 28
623 622 621	Crystal structure of Korean pine (Pinus koraiensis) 7S seed storage protein with copper ligands. 2014, 62, 222-8  Thermal adaptation of the mylases: a review. 2014, 18, 937-44  Molecular phylogeny and intricate evolutionary history of the three isofunctional enzymes involved in the oxidation of protoporphyrinogen IX. 2014, 6, 2141-55	17 28 37
623 622 621	Crystal structure of Korean pine (Pinus koraiensis) 7S seed storage protein with copper ligands. 2014, 62, 222-8  Thermal adaptation of Emylases: a review. 2014, 18, 937-44  Molecular phylogeny and intricate evolutionary history of the three isofunctional enzymes involved in the oxidation of protoporphyrinogen IX. 2014, 6, 2141-55  Tryptophan 19 residue is the origin of bovine Eactoglobulin fluorescence. 2014, 91, 144-50	17 28 37 42
623 622 621 620	Crystal structure of Korean pine (Pinus koraiensis) 7S seed storage protein with copper ligands. 2014, 62, 222-8  Thermal adaptation of Eamylases: a review. 2014, 18, 937-44  Molecular phylogeny and intricate evolutionary history of the three isofunctional enzymes involved in the oxidation of protoporphyrinogen IX. 2014, 6, 2141-55  Tryptophan 19 residue is the origin of bovine Eactoglobulin fluorescence. 2014, 91, 144-50  Your personalized protein structure: Andrei N. Lupas fused to GCN4 adaptors. 2014, 186, 380-5  Designer nodal/BMP2 chimeras mimic nodal signaling, promote chondrogenesis, and reveal a	17 28 37 42

615 The 11-Heme Cell-Surface Cytochrome UndA of Shewanella sp. HRCR-6. **2014**, 1-6

614	MUFOLD-DB: a processed protein structure database for protein structure prediction and analysis. <b>2014</b> , 15 Suppl 11, S2	5
613	Lethal Neonatal Progression of Fetal Cardiomegaly Associated to ACAD9 Deficiency. <b>2015</b> , 1	10
612	Inhibition of human GLUT1 and GLUT5 by plant carbohydrate products; insights into transport specificity. <b>2015</b> , 5, 12804	35
611	Interaction of Epac with Non-canonical Cyclic Nucleotides. <b>2017</b> , 238, 135-147	3
610	Cross-strand disulfides in the non-hydrogen bonding site of antiparallel	4
609	Structure of importin-bound to a non-classical nuclear localization signal of the influenza A virus nucleoprotein. <b>2015</b> , 5, 15055	29
608	Structure of a thermophilic F1-ATPase inhibited by an Bubunit: deeper insight into the Enhibition mechanism. <b>2015</b> , 282, 2895-913	63
607	Theoretical investigation on the glycan-binding specificity of Agrocybe cylindracea galectin using molecular modeling and molecular dynamics simulation studies. <b>2015</b> , 28, 528-38	10
606	Comparison of epsilon- and delta-class glutathione S-transferases: the crystal structures of the glutathione S-transferases DmGSTE6 and DmGSTE7 from Drosophila melanogaster. <b>2015</b> , 71, 2089-98	7
605	Tandem fusion of hepatitis B core antigen allows assembly of virus-like particles in bacteria and plants with enhanced capacity to accommodate foreign proteins. <b>2015</b> , 10, e0120751	73
604	An Accurate Model for Biomolecular Helices and Its Application to Helix Visualization. <b>2015</b> , 10, e0129653	2
603	Sbi00515, a Protein of Unknown Function from Streptomyces bingchenggensis, Highlights the Functional Versatility of the Acetoacetate Decarboxylase Scaffold. <b>2015</b> , 54, 3978-88	2
602	The Radical S-Adenosyl-L-methionine Enzyme QhpD Catalyzes Sequential Formation of Intra-protein Sulfur-to-Methylene Carbon Thioether Bonds. <b>2015</b> , 290, 11144-66	31
601	A positive genotype-phenotype correlation in a large cohort of patients with Pseudohypoparathyroidism Type Ia and Pseudo-pseudohypoparathyroidism and 33 newly identified mutations in the GNAS gene. <b>2015</b> , 3, 111-20	38
600	Functional significance of protein assemblies predicted by the crystal structure of the restriction endonuclease BsaWl. <b>2015</b> , 43, 8100-10	7
599	Structural Basis of Species-Dependent Differential Affinity of 6-Alkoxy-5-Aryl-3-Pyridinecarboxamide Cannabinoid-1 Receptor Antagonists. <b>2015</b> , 88, 238-44	13
598	Streptomyces wadayamensis MppP Is a Pyridoxal 5'-Phosphate-Dependent L-Arginine Deaminase, Elydroxylase in the Enduracididine Biosynthetic Pathway. <b>2015</b> , 54, 7029-40	27

597	Nicotinamide mononucleotide adenylyltransferase displays alternate binding modes for nicotinamide nucleotides. <b>2015</b> , 71, 2032-9	2
596	Residues required for phosphorylation of translation initiation factor eIF2 under diverse stress conditions are divergent between yeast and human. <b>2015</b> , 59, 135-41	4
595	Crystal and molecular structure of the analgesic tetrapeptide, L-Phe-L-Leu-L-Pro-L-Ser. <b>2015</b> , 104, 84-90	
594	Structure and function of a short LOV protein from the marine phototrophic bacterium Dinoroseobacter shibae. <b>2015</b> , 15, 30	23
593	The mammalian autophagy initiator complex contains 2 HORMA domain proteins. 2015, 11, 2300-8	22
592	Functionalization of fluorinated benzenesulfonamides and their inhibitory properties toward carbonic anhydrases. <b>2015</b> , 10, 662-87	30
591	Beyond the International Year of Crystallography. <i>Journal of Applied Crystallography</i> , <b>2015</b> , 48, 1-2 3.8	2
590	Geometry Optimization of Carbohydrate Binding Sites of Influenza: A Quantum Mechanical Approach. <b>2015</b> , 34, 409-429	2
589	A cerato-platanin-like protein HaCPL2 from Heterobasidion annosum sensu stricto induces cell death in Nicotiana tabacum and Pinus sylvestris. <b>2015</b> , 84, 41-51	16
588	Plant immunophilins: a review of their structure-function relationship. <b>2015</b> , 1850, 2145-58	29
587	Conformational Polymorphism in Autophagy-Related Protein GATE-16. <b>2015</b> , 54, 5469-79	14
586	Antipsychotics inhibit glucose transport: Determination of olanzapine binding site in Staphylococcus epidermidis glucose/H(+) symporter. <b>2015</b> , 5, 335-40	7
585	Crystal structure of the HIV neutralizing antibody 2G12 in complex with a bacterial oligosaccharide analog of mammalian oligomannose. <b>2015</b> , 25, 412-9	23
584	Soluble human TLR2 ectodomain binds diacylglycerol from microbial lipopeptides and glycolipids. <b>2015</b> , 21, 175-93	21
583	Roll of hemagglutinin gene in the biology of avian influenza virus. <b>2016</b> , 6, 443-446	
582	Crystal Structure of a Complex of Surfactant Protein D (SP-D) and Haemophilus influenzae Lipopolysaccharide Reveals Shielding of Core Structures in SP-D-Resistant Strains. <b>2016</b> , 84, 1585-1592	12
581	Restriction endonuclease Agel is a monomer which dimerizes to cleave DNA. 2017, 45, 3547-3558	10
580	Towards recognition of protein function based on its structure using deep convolutional networks. <b>2016</b> ,	9

579	Nucleosomal arrays self-assemble into supramolecular globular structures lacking 30-nm fibers. <b>2016</b> , 35, 1115-32	124
578	Structure analysis of a glycosides hydrolase family 42 cold-adapted 暇alactosidase from Rahnella sp. R3. <b>2016</b> , 6, 37362-37369	6
577	Biochemical and biophysical combined study of bicarinalin, an ant venom antimicrobial peptide. <b>2016</b> , 79, 103-13	25
576	The Pichia pastoris transmembrane protein GT1 is a glycerol transporter and relieves the repression of glycerol on AOX1 expression. <b>2016</b> , 16,	15
575	Identification and Characterization of a New Pecan [Carya illinoinensis (Wangenh.) K. Koch] Allergen, Car i 2. <b>2016</b> , 64, 4146-51	19
574	S-Nitrosylation Induces Structural and Dynamical Changes in a Rhodanese Family Protein. <b>2016</b> , 428, 3737-51	9
573	Iron Storage Proteins. <b>2016</b> , 300-345	1
572	Signaling States of a Short Blue-Light Photoreceptor Protein PpSB1-LOV Revealed from Crystal Structures and Solution NMR Spectroscopy. <b>2016</b> , 428, 3721-36	21
571	UDP-galactose and acetyl-CoA transporters as Plasmodium multidrug resistance genes. <b>2016</b> , 1, 16166	67
570	Discovery of a specific inhibitor of human GLUT5 by virtual screening and in vitro transport evaluation. <b>2016</b> , 6, 24240	30
569	Complete structure of the bacterial flagellar hook reveals extensive set of stabilizing interactions. <b>2016</b> , 7, 13425	35
568	Periplasmic Cytophaga hutchinsonii Endoglucanases Are Required for Use of Crystalline Cellulose as the Sole Source of Carbon and Energy. <b>2016</b> , 82, 4835-4845	31
567	Molecular mechanism underlying promiscuous polyamine recognition by spermidine acetyltransferase. <b>2016</b> , 76, 87-97	6
566	Global molecular analysis and APOE mutations in a cohort of autosomal dominant hypercholesterolemia patients in France. <b>2016</b> , 57, 482-91	17
565	The structure of the Guanine Nucleotide Exchange Factor Rlf in complex with the small G-protein Ral identifies conformational intermediates of the exchange reaction and the basis for the selectivity. <b>2016</b> , 193, 106-14	6
564	Mechanistic Insights from Structural Analyses of Ran-GTPase-Driven Nuclear Export of Proteins and RNAs. <b>2016</b> , 428, 2025-39	32
563	Enzymatic Conversion of CO2 (Carboxylation Reactions and Reduction to Energy-Rich C1 Molecules). <b>2016</b> , 347-371	4
562	NtRING1, putative RING-finger E3 ligase protein, is a positive regulator of the early stages of elicitin-induced HR in tobacco. <b>2016</b> , 35, 415-28	7

561	Structures of the Karyopherins Kap121p and Kap60p Bound to the Nuclear Pore-Targeting Domain of the SUMO Protease Ulp1p. <b>2017</b> , 429, 249-260	5
560	A RuBisCO-mediated carbon metabolic pathway in methanogenic archaea. <b>2017</b> , 8, 14007	60
559	Novel calcium recognition constructions in proteins: Calcium blade and EF-hand zone. 2017, 483, 958-963	3
558	Crystal structures of the NO sensor NsrR reveal how its iron-sulfur cluster modulates DNA binding. <b>2017</b> , 8, 15052	40
557	Protein-phospholipid interplay revealed with crystals of a calcium pump. <b>2017</b> , 545, 193-198	96
556	Intrinsic Thermodynamics and Structures of 2,4- and 3,4-Substituted Fluorinated Benzenesulfonamides Binding to Carbonic Anhydrases. <b>2017</b> , 12, 161-176	18
555	Dynamics of Lysine as a Heme Axial Ligand: NMR Analysis of the Chlamydomonas reinhardtii Hemoglobin THB1. <b>2017</b> , 56, 551-569	14
554	CYPome of the conifer pathogen Heterobasidion irregulare: Inventory, phylogeny, and transcriptional analysis of the response to biocontrol. <b>2017</b> , 121, 158-171	7
553	CELSR2, encoding a planar cell polarity protein, is a putative gene in Joubert syndrome with cortical heterotopia, microophthalmia, and growth hormone deficiency. <b>2017</b> , 173, 661-666	17
552	Building kit for metal cation binding sites in proteins. <b>2017</b> , 494, 311-317	1
551	Theoretical investigation on the binding specificity of fluorinated sialyldisaccharides Neu5Act也)Gal and Neu5Act也)Gal with influenza hemagglutinin H1 A Molecular Dynamics Study. <b>2017</b> , 36, 111-128	4
550	Rhorix: An interface between quantum chemical topology and the 3D graphics program blender. <b>2017</b> , 38, 2538-2552	7
549	Small molecule metalloprotease inhibitor with inlyitro, exlyivo and inlyivo efficacy against botulinum neurotoxin serotype A. <b>2017</b> , 137, 36-47	7
548	Fumarate and Nitrate Reduction Regulator (FNR). 2017, 1-11	1
547	Crystal structure of tripartite-type ABC transporter MacB from Acinetobacter baumannii. 2017, 8, 1336	50
546	Radical S-Adenosyl-l-Methionine Carbon Monoxide and Cyanide Synthase HydG. <b>2017</b> , 1-10	
545	Streptomyces wadayamensis MppP is a PLP-Dependent Oxidase, Not an Oxygenase. <b>2018</b> , 57, 3252-3264	12
544	Crystallographic Trapping of Reaction Intermediates in Quinolinic Acid Synthesis by NadA. <b>2018</b> , 13, 1209-12	1 <b>7</b> 5

543	On the Trails of the Proteasome Fold: Structural and Functional Analysis of the Ancestral <b>Subunit</b> Protein Anbu. <b>2018</b> , 430, 628-640	3
542	Loss of function mutations in VARS encoding cytoplasmic valyl-tRNA synthetase cause microcephaly, seizures, and progressive cerebral atrophy. <b>2018</b> , 137, 293-303	10
541	Top surface blade residues and the central channel water molecules are conserved in every repeat of the integrin-like 中ropeller structures. <b>2018</b> , 201, 155-161	2
540	Simulated Raman spectra of four tetraphenylbutadiene polymorphs. <b>2018</b> , 118, e25503	2
539	VIPERdb: A Tool for Virus Research. <b>2018</b> , 5, 477-488	20
538	Peptide and Protein Structure Prediction with a Simplified Continuum Solvent Model. <b>2018</b> , 122, 11355-1136	52 1
537	Chemical Ligand Space of Cereblon. 2018, 3, 11163-11171	21
536	Bouganin, an Attractive Weapon for Immunotoxins. 2018, 10,	7
535	Homology Modeling for Enzyme Design. <b>2018</b> , 1796, 301-320	1
534	Identifying G protein-coupled receptor dimers from crystal packings. <b>2018</b> , 74, 655-670	13
533	Improving Docking Performance Using Negative Image-Based Rescoring. 2018, 9, 260	16
532	Perspectives on Structural Molecular Biology Visualization: From Past to Present. <b>2018</b> , 430, 3997-4012	44
531	Mechanistic Basis of the Fast Dark Recovery of the Short LOV Protein DsLOV from Dinoroseobacter shibae. <b>2018</b> , 57, 4833-4847	9
530	Structure-Activity Relationship Analysis of 3-Phenylcoumarin-Based Monoamine Oxidase B Inhibitors. <b>2018</b> , 6, 41	28
529	Molecular Illustration in Research and Education: Past, Present, and Future. 2018, 430, 3969-3981	34
528	RitR is an archetype for a novel family of redox sensors in the streptococci that has evolved from two-component response regulators and is required for pneumococcal colonization. <b>2018</b> , 14, e1007052	11
527	Discovery of Retinoic Acid-Related Orphan Receptor Il Inverse Agonists via Docking and Negative Image-Based Screening. <b>2018</b> , 3, 6259-6266	5
526	Machilin A Inhibits Tumor Growth and Macrophage M2 Polarization Through the Reduction of Lactic Acid. <b>2019</b> , 11,	15

525	Investigation on the binding specificity of Agrocybe cylindracea galectin towards 仅,6)-linked sialyllactose by molecular modeling and molecular dynamics simulations. <b>2019</b> , 38, 566-585	1
524	De Novo Heterozygous POLR2A Variants Cause a Neurodevelopmental Syndrome with Profound Infantile-Onset Hypotonia. <b>2019</b> , 105, 283-301	20
523	Fragment- and negative image-based screening of phosphodiesterase 10A inhibitors. <b>2019</b> , 94, 1799-1812	7
522	Solution structure of the autophagy-related protein LC3C reveals a polyproline II motif on a mobile tether with phosphorylation site. <b>2019</b> , 9, 14167	8
521	Illustrate: Software for Biomolecular Illustration. <b>2019</b> , 27, 1716-1720.e1	57
520	Enhancing Understanding in Biochemistry Using 3D Printing and Cheminformatics Technologies: A Student Perspective. <b>2019</b> , 96, 2497-2502	7
519	Web 3DNA 2.0 for the analysis, visualization, and modeling of 3D nucleic acid structures. <b>2019</b> , 47, W26-W34	81
518	Functional characterisation of a novel class of in-frame insertion variants of KRAS and HRAS. <b>2019</b> , 9, 8239	2
517	Biallelic HEPHL1 variants impair ferroxidase activity and cause an abnormal hair phenotype. <b>2019</b> , 15, e1008143	13
516	A Practical Perspective: The Effect of Ligand Conformers on the Negative Image-Based Screening. <b>2019</b> , 20,	6
515	Importance of the Cys-Cys intermolecular disulfide bonding for oligomeric assembly and hemolytic activity of the Helicobacter pylori TlyA hemolysin. <b>2019</b> , 514, 365-371	2
514	The Evolution of SlyA/RovA Transcription Factors from Repressors to Countersilencers in. <b>2019</b> , 10,	12
513	GLS hyperactivity causes glutamate excess, infantile cataract and profound developmental delay. <b>2019</b> , 28, 96-104	11
512	Identification of a Loss-of-Function Mutation in the Context of Glutaminase Deficiency and Neonatal Epileptic Encephalopathy. <b>2019</b> , 76, 342-350	17
511	A comprehensive analysis of the protein-ligand interactions in crystal structures of Mycobacterium tuberculosis EthR. <b>2019</b> , 1867, 248-258	8
510	Unique mechanism of target recognition by PfoI restriction endonuclease of the CCGG-family. <b>2019</b> , 47, 997-1010	3
509	Distinctive structural motifs co-ordinate the catalytic nucleophile and the residues of the oxyanion hole in the alpha/beta-hydrolase fold enzymes. <b>2019</b> , 28, 344-364	13
508	Design of fluorinated sialic acid analog inhibitor to H5 hemagglutinin of H5N1 influenza virus through molecular dynamics simulation study. <b>2020</b> , 38, 3504-3513	1

507	Cyclization mechanism catalyzed by an ATP-grasp enzyme essential for d-cycloserine biosynthesis. <b>2020</b> , 287, 2763-2778	3
506	LARMD: integration of bioinformatic resources to profile ligand-driven protein dynamics with a case on the activation of estrogen receptor. <b>2020</b> , 21, 2206-2218	65
505	What ATP binding does to the Ca pump and how nonproductive phosphoryl transfer is prevented in the absence of Ca. <b>2020</b> , 117, 18448-18458	7
504	A monodomain class II terpene cyclase assembles complex isoprenoid scaffolds. <b>2020</b> , 12, 968-972	10
503	Papain-like cysteine proteinase zone (PCP-zone) and PCP structural catalytic core (PCP-SCC) of enzymes with cysteine proteinase fold. <b>2020</b> , 165, 1438-1446	2
502	Interferon Beta Activity Is Modulated via Binding of Specific S100 Proteins. <b>2020</b> , 21,	2
501	NBCZone: Universal three-dimensional construction of eleven amino acids near the catalytic nucleophile and base in the superfamily of (chymo)trypsin-like serine fold proteases. <b>2020</b> , 153, 399-411	4
500	A point mutation in the nuclease domain of MLH3 eliminates repeat expansions in a mouse stem cell model of the Fragile X-related disorders. <b>2020</b> , 48, 7856-7863	13
499	Biochemical and Molecular Characterization of Cells Expressing Multiple TMOF Genes (A) for Mosquito Larval Control. <b>2020</b> , 11, 527	1
498	Inhibition of human CYP1 enzymes by a classical inhibitor Enaphthoflavone and a novel inhibitor N-(3, 5-dichlorophenyl)cyclopropanecarboxamide: An in vitro and in silico study. <b>2020</b> , 95, 520-533	6
497	The acid-base-nucleophile catalytic triad in ABH-fold enzymes is coordinated by a set of structural elements. <b>2020</b> , 15, e0229376	8
496	Structural and functional relationship of Cassia obtusifolia trypsin inhibitor to understand its digestive resistance against Pieris rapae. <b>2020</b> , 148, 908-920	7
495	System Approach for Building of Calcium-Binding Sites in Proteins. <b>2020</b> , 10,	
494	An insight on egg white: From most common functional food to biomaterial application. <b>2021</b> , 109, 1045-105	58 11
493	Research progress of single molecule force spectroscopy technology based on atomic force microscopy in polymer materials: Structure, design strategy and probe modification. <b>2021</b> , 2, 909-931	3
492	Structural determinants underlying the adduct lifetime in the LOV proteins of Pseudomonas putida. <b>2021</b> , 288, 4955-4972	1
491	Structural leitmotif and functional variations of the structural catalytic core in (chymo)trypsin-like serine/cysteine fold proteinases. <b>2021</b> , 179, 601-609	2
490	Treatment of ARS deficiencies with specific amino acids. <b>2021</b> , 23, 2202-2207	6

489	N1 neuraminidase of H5N1 avian influenza A virus complexed with sialic acid and zanamivir - A study by molecular docking and molecular dynamics simulation. <b>2021</b> , 1-14	1
488	Crystal structure of restriction endonuclease Kpn2I of CCGG-family. <b>2021</b> , 1865, 129926	
487	Crystallographic investigation of the ubiquinone binding site of respiratory Complex II and its inhibitors. <b>2021</b> , 1869, 140679	4
486	PTMdyna: exploring the influence of post-translation modifications on protein conformational dynamics. <b>2021</b> ,	1
485	Pancreatic adenocarcinoma: molecular drivers and the role of targeted therapy. <b>2021</b> , 40, 355-371	3
484	Numerical criteria for the evaluation of ab initio predictions of protein structure. <b>1997</b> , 29, 140-150	1
483	Assessment of comparative modeling in CASP2. <b>1997</b> , 29, 14-28	9
482	Successful ab initio prediction of the tertiary structure of NK-lysin using multiple sequences and recognized supersecondary structural motifs. <b>1997</b> , 29, 185-191	13
481	Dissection of multi-protein complexes using mass spectrometry: Subunit interactions in transthyretin and retinol-binding protein complexes. <b>1998</b> , 33, 3-11	8
480	Successful recognition of protein folds using threading methods biased by sequence similarity and predicted secondary structure. <b>1999</b> , 37, 104-111	26
479	Ab initio protein structure prediction of CASP III targets using ROSETTA. <b>1999</b> , 37, 171-176	82
478	Angiogenin.	1
477	Prediction of Protein Structure Through Evolution. 1789-1811	5
476	Adsorption of proteins onto charged surfaces: A Monte Carlo approach with explicit ions. <b>1996</b> , 17, 1783-1803	3 20
475	Is the binding of beta-amyloid protein to antichymotrypsin in Alzheimer plaques mediated by a beta-strand insertion?. <b>1996</b> , 25, 420-4	12
474	Molecular mechanisms of pressure induced conformational changes in BPTI. <b>1996</b> , 25, 446-55	53
473	Comparative Binding Energy Analysis. <b>2002</b> , 19-34	2
472	The Structures of Photosynthetic Reaction Centers from Purple Bacteria as Revealed by X-Ray Crystallography. <b>1995</b> , 503-526	1

471	Thioredoxins in Cyanobacteria: Structure and Redox Regulation of Enzyme Activity. <b>1994</b> , 715-729	1
470	Structural Analysis of Rho Protein Complexes. <b>2005</b> , 31-72	1
469	3 Structure of ribonucleases. 3001-3006	1
468	Multiple Alignment of Protein Structures in Three Dimensions. <b>2005</b> , 67-78	27
467	VIII. Protein Folding Simulations by a Generalized-Ensemble Algorithm Based on Tsallis Statistics. <b>2001</b> , 259-274	1
466	Protein engineering of cytochrome P450cam. <b>1997</b> , 175-207	19
465	X-ray Diffraction for Characterizing Structure in Protein Aggregates. <b>2006</b> , 167-191	2
464	Nucleotide Exchange Factors for Hsp70 Molecular Chaperones. <b>2007</b> , 1-12	3
463	Protein Contact Map Prediction. <b>2007</b> , 255-277	5
462	Wild Type p53 Conformation, Structural Consequences of p53 Mutations and Mechanisms of Mutant p53 Rescue. <b>2007</b> , 377-397	3
461	Atomistic Visualization. 2005, 1051-1068	9
460	Gonadotropic regulation of oocyte development. <b>2007</b> , 175-202	11
459	Electron Crystallography in Photosynthesis Research. 2008, 125-150	2
458	Function Diversity Within Folds and Superfamilies. <b>2009</b> , 143-166	3
457	Crystal structure of diphtheria toxin bound to nicotinamide adenine dinucleotide. <b>1997</b> , 419, 35-43	13
456	Selection of diphtheria toxin active-site mutants in yeast. Rediscovery of glutamic acid-148 as a key residue. <b>1997</b> , 419, 45-52	10
455	Switch 1 Opens on Strong Binding to Actin. <b>2003</b> , 159-167	4
454	Denitrification by Pseudomonads: Control and Assembly Processes. <b>2004</b> , 193-227	5

453	Structural Conservation and Functional Versatility: Allostery as a Common Annexin Feature. 2003, 38-60	2
452	Insights into binding of fatty acids by fatty acid binding proteins. <b>2002</b> , 45-54	3
451	Pursuing Laplace Vision on Modern Computers. <b>1996</b> , 219-247	11
450	Electrochemical Investigations of the Interfacial Behavior of Proteins. <b>1996</b> , 319-399	10
449	Protein quality control in bacterial cells: integrated networks of chaperones and ATP-dependent proteases. <b>2002</b> , 24, 17-47	7
448	Enzyme stabilization by directed evolution. <b>2000</b> , 22, 55-76	6
447	The Cytochromes c of Cyanobacteria. <b>1999</b> , 259-268	2
446	Electron Transfer Between Cytochrome f and Plastocyanin in Phormidium Laminosum. <b>1999</b> , 315-328	5
445	Mutational Analysis of ATP Synthase An Approach to Catalysis and Energy Coupling. 1999, 399-421	1
444	Investigation of an allosteric site of HIV-1 proteinase involved in inhibition by Cu2+. <b>1998</b> , 436, 99-103	13
443	Overcoming the unfavourable entropic contribution of ligand binding with a macrocyclic inhibitor bound to penicillopepsin. <b>1998</b> , 436, 355-9	4
442	Structural and functional aspects of cardosins. <b>1998</b> , 436, 423-33	12
441	Antithrombin. <b>1997</b> , 17-33	46
440	Functional, Conformational, and Molecular Modelling Studies of Voltage-Sensitivity and Selectivity of Synthetic Peptides Derived from Ion Channels. <b>1996</b> , 41-62	2
439	The Iron Responsive Element (IRE), the Iron Regulatory Protein (IRP), and Cytosolic Aconitase. <b>1998</b> , 157-216	12
438	Molecular Dynamics Studies of Protein and Peptide Folding and Unfolding. <b>1994</b> , 193-230	15
437	Structural Studies on Prokaryotic Cytochromes P450. <b>1995</b> , 125-150	27
436	Bacterial P450s. <b>1995</b> , 151-180	28

435	Ligand Binding Sites Within the Integrins. <b>1997</b> , 199-217	1
434	Structural Studies on Angiogenin, a Protein Implicated in Neovascularization during Tumour Growth. <b>1998</b> , 165-178	2
433	A family of RNA-binding enzymes. the aminoacyl-tRNA synthetases. <b>1995</b> , 24, 323-76	5
432	Molecular modeling of peptides. <b>2015</b> , 1268, 15-41	4
431	Conformational Plasticity of GPCR Binding Sites. <b>2005</b> , 363-388	1
430	Computational identification of plant transcription factors and the construction of the PlantTFDB database. <b>2010</b> , 674, 351-68	13
429	Active-site engineering of carbonic anhydrase and its application to biosensors. 2000, 221-40	2
428	Folding and stability of human carbonic anhydrase II. <b>2000</b> , 241-59	8
427	X-ray crystallographic studies of mammalian carbonic anhydrase isozymes. <b>2000</b> , 159-74	14
426	Structural characteristics of the matrix metalloproteinases. <b>1999</b> , 1-16	1
426 425	Structural characteristics of the matrix metalloproteinases. <b>1999</b> , 1-16  Classification of chitinases modules. <b>1999</b> , 87, 137-56	66
425	Classification of chitinases modules. <b>1999</b> , 87, 137-56	66
425 424	Classification of chitinases modules. <b>1999</b> , 87, 137-56  The ETS Family of Transcriptional Regulators. <b>1997</b> , 29-88  Interaction of protein domains in the assembly and mechanism of 2-oxo acid dehydrogenase	66 34
425 424 423	Classification of chitinases modules. <b>1999</b> , 87, 137-56  The ETS Family of Transcriptional Regulators. <b>1997</b> , 29-88  Interaction of protein domains in the assembly and mechanism of 2-oxo acid dehydrogenase multienzyme complexes. <b>1996</b> , 1-15	66 34 6
425 424 423 422	Classification of chitinases modules. 1999, 87, 137-56  The ETS Family of Transcriptional Regulators. 1997, 29-88  Interaction of protein domains in the assembly and mechanism of 2-oxo acid dehydrogenase multienzyme complexes. 1996, 1-15  Lipoamide dehydrogenase. 1996, 53-70	66 34 6 9
425 424 423 422 421	Classification of chitinases modules. 1999, 87, 137-56  The ETS Family of Transcriptional Regulators. 1997, 29-88  Interaction of protein domains in the assembly and mechanism of 2-oxo acid dehydrogenase multienzyme complexes. 1996, 1-15  Lipoamide dehydrogenase. 1996, 53-70  Lysozyme: a model enzyme in protein crystallography. 1996, 75, 185-222  Familial hypertrophic cardiomyopathic myosin mutations that affect the actin-myosin interaction.	66 34 6 9 41

417	General Introduction of Various Endoglycosidases. 55-127	1
416	Generalized-Ensemble Algorithms for Studying Protein Folding. <b>2009</b> , 61-95	2
415	The Transthyretin <b>R</b> etinol-Binding Protein Complex. <b>2009</b> , 123-142	4
414	Regulation of the actin cytoskeleton by PI(4,5)P2 and PI(3,4,5)P3. <b>2004</b> , 282, 117-63	85
413	A Test Set for Molecular Dynamics Algorithms. <b>2002</b> , 73-103	3
412	Calcium-Binding EGF-like Domains. <b>2000</b> , 83-99	2
411	Cytoplasmic inorganic pyrophosphatase. <b>1999</b> , 23, 127-50	68
410	Lens crystallins of invertebrates. <b>1996</b> , 1-17	1
409	New Insights into the X-Ray Structure of the Reaction Center from Rhodopseudomonas viridis. <b>1996</b> , 23-35	5
408	Three-Dimensional Structure of the Hammerhead Ribozyme. <b>1996</b> , 161-172	5
407	Diphtheria toxin fusion proteins. <b>1998</b> , 234, 63-81	32
406	Consequences of HMG-Domain Protein Binding to Cisplatin-Modified DNA. <b>1995</b> , 264-284	12
405	DNA Recognition by Helix-Loop-Helix Proteins. <b>1995</b> , 285-298	7
404	Structure of the receptor binding domain of adenovirus type 5 fiber protein. <b>1995</b> , 199 ( Pt 1), 39-46	15
403	Pleckstrin homology domains. <b>1998</b> , 228, 39-74	71
402	Anticancer Activity of Cisplatin and Related Complexes. <b>1999</b> , 1-43	15
401	Psychrophilic enzymes: insights into cold adaptation and catalysis from the first high resolution crystal structures. <b>1999</b> , 277-295	1
400	Structure of Toxic Shock Syndrome Toxin-1. <b>1996</b> , 217-229	1

399	Structure of Staphylococcal Enterotoxins. <b>1996</b> , 231-251	2
398	The Structures and Evolution of Snake Toxins of the Three-Finger Folding Type. <b>1996</b> , 271-290	2
397	Insights into Membrane Insertion Based on Studies of Colicins. <b>1996</b> , 5-23	5
396	Structure and Assembly of the Channel-Forming Aeromonas Toxin Aerolysin. <b>1996</b> , 79-95	1
395	The Cholera Family of Enterotoxins. <b>1996</b> , 123-146	2
394	E. Coli Heat Labile Enterotoxin and Cholera Toxin B-Pentamer <b>©</b> rystallographic Studies of Biological Activity. <b>1996</b> , 147-172	2
393	Modeling of the F-actin structure. <b>2007</b> , 592, 385-401	12
392	The Phylogeny and Structural Properties of 2/2 Haemoglobins. 2008, 31-43	1
391	Carboxylate Shifts in the Active Site of the Hydroxylase Component of Soluble Methane Monooxygenase from Methylococcus capsulatus (Bath). <b>1996</b> , 141-149	9
390	Protein Engineering of Microbial Lipases with Industrial Interest. <b>1996</b> , 203-217	4
389	A census of carbohydrate-active enzymes in the genome of Arabidopsis thaliana. <b>2001</b> , 55-72	14
388	Calcium Binding to Extracellular Matrix Proteins, Functional and Pathological Effects. 2000, 151-164	1
387	Thioredoxins in Cyanobacteria: Structure and Redox Regulation of Enzyme Activity. <b>1994</b> , 715-729	5
386	Essential Degrees of Freedom of Proteins. <b>1995</b> , 85-93	6
385	Assembly of Escherichia coli heat-labile enterotoxin and its secretion from Vibrio cholerae. <b>1994</b> , 293-309	2
384	Pressure Denaturation of Proteins. <b>1999</b> , 473-495	3
383	On the Mechanism of Nitrite Reductase: Complex between Pseudoazurin and Nitrite Reductase from A. Cycloclastes. <b>1998</b> , 115-128	2
382	Complex Structures of Nitrogenase. <b>1998,</b> 11-16	8

381	Structure of prostaglandin H2 synthase-1 (COX-1) and its NSAID binding sites. 1996, 13-21	2
<b>3</b> 80	Molecular Modeling of Globular Proteins : Strategy 1D => 3D: Secondary Structures and Epitopes. <b>1997</b> , 121-150	3
379	The Interaction Between Cytochrome f and Plastocyanin or Cytochrome c6. <b>2016</b> , 631-655	1
378	Function Diversity Within Folds and Superfamilies. <b>2017</b> , 295-325	2
377	MILK PROTEINS   Beta-Lactoglobulin. <b>2002</b> , 1932-1939	1
376	Measuring Global and Local Structural Free Energy Changes in Staphylococcal Nuclease by NMR-Observed Hydrogen Exchange. <b>1994</b> , 431-438	1
375	Comparative three-dimensional structure of cholesterol-dependent cytolysins. 2006, 659-670	3
374	Erythropoietin Receptor as a Paradigm for Cytokine Signaling. <b>2003</b> , 251-258	1
373	tRNA Recognition by Aminoacyl-tRNA Synthetases. <b>1998</b> , 55-65	6
372	Structure and Function of CheA, the Histidine Kinase Central to Bacterial Chemotaxis. <b>2003</b> , 47-72	6
372	Structure and Function of CheA, the Histidine Kinase Central to Bacterial Chemotaxis. <b>2003</b> , 47-72  Interleukin-4. <b>1998</b> , 53-68	3
371	Interleukin-4. <b>1998</b> , 53-68	3
371	Interleukin-4. <b>1998</b> , 53-68  Recombinant Hemoglobins with Low Oxygen Affinity and High Cooperativity. <b>1998</b> , 281-296	3
371 370 369	Interleukin-4. <b>1998</b> , 53-68  Recombinant Hemoglobins with Low Oxygen Affinity and High Cooperativity. <b>1998</b> , 281-296  On the Evolutionary Search for Solutions to the Protein Folding Problem. <b>2003</b> , 115-136	3 3 5
371 370 369 368	Interleukin-4. 1998, 53-68  Recombinant Hemoglobins with Low Oxygen Affinity and High Cooperativity. 1998, 281-296  On the Evolutionary Search for Solutions to the Protein Folding Problem. 2003, 115-136  The Architecture of Loops in Proteins. 1996, 239-259  Repair of spontaneously deamidated HPr phosphocarrier protein catalyzed by the	3 3 5
371 370 369 368 367	Interleukin-4. 1998, 53-68  Recombinant Hemoglobins with Low Oxygen Affinity and High Cooperativity. 1998, 281-296  On the Evolutionary Search for Solutions to the Protein Folding Problem. 2003, 115-136  The Architecture of Loops in Proteins. 1996, 239-259  Repair of spontaneously deamidated HPr phosphocarrier protein catalyzed by the L-isoaspartate-(D-aspartate) O-methyltransferase 1994, 269, 24586-24595  The solution structure of sarafotoxin-c. Implications for ligand recognition by endothelin	3 3 5 1

363	Role of the proximal ligand in peroxidase catalysis. Crystallographic, kinetic, and spectral studies of cytochrome c peroxidase proximal ligand mutants <b>1994</b> , 269, 20239-20249	93
362	Mutagenesis study at a postulated hydrophobic region near the active site of aromatase cytochrome P450 <b>1994</b> , 269, 19501-19508	40
361	The crystal structure of succinyl-CoA synthetase from Escherichia coli at 2.5-A resolution <b>1994</b> , 269, 10883-10890	113
360	A unique interhelical insertion in plasminogen activator inhibitor-2 contains three glutamines, Gln83, Gln84, Gln86, essential for transglutaminase-mediated cross-linking <b>1994</b> , 269, 15394-15398	45
359	Capsid assembly in a family of animal viruses primes an autoproteolytic maturation that depends on a single aspartic acid residue <b>1994</b> , 269, 13680-13684	70
358	Interaction of a legume lectin with two components of the bacterial cell wall. A crystallographic study. <b>1994</b> , 269, 9429-9435	30
357	Functional and structural role of a tryptophan generally observed in protein-carbohydrate interaction. TRP-62 of hen egg white lysozyme <b>1994</b> , 269, 7070-7075	44
356	Spectroscopic characterization of tyrosine-Z in histidine 190 mutants of the D1 protein in photosystem II (PSII) in Chlamydomonas reinhardtii. Implications for the structural model of the donor side of PSII <b>1994</b> , 269, 5115-5121	75
355	Binding of sugar ligands to Ca(2+)-dependent animal lectins. I. Analysis of mannose binding by site-directed mutagenesis and NMR <b>1994</b> , 269, 15505-15511	92
354	Refined structure for the complex of acarbose with glucoamylase from Aspergillus awamori var. X100 to 2.4-A resolution <b>1994</b> , 269, 15631-15639	124
353	The bacterial periplasmic histidine-binding protein. structure/function analysis of the ligand-binding site and comparison with related proteins <b>1994</b> , 269, 4135-4143	73
352	Translation initiation factor eIF-2. Cloning and expression of the human cDNA encoding the gamma-subunit <b>1994</b> , 269, 3415-3422	51
351	Identification and characterization of the second regulatory disulfide bridge of recombinant sorghum leaf NADP-malate dehydrogenase <b>1994</b> , 269, 3511-3517	60
350	An Escherichia coli protein consisting of a domain homologous to FK506-binding proteins (FKBP) and a new metal binding motif <b>1994</b> , 269, 2895-2901	108
349	Molecular cloning of a proteolytic antibody light chain <b>1994</b> , 269, 32389-32393	56
348	Probing protein-protein interactions. The ribose-binding protein in bacterial transport and chemotaxis <b>1994</b> , 269, 30206-30211	73
347	The C-terminal peptide produced upon proteolytic activation of the cytolytic toxin aerolysin is not involved in channel formation <b>1994</b> , 269, 30496-30501	29
346	Adipocyte lipid-binding protein complexed with arachidonic acid. Titration calorimetry and X-ray crystallographic studies <b>1994</b> , 269, 25339-25347	73

345	Structure-function studies on recombinant human macrophage colony-stimulating factor (M-CSF) <b>1994</b> , 269, 31171-31177	16
344	Three-dimensional models of four mouse mast cell chymases. Identification of proteoglycan binding regions and protease-specific antigenic epitopes <b>1993</b> , 268, 9023-9034	88
343	Reduction of mutant phage T4 glutaredoxins by Escherichia coli thioredoxin reductase <b>1993</b> , 268, 3845-3849	7
342	Structure of a non-peptide inhibitor complexed with HIV-1 protease. Developing a cycle of structure-based drug design. <b>1993</b> , 268, 15343-15346	113
341	The three-dimensional structure of the ligand-binding domain of a wild-type bacterial chemotaxis receptor. Structural comparison to the cross-linked mutant forms and conformational changes upon ligand binding. <b>1993</b> , 268, 9787-9792	77
340	Expression, purification, and characterization of a recombinant ribonuclease H from Thermus thermophilus HB8 <b>1992</b> , 267, 10184-10192	53
339	Self Recognition in the Ig Superfamily. 2000, 275, 26935-26943	31
338	Differential Influence of Nucleoside Analog-resistance Mutations K65R and L74V on the Overall Mutation Rate and Error Specificity of Human Immunodeficiency Virus Type 1 Reverse Transcriptase. <b>2000</b> , 275, 27037-27044	57
337	Crystal Structure and Thermodynamic Analysis of Human Brain Fatty Acid-binding Protein. <b>2000</b> , 275, 27045-27054	124
336	A Novel Anti-tumor Cytokine Contains an RNA Binding Motif Present in Aminoacyl-tRNA Synthetases. <b>2000</b> , 275, 27062-27068	37
335	Escherichia coli-derived rat intestinal fatty acid binding protein with bound myristate at 1.5 A resolution and I-FABPArg106ਊGln with bound oleate at 1.74 A resolution <b>1993</b> , 268, 26375-26385	46
334	Probing the active site of human aldose reductase. Site-directed mutagenesis of Asp-43, Tyr-48, Lys-77, and His-110 <b>1993</b> , 268, 25687-25693	92
333	Crystal Structure of the RUN Domain of the RAP2-interacting Protein x. 2006, 281, 31843-31853	6
332	Crystal Structure of the B Subunit of Escherichia coli Heat-labile Enterotoxin Carrying Peptides with Anti-herpes Simplex Virus Type 1 Activity. <b>1999</b> , 274, 8764-8769	9
331	The crystal structure of manganese peroxidase from Phanerochaete chrysosporium at 2.06-A resolution. <b>1994</b> , 269, 32759-32767	292
330	Crystal structures of ribonuclease HI active site mutants from Escherichia coli <b>1993</b> , 268, 22092-22099	31
329	Conformational lability of lipases observed in the absence of an oil-water interface: crystallographic studies of enzymes from the fungi Humicola lanuginosa and Rhizopus delemar <b>1994</b> , 35, 524-534	167
328	Intrasteric regulation of protein kinases. <b>1997</b> , 31, 29-40	16

327	Molecular Light Scattering and Optical Activity. <b>2004</b> ,	1015
326	Molecular scattering of polarized light. <b>2004</b> , 123-169	2
325	Identification of a new Leu354Pro mutation responsible for factor XIII deficiency. 2001, 66, 133-6	11
324	Structural evidence for dimerization-regulated activation of an integral membrane phospholipase. <b>1999</b> , 401, 717-21	132
323	Structure of the Bcr-Abl oncoprotein oligomerization domain. <b>2002</b> , 9, 117-20	79
322	Thermodynamic stability of wild-type and mutant p53 core domain. <b>1997</b> , 94, 14338-42	312
321	Crystal structures of eukaryotic translation initiation factor 5A from Methanococcus jannaschii at 1.8 A resolution. <b>1998</b> , 95, 10419-24	94
320	Semirational design of active tumor suppressor p53 DNA binding domain with enhanced stability. <b>1998</b> , 95, 14675-80	186
319	In vivo identification of intermediate stages of the DNA inversion reaction catalyzed by the Salmonella Hin recombinase. <b>1998</b> , 149, 1649-63	17
318	The necrotic gene in Drosophila corresponds to one of a cluster of three serpin transcripts mapping at 43A1.2. <b>2000</b> , 156, 1117-27	56
317	Saccharomyces cerevisiae SMT4 encodes an evolutionarily conserved protease with a role in chromosome condensation regulation. <b>2001</b> , 158, 95-107	100
316	Mutational analysis of the gephyrin-related molybdenum cofactor biosynthetic gene cnxE from the lower eukaryote Aspergillus nidulans. <b>2002</b> , 161, 623-32	13
315	Evolutionary, structural and biochemical evidence for a new interaction site of the leptin obesity protein. <b>2003</b> , 163, 1549-53	31
314	The ESS1 prolyl isomerase and its suppressor BYE1 interact with RNA pol II to inhibit transcription elongation in Saccharomyces cerevisiae. <b>2003</b> , 165, 1687-702	37
313	DSSR-enabled innovative schematics of 3D nucleic acid structures with PyMOL. <b>2020</b> , 48, e74	5
312	Characterization and functional analysis of Serp3: a novel myxoma virus-encoded serpin involved in virulence. <b>2001</b> , 82, 1407-1417	31
311	YeiL, the third member of the CRP-FNR family in Escherichia coli. <b>2000</b> , 146 Pt 12, 3157-3170	12
310	MabA (FabG1), a Mycobacterium tuberculosis protein involved in the long-chain fatty acid elongation system FAS-II. <b>2002</b> , 148, 951-960	85

309	'New uses for an Old Enzyme'the Old Yellow Enzyme family of flavoenzymes. 2002, 148, 1607-1614	216
308	Molecular cloning and characterization of the ferric hydroxamate uptake (fhu) operon in Actinobacillus pleuropneumoniae. <b>2002</b> , 148, 2869-2882	25
307	Sustained software development, not number of citations or journal choice, is indicative of accurate bioinformatic software.	5
306	The Evolution of SlyA/RovA Transcription Factors From Repressors to Counter-Silencers inEnterobacteriaceae.	1
305	Phylogeny of the Serpin Superfamily: Implications of Patterns of Amino Acid Conservation for Structure and Function. <b>2000</b> , 10, 1845-1864	92
304	X-ray crystallographic studies of eukaryotic transcription factors. <b>1998</b> , 63, 33-40	2
303	DNA polymerase beta and mammalian base excision repair. <b>2000</b> , 65, 143-55	40
302	Analysis of the fission yeast checkpoint Rad proteins. <b>2000</b> , 65, 451-6	7
301	Interactions of the eukaryotic translation initiation factor eIF4E. 2001, 66, 397-402	4
300	Structural studies of eukaryotic elongation factors. <b>2001</b> , 66, 425-37	13
299	The susceptibility of disulfide bonds towards radiation damage may be explained by S?O interactions. <b>2020</b> , 7, 825-834	3
298	Structural characterization of three noncanonical NTF2-like superfamily proteins: implications for polyketide biosynthesis. <b>2020</b> , 76, 372-383	5
297	Molecular basis of oculocutaneous albinism. <b>1994</b> , 103, 131S-136S	42
296	Solution structure of porcine pancreatic procolipase as determined from 1H homonuclear two-dimensional and three-dimensional NMR. <b>1995</b> , 227, 663-72	19
295	Refined crystal structure of the interleukin-1 receptor antagonist. Presence of a disulfide link and a cis-proline. <b>1995</b> , 227, 838-47	56
294	1H and 15N Resonance Assignments and Structure of the N-Terminal Domain of Escherichia coli Initiation Factor 3. <b>1995</b> , 228, 395-402	36
293	X-ray structures of human neutrophil collagenase complexed with peptide hydroxamate and peptide thiol inhibitors. Implications for substrate binding and rational drug design. <b>1995</b> , 228, 830-41	156
292	1H, 13C, 15N-NMR resonance assignments of oxidized thioredoxin h from the eukaryotic green alga Chlamydomonas reinhardtii using new methods based on two-dimensional triple-resonance NMR spectroscopy and computer-assisted backbone assignment. <b>1995</b> , 229, 473-85	20

291	Insights into thermal stability from a comparison of the glutamate dehydrogenases from Pyrococcus furiosus and Thermococcus litoralis. <b>1995</b> , 229, 688-95	88
290	Investigation of the energy requirement and targeting signal for the import of glycolate oxidase into glyoxysomes. <b>1995</b> , 230, 157-63	27
289	Folding of protein G B1 domain studied by the conformational characterization of fragments comprising its secondary structure elements. <b>1995</b> , 230, 634-49	154
288	Identification of residues potentially involved in the interactions between subunits in yeast alcohol dehydrogenases. <b>1995</b> , 231, 214-9	11
287	Structural Influence of Calcium on the Heme Cavity of Cationic Peanut Peroxidase as Determined by 1H-NMR Spectroscopy. <b>1995</b> , 232, 825-833	27
286	Crystal and Molecular Structure at 0.16-nm Resolution of the Hybrid Bacillus Endo-1,3-1,4-beta-D-Glucan 4-Glucanohydrolase H(A16-M). <b>1995</b> , 232, 849-858	46
285	Antibody Structure. 49-62	1
284	Structure and Function of Picornavirus Proteinases. 199-212	15
283	Poliovirus RNA-Dependent RNA Polymerase (3Dpol): Structure, Function, and Mechanism. 255-267	6
282	Picornavirus Structure Overview. 25-38	2
281	Termination of Chromosome Replication. 87-95	8
280	The States, Conformational Dynamics, and Fusidic Acid-Resistant Mutants of Elongation Factor G. 359-365	1
279	Recognition of Aminoacyl-tRNAs by Protein Elongation Factors. 423-442	10
278	Hemoglobin biosynthesis in Vitreoscilla stercoraria DW: cloning, expression, and characterization of a new homolog of a bacterial globin gene. <b>1998</b> , 64, 2220-8	14
277	Substrate specificity of and product formation by muconate cycloisomerases: an analysis of wild-type enzymes and engineered variants. <b>1998</b> , 64, 3290-9	30
276	Structural and evolutionary inference from molecular variation in Neisseria porins. <b>1999</b> , 67, 2406-13	112
275	How photosynthetic bacteria harvest solar energy. <b>1999</b> , 181, 3869-79	84
274	Localization of synthesis of beta1,6-glucan in Saccharomyces cerevisiae. <b>1999</b> , 181, 7414-20	75

273	Unusual ribulose 1,5-bisphosphate carboxylase/oxygenase of anoxic Archaea. <b>1999</b> , 181, 1569-75	88
272	Structure of human rhinovirus complexed with Fab fragments from a neutralizing antibody. <b>1993</b> , 67, 1148-58	115
271	Sequence and structure alignment of paramyxovirus hemagglutinin-neuraminidase with influenza virus neuraminidase. <b>1993</b> , 67, 2972-80	194
270	Antigenicity of the N8 influenza A virus neuraminidase: existence of an epitope at the subunit interface of the neuraminidase. <b>1994</b> , 68, 1790-6	22
269	Steps in maturation of influenza A virus neuraminidase. <b>1995</b> , 69, 5011-7	34
268	Reversion of a human immunodeficiency virus type 1 integrase mutant at a second site restores enzyme function and virus infectivity. <b>1996</b> , 70, 8277-84	25
267	Crystal structure of the top domain of African horse sickness virus VP7: comparisons with bluetongue virus VP7. <b>1996</b> , 70, 3797-806	49
266	Characteristics of the Pro225His mutation in human immunodeficiency virus type 1 (HIV-1) reverse transcriptase that appears under selective pressure of dose-escalating quinoxaline treatment of HIV-1. <b>1997</b> , 71, 8195-203	15
265	Dissecting the roles of VP0 cleavage and RNA packaging in picornavirus capsid stabilization: the structure of empty capsids of foot-and-mouth disease virus. <b>1997</b> , 71, 9743-52	116
264	The refined crystal structure of the 3C gene product from hepatitis A virus: specific proteinase activity and RNA recognition. <b>1997</b> , 71, 2436-48	133
263	Structure-function studies of the human immunodeficiency virus type 1 matrix protein, p17. <b>1997</b> , 71, 3474-83	67
262	Characterization of human immunodeficiency virus type 1 matrix revertants: effects on virus assembly, Gag processing, and Env incorporation into virions. <b>1997</b> , 71, 4409-18	77
261	Poliovirus Sabin type 1 neutralization epitopes recognized by immunoglobulin A monoclonal antibodies. <b>1997</b> , 71, 6905-12	18
260	Active-site residues of cyclophilin A are crucial for its incorporation into human immunodeficiency virus type 1 virions. <b>1997</b> , 71, 7110-3	41
259	Rapid selection in modified BHK-21 cells of a foot-and-mouth disease virus variant showing alterations in cell tropism. <b>1998</b> , 72, 10171-9	52
258	Mutational scan of the human immunodeficiency virus type 2 integrase protein. <b>1998</b> , 72, 3916-24	24
257	Structure-based mutational analysis of the C-terminal DNA-binding domain of human immunodeficiency virus type 1 integrase: critical residues for protein oligomerization and DNA binding. <b>1998</b> , 72, 4841-8	108
256	Reversion of a human immunodeficiency virus type 1 matrix mutation affecting Gag membrane binding, endogenous reverse transcriptase activity, and virus infectivity. <b>1999</b> , 73, 4728-37	24

255	Three-dimensional structure of Aleutian mink disease parvovirus: implications for disease pathogenicity. <b>1999</b> , 73, 6882-91	59
254	Mutations at KFRDI and VGK domains of enterovirus 71 3C protease affect its RNA binding and proteolytic activities. <b>2004</b> , 11, 239	3
253	Remarkably similar antigen receptors among a subset of patients with chronic lymphocytic leukemia. <b>2004</b> , 113, 1008-16	162
252	Inherited human cPLA(2alpha) deficiency is associated with impaired eicosanoid biosynthesis, small intestinal ulceration, and platelet dysfunction. <b>2008</b> , 118, 2121-31	95
251	Saturation Mutagenesis of the Bubunit of the Human Granulocyte-Macrophage Colony-Stimulating Factor Receptor Shows Clustering of Constitutive Mutations, Activation of ERK MAP Kinase and STAT Pathways, and Differential Bubunit Tyrosine Phosphorylation. <b>1998</b> , 92, 1989-2002	5
250	Structure of the activation domain of the GM-CSF/IL-3/IL-5 receptor common	3
249	Identification and characterization of human eosinophil cationic protein by an epitope-specific antibody. <b>2001</b> , 69, 1027-1035	5
248	Catalysis by Nitrogenases and Synthetic Analogs. <b>1999</b> , 153-207	1
247	PDE2 Structure and Functions. <b>2006</b> ,	2
246	The Role of Nitrate Ester Reductase Enzymes in the Biodegradation of Explosives. 2000,	1
245	Thiolation-enhanced substrate recognition by D-alanyl carrier protein ligase DltA from Bacillus cereus. <b>2014</b> , 3, 106	5
244	A high performance prediction system of coiled coil domains containing heptad breaks: SOSUIcoil. <b>2008</b> , 8, 96-111	7
243	Prediction of fragile points of coiled coils. <b>2009</b> , 9, 12-29	2
242	Structure and evolutionary origin of Ca(2+)-dependent herring type II antifreeze protein. 2007, 2, e548	55
241	UPF201 archaeal specific family members reveal structural similarity to RNA-binding proteins but low likelihood for RNA-binding function. <b>2008</b> , 3, e3903	1
240	Structural relationships in the lysozyme superfamily: significant evidence for glycoside hydrolase signature motifs. <b>2010</b> , 5, e15388	62
239	Structural basis for dual-inhibition mechanism of a non-classical Kazal-type serine protease inhibitor from horseshoe crab in complex with subtilisin. <b>2011</b> , 6, e18838	10
238	Conservation of the human integrin-type beta-propeller domain in bacteria. <b>2011</b> , 6, e25069	18

237	Chemoinformatic identification of novel inhibitors against Mycobacterium tuberculosis L-aspartate Edecarboxylase. <b>2012</b> , 7, e33521	13
236	SNPs altering ammonium transport activity of human Rhesus factors characterized by a yeast-based functional assay. <b>2013</b> , 8, e71092	3
235	High resolution crystal structure of the Grb2 SH2 domain with a phosphopeptide derived from CD28. <b>2013</b> , 8, e74482	13
234	Single, double and quadruple alanine substitutions at oligomeric interfaces identify hydrophobicity as the key determinant of human neutrophil alpha defensin HNP1 function. <b>2013</b> , 8, e78937	20
233	Addressing mechanism of fibrillization/aggregation and its prevention in presence of osmolytes: spectroscopic and calorimetric approach. <b>2014</b> , 9, e104600	20
232	Structural dynamics of the cereblon ligand binding domain. <b>2015</b> , 10, e0128342	17
231	GrpE, a nucleotide exchange factor for DnaK. <b>2003</b> , 8, 218-24	86
230	S-Sulfhydration of the Catalytic Cysteine in the Rhodanese Domain of YgaP is Complex Dynamic Process.	1
229	Bacterial toxins: friends or foes?. <b>1999</b> , 5, 224-34	95
228	Structural and Functional Characterization of SoxW-a Thioredoxin Involved in the Transport of Reductants During Sulfur Oxidation by the Global Sulfur Oxidation Reaction Cycle. <b>2006</b> , 1, 392-400	2
227	Homology Modeling and Molecular Dynamics Study of the Interactions of SoxY and SoxZ: The Central Player of Biochemical Oxidation of Sulfur Anions in Pseudaminobacter salicylatoxidans. <b>2007</b> , 2, 569-576	3
226	Genetic polymorphism at the candidate gene in Iranian Sistani cattle (Bos indicus). 2007, 10, 3368-73	1
225	Photoreactions of 2- and 4-Pyridones in Their Inclusion Crystal with a Host Compound. 2003, 59, 735	6
224	An interactive 3D viewer of molecules compatible with the suite of ANTHEPROT programs. <b>2012</b> , 03, 35-38	4
223	Two flexible loops in subtilisin-like thermophilic protease, thermicin, from Thermoanaerobacter yonseiensis. <b>2002</b> , 35, 498-507	5
222	Structure and function of HtrA family proteins, the key players in protein quality control. 2005, 38, 266-74	104
221	Analysis of the crystal structure of an active MCM hexamer. <b>2014</b> , 3, e03433	47
220	<b>严</b> coiled coils. <b>2016</b> , 5,	18

219	Crystal structure correlations with the intrinsic thermodynamics of human carbonic anhydrase inhibitor binding. <b>2018</b> , 6, e4412	7
218	NAA80 bi-allelic missense variants result in high-frequency hearing loss, muscle weakness and developmental delay. <b>2021</b> , 3, fcab256	2
217	Transient Formation of a Second Active Site Cavity during Quinolinic Acid Synthesis by NadA. <b>2021</b> , 16, 2423-2433	О
216	Protein Folding Simulations by Monte Carlo Simulated Annealing and Multicanonical Algorithm. <b>2000</b> , 73-90	
215	Inhibition and Structural Changes of O-Acetylserine Sulfhydrylase-A from Salmonella typhimurium Upon Binding Sulfate and Chloride Anions. <b>2000</b> , 271-276	
214	IL-1 antagonist discovery. <b>2000</b> , 205-222	
213	Generation of mutants of CK2⊞which are dependent on the ⊞ubunit for catalytic activity. <b>2001</b> , 13-19	
212	Structural Views of the Ran GTPase Cycle. <b>2001</b> , 177-201	
211	Structure-function relationships of む-glucan endo- and exohydrolases from higher plants. <b>2001</b> , 73-91	2
210	Comparison of Conformational Transitions in Proteins. <b>2002</b> , 91-101	
209	Solution structure of fatty acid-binding protein from human brain. <b>2002</b> , 61-68	1
208	EGF Motif.	
207	Beta-Sheet.	
206	TIM Barrel.	
205	Imaging Science in Biochemistry.	
204	Kringle Domain.	
203	Gamma-Turns.	
202	Fv Immunoglobulins.	

201	Odorant-Binding Proteins (OBP).
<b>2</b> 00	Granulocyte Colony-Stimulating Factor (G-CSF).
199	Beta-Bulge.
198	Beta-Helix.
197	PTB (Phosphotyrosine-Binding) Domains.
196	Insulin: Sequence, Structure and Function - A Story of Surprises. <b>2002</b> , 29-39
195	Macrophage Colony-Stimulating Factor (M-CSF).
194	Peptide.
193	Nucleotide-Binding Motif.
192	Leucine-Rich Repeat.
191	Up-And-Down Barrel.
190	Corticosteroid-Binding Globulin (CBG).
189	Four-Helix Bundle Motif.
188	Secondary Structure, Protein.
187	Actin.
186	Staphylokinase.
185	Hemoglobin.
184	Alpha-Helix (310-Helix and Pi-Helix).

183	Riboflavin-Binding Protein RfBP.
182	Heparin-binding Protein.
181	Cystine Knot.
180	Carbonic Anhydrase.
179	Polyproline.
178	Protein Structure.
177	Phosphofructokinases.
176	Beta-Lactoglobulin.
175	Omega Loop.
174	Interleukin-1 Motif.
174 173	Interleukin-1 Motif.  DEAD and DEAH Domains.
173	DEAD and DEAH Domains.
173 172	DEAD and DEAH Domains.  Beta-Turns.
173 172 171	DEAD and DEAH Domains.  Beta-Turns.  Factor X, Coagulation.
173 172 171 170	DEAD and DEAH Domains.  Beta-Turns.  Factor X, Coagulation.  Barnase and Barstar.
173 172 171 170	DEAD and DEAH Domains.  Beta-Turns.  Factor X, Coagulation.  Barnase and Barstar.  Granulocyte-Macrophage Colony-Stimulating Factor.

165	""Smart[Materials for Colorimetric Detection of Pathogenic Agents. 2002,	
164	Self-assembling Symmetric Protein Materials. 2002,	
163	Structural Biology of Programmed Cell Death. <b>2003</b> , 47-65	
162	Effects of pH on kinetics of the structural rearrangement that gates the electron-transfer reaction between zinc cytochrome c and plastocyanin: Analysis of protonation states in a diprotein complex. <b>2003</b> , 68, 327-337	
161	Pleckstrin Homology (PH) Domains. 2003, 161-169	
160	AntibodyAntigen Recognition and Conformational Changes. 2003, 33-38	1
159	Protein Folding. <b>2003</b> , 179-190	0
158	Molek[modelle und Modellmolek[e: Strukturanalyse großr biologischer Molek[e ff]die Medizin. <b>2003</b> , 340-359	
157	The Structures and Active Sites of Pectinases. <b>2003</b> , 267-275	
156	Effects of genotypic variations on hepatitis C virus nonstructural protein 5B structure and activity. <b>2003</b> , 109-121	1
155	Structure of a Biological Cell. <b>2003</b> , 159-228	
154	Solvent and Carbon Kinetic Isotope Effects on Active-Site and Regulatory-Site Variants of Yeast Pyruvate Decarboxylase. <b>2003</b> ,	
153	Insights into the Mechanism and Regulation of Bacterial Acetohydroxyacid Synthases. 2003,	
152	Sialidases. 2003,	
151	Protein Structures. 2003,	
150	Structure and Intersubunit Information Transfer in the E. coli Pyruvate Dehydrogenase Multienzyme Complex. <b>2003</b> ,	
149	VanX d-,d-dipeptidase. <b>2004</b> , 860-866	
148	PairAnalyzer: Extracting and Visualizing RNA Structure Elements Formed by Base Pairing. <b>2004</b> , 279-286	

147	DNA-Protein Interactions. <b>2004</b> , 241-278
146	Preface to the second edition. <b>2004</b> , xv-xvii
145	References. <b>2004</b> , 423-435
144	Preface to the first edition. <b>2004</b> , xi-xiv
143	Natural vibrational optical activity. <b>2004</b> , 331-384
142	A historical review of optical activity phenomena. <b>2004</b> , 1-52
141	Natural electronic optical activity. <b>2004</b> , 264-310
140	Symmetry and optical activity. <b>2004</b> , 170-263
139	Molecules in electric and magnetic fields. <b>2004</b> , 53-122
138	Magnetic electronic optical activity. <b>2004</b> , 311-330
137	Antisymmetric scattering and magnetic Raman optical activity. 2004, 385-422
136	References. 2004,
135	Strategies for Crystallizing the N-Terminal Growth Factor Domain of Amyloid Precursor Protein. <b>2004</b> ,
134	A Novel Model for Prediction of RNA binding Proteins. <b>2005</b> , 5, 1-14
133	Relating Protein Dynamics to Function and Structure: The Purple Membrane. <b>2006</b> , 419-434
132	Scaffold proteins and the regeneration of visual pigments. <b>2006</b> , 82, 1482-8
131	Structural Identification of the Interactions of SoxA and SoxX During the Oxidation of Sulfur Anions via the Novel Global Sulfur Oxidizing (Sox) Operon. <b>2006</b> , 1, 172-182
130	Chloroperoxidase.

Bacillus Subtilis D-Aminopeptidase DppA. 129 Mining Molecular Structure Data for the Patterns of Interactions Between Protein and RNA. 2007, 94-101 128 Neprilysin. 2007, 1-7 127 What We can Learn about Protein Folding from Recent Progress in Structure Prediction. 2007, 149-155 126 Resources and Infrastructure for Structural Bioinformatics. 2007, 207-227 125 Mechanisms of VCAM-1 and fibronectin binding to integrin alpha 4 beta 1: implications for integrin 124 7 function and rational drug design. 1995, 189, 177-91; discussion 191-9 References. 2009, 231-261 123 Probing of Structure and Function of Proteins by Mass Spectrometry -Analysis of Structure and 122 Function of a Protein by the pH Titration Using ESI-MS-. 2010, 58, 155-165 Macromolecular Crystallographic Computing. 2010, 1-36 121 Erythropoietin Receptor as a Paradigm for Cytokine Signaling. 2010, 245-252 120 Keratin mutations in patients with epidermolysis bullosa simplex: correlations between phenotype 119 severity and disturbance of intermediate filament molecular structure. 2010, The Morphology and Structure of Viruses. 118 Membrane-Related Diseases. 2012, 151-170 117 1 Carbinolamine formation and dehydration in a DNA repair enzyme active site. 2012, 7, e31377 116 Materials and Methods. 2013, 21-39 115 Materials and Methods. 2014, 25-40 114 Protein-Folding Systems. 209-223 113 Response: Similarity of Protein G and Ubiquitin. 1991, 254, 581-581 112

111	Three-Dimensional Structure of the Human Retinoic Acid Receptor- ®DNA Binding Domain: Implications for DNA-Binding. <b>1993</b> , 153-168	
110	Model Calculations of Protein-Water Systems and of Long Time Dynamics of Proteins. <b>1993</b> , 89-100	
109	Structure and Post-Translational Modification of the Lipoyl Domain of 2-Oxo Acid Dehydrogenase Complexes: A New Family of Protein Domains. <b>1993</b> , 283-288	
108	Complement System Genes and the Structures of the Proteins They Encode. <b>1993</b> , 525-532	
107	Toward the Structure of Mosaic Proteins: Expression, Purification and Structural Analysis of a Pair of Fibronectin Type1 Modules. <b>1993</b> , 623-631	
106	Structure of a Human Rhinovirus Complexed with its Receptor Molecule. <b>1993</b> , 1-12	1
105	NMR Studies of the Structure and Role of Modules Involved in Protein-Protein Interactions. <b>1993</b> , 134-158	
104	Structure and Function of the Glucocorticoid Receptor DNA-Binding Domain. <b>1993</b> , 120-147	
103	Application of computational neural networks to the prediction of protein structural features. <b>1993</b> , 15, 1-19	1
102	NMR studies of the structure of peptide complexes that duplicate functional interactions between proteins. <b>1994</b> , 921-923	
101	Diphtheria toxin-related cytokine fusion proteins: elongation factor 2 as a target for the treatment of neoplastic disease. <b>1994</b> , 151-156	
100	Molecular Dynamics Simulation of a DNA Binding Protein free and in Complex with DNA. <b>1994</b> , 441-456	1
99	Preferred Local Conformations of Peptides comprising the Entire Sequence of Bovine Pancreatic Trypsin Inhibitor (BPTI) and their Roles in Protein Folding. <b>1994</b> , 139-153	1
98	Crystallographic and cryo EM analysis of virion-receptor interactions. <b>1994</b> , 9, 531-41	12
97	Protein Fold Families and Structural Motifs. <b>1994</b> , 253-275	
96	Rack-induced bonding in blue-copper proteins. <b>1994</b> , 157-164	
95	Proteins under pressure. <b>1994</b> , 91-104	2
94	Identical mutations at corresponding positions in two homologous proteins with nonidentical effects. <b>1994</b> , 269, 11196-11200	6

93	Structure of the Thioredoxin 2 from Anabaena sp. pcc7120. <b>1995</b> , 1703-1706	
92	NMR structural studies on the zinc finger domains of nuclear hormone receptors. <b>1995</b> , 73, 279-95	1
91	Molecular Dissection of Regulatory Light Chain Function in Vertebrate Smooth Muscle Myosins. <b>1995</b> , 111-130	
90	Cathepsin D crystal structures and lysosomal sorting. <b>1995</b> , 362, 193-200	1
89	Dynamics of Nucleic Acids and Nucleic Acid:Protein Complexes. <b>1995</b> , 156-164	
88	Dynamic Domains: A Simple Method of Analysing Structural Movements in Proteins. <b>1995,</b> 137-149	
87	A Model of HIV-I Reverse Transcriptase: Possible Mechanisms for AZT Resistance. <b>1995</b> , 99-106	
86	The Sedoheptulose Bisphosphatase of Chlamydomonas Reinhardtii Contains a Potential Inter-Domain Disulphide and is Redox-Sensitive. <b>1995</b> , 3963-3966	
85	The Structure of Lentiviral Tat Proteins in Solution. <b>1996</b> , 287-303	
84	Structural Insights into Pertussis Toxin Action. <b>1996</b> , 191-216	
83	Shiga Toxin. <b>1996</b> , 173-190	2
82	Determination of protein and solvent volumes in protein crystals from contrast variation data. <b>1996</b> , 64, 333-43	
81	How Conventional Antigens and Superantigens Interact with the Human MHC Class II Molecule HLA-DR1. <b>1996</b> , 163-172	
80	Molecular Recognition: The Lipocalins. <b>1996</b> , 415-427	O
79	What Limits Protein Folding. <b>1996</b> , 65-71	
78	Molecular Evolution of Aphthoviruses. <b>1996</b> , 125-135	
77	Biology and Biochemistry. <b>1996</b> ,	
76	Insights into Protein Dynamics by NMR Techniques. <b>1996</b> , 127-138	

75	The Cooperative Substructure of Protein Molecules. <b>1996</b> , 1-7	
74	Structural studies of aldo-keto reductase inhibition. <b>1997</b> , 414, 435-42	
73	Oxygenic photosynthesis. <b>1996</b> , 121-133	
72	Prediction of the Structure of an Integral Membrane Protein: The Light-Harvesting Complex II of Rhodospirillum molischianum. <b>1996</b> , 503-533	
71	Computer Simulations of Protein-DNA Interactions. <b>1997</b> , 279-286	
70	Chapter The secondary structure of proteins. <b>1997</b> , 99-136	
69	Structure of the POU Domain. <b>1997</b> , 237-250	
68	Structural Studies of Eukaryotic Transcription Initiation. <b>1997</b> , 251-264	
67	Three-Dimensional Structure of Neocarzinostatin. <b>1997</b> , 109-128	
66	Chapter 4 Computational methods relating protein sequence and structure. <b>1997</b> , 165-268	
66	Chapter 4 Computational methods relating protein sequence and structure. <b>1997</b> , 165-268  Structural Relation of Peridinin-Chlorophyll A-Protein (PCP) and Proteins with Globin-Like Fold. <b>1998</b> , 277-284	
	Structural Relation of Peridinin-Chlorophyll A-Protein (PCP) and Proteins with Globin-Like Fold.	
65	Structural Relation of Peridinin-Chlorophyll A-Protein (PCP) and Proteins with Globin-Like Fold. <b>1998</b> , 277-284	
65 64	Structural Relation of Peridinin-Chlorophyll A-Protein (PCP) and Proteins with Globin-Like Fold.  1998, 277-284  Six Previously Undescribed Pyruvate Kinase Mutations Causing Enzyme Deficiency. 1998, 92, 647-652	
65 64 63	Structural Relation of Peridinin-Chlorophyll A-Protein (PCP) and Proteins with Globin-Like Fold.  1998, 277-284  Six Previously Undescribed Pyruvate Kinase Mutations Causing Enzyme Deficiency. 1998, 92, 647-652  Intermolecular Interactions of Proteins Involved in the Control of Gene Expression. 1999, 247-254	2
65 64 63 62	Structural Relation of Peridinin-Chlorophyll A-Protein (PCP) and Proteins with Globin-Like Fold.  1998, 277-284  Six Previously Undescribed Pyruvate Kinase Mutations Causing Enzyme Deficiency. 1998, 92, 647-652  Intermolecular Interactions of Proteins Involved in the Control of Gene Expression. 1999, 247-254  Struktur und Funktion des Thrombins. 1999, 269-284	2
65 64 63 62 61	Structural Relation of Peridinin-Chlorophyll A-Protein (PCP) and Proteins with Globin-Like Fold.  1998, 277-284  Six Previously Undescribed Pyruvate Kinase Mutations Causing Enzyme Deficiency. 1998, 92, 647-652  Intermolecular Interactions of Proteins Involved in the Control of Gene Expression. 1999, 247-254  Struktur und Funktion des Thrombins. 1999, 269-284  Human Herpesvirus Proteases. 1999, 93-115	

Host Receptors of Bacterial Origin. 49-68 57 The Aspartic Acid tRNA System: Recognition by a Class II Aminoacyl-tRNA Synthetase. 411-422 56 Bibliography. 2015, 243-260 55 Visualizing Protein Structures in Virtual Interactive Interface. 2015, 4, 422-425 54 Identifying G protein-coupled receptor dimers from crystal packings. 53 Application of Deep Architecture in Bioinformatics. 2020, 167-186 52 Exploration of Ion Channels in Mycobacterium tuberculosis: Implication on Drug Discovery and 51 1 Potent Drug Targets Against Tuberculosis. 2020, 14, 14-29 Some Consequences of the High Resolution X-Ray Structure Analysis of Cytochrome f. 1996, 431-437 50 The Structure and Function of the LH2 Complex from Rhodopseudomonas acidophila Strain 10050, 49 with Special Reference to the Bound Carotenoid. 1999, 71-80 48 FTIR Studies of Viral Ion Channels. 2005, 91-100 Atomistic Visualization. 2005, 1051-1068 47 1 Structural Insights into Smad Function and Specificity. 2006, 215-233 46 Figs. 4. 3043-3043 45 References for 3. 3082-3087 44 References for 2. 2028-2029 43 Understanding the Effects of Cancer-Associated Mutations in the Tumor Suppressor Protein p53: 42 Structural Consequences of Mutations and Possible Ways of Rescuing Oncogenic Mutants. 345-361 Molek[modelle und Modellmolek[e: Strukturanalyse großr biologischer Molek[e fildie 41 Medizin. 2008, 275-294 Protein Structure and Its Folding Rate. 2008, 273-301 40

39	Structure <b>E</b> unction Relationships of the NsrR and RsrR Transcription Regulators. 1-23	
38	Structural Determination of Uridine Diphosphate Glycosyltransferases Using X-Ray Crystallography. <b>2022</b> , 2396, 227-241	O
37	Structural and functional significance of the amino acid differences ValThr, SerAla, AsnSer, and AlaSer in 3C-like proteinases from SARS-CoV-2 and SARS-CoV. <b>2021</b> , 193, 2113-2113	1
36	Coumarins as Tool Compounds to Aid the Discovery of Selective Function Modulators of Steroid Hormone Binding Proteins. <b>2021</b> , 26, 5142	1
35	Reactivating chaperones for coenzyme B-dependent diol and glycerol dehydratases and ethanolamine ammonia-lyase <b>2022</b> , 668, 243-284	
34	Structural diversity of marine anti-freezing proteins, properties and potential applications: a review. <b>2022</b> , 9,	1
33	Coenzyme B-dependent eliminases: Diol and glycerol dehydratases and ethanolamine ammonia-lyase <b>2022</b> , 668, 181-242	
32	Novel Macrocyclic Peptidomimetics Targeting the Polo-Box Domain of Polo-Like Kinase 1 2022,	О
31	Sustained software development, not number of citations or journal choice, is indicative of accurate bioinformatic software <b>2022</b> , 23, 56	2
30	Engineering a more specific E. coli glyoxylate/hydroxypyruvate reductase for coupled steady state kinetics assays.	
29	Investigation on the Binding Properties of N1 Neuraminidase of H5N1 Influenza Virus in Complex with Fluorinated Sialic Acid Analog Compounds Study by Molecular Docking and Molecular Dynamics Simulations. <b>2022</b> , 52,	2
28	Montelarlo Simulated Annealing in Protein Folding. <b>2001</b> , 1515-1529	
27	Protein Folding: Generalized-Ensemble Algorithms. <b>2001</b> , 2062-2071	
26	X-ray Diffraction for Characterizing Structure in Protein Aggregates. <b>2006</b> , 167-191	
25	Monte-Carlo Simulated Annealing in Protein Folding. 2008, 2323-2337	
24	DataSheet1.docx. <b>2018</b> ,	
23	DataSheet1.zip. <b>2018</b> ,	
22	Quinolinate Synthase: An Example of the Roles of the Second and Outer Coordination Spheres in Enzyme Catalysis <b>2022</b> ,	1

21	Design 🖟 new way to look at old molecules. <b>2022</b> ,	1
20	Newly identified disorder of copper metabolism caused by variants in CTR1, a high-affinity copper transporter.	1
19	Canonical structural-binding modes in the calmodulinEarget protein complexes. 1-13	1
18	Metal-free PPi activates hydrolysis of MgPPi by an Escherichia coli inorganic pyrophosphatase. <b>2005</b> , 70, 69-78	O
17	The protein conformational basis of isoflavone biosynthesis. <b>2022</b> , 5,	О
16	Structural and conformational dynamics of human milk oligosaccharides, lacto-N-fucopentaose I and II, through molecular dynamics simulation. <b>2022</b> , 41, 385-404	O
15	Structural and binding studies of 2?- and 3-fucosyllactose and its complexes with norovirus capsid protein by molecular dynamics simulations. 1-14	О
14	Maturation of Qa-1b Class I Molecules Requires ₹-Microglobulin But Is TAP Independent. <b>1998</b> , 160, 3217-3224	6
13	The Leukocyte Function-Associated Antigen-1 (LFA-1)-Binding Site on ICAM-3 Comprises Residues on Both Faces of the First Immunoglobulin Domain. <b>1998</b> , 161, 1363-1370	6
12	The MHC Class I-Restricted Immune Response to HIV-gag in BALB/c Mice Selects a Single Epitope That Does Not Have a Predictable MHC-Binding Motif and Binds to Kd Through Interactions Between a Glutamine at P3 and Pocket D. <b>1998</b> , 161, 2985-2993	21
11	B Cell Tolerance to a Minor, But Not to a Major, Antigenic Surface of the Self Antigen, Cytochrome c. <b>1998</b> , 161, 2841-2847	2
10	A Site for CD4 Binding in the <b>#</b> Domain of the MHC Class II Protein HLA-DR1. <b>1998</b> , 161, 5472-5480	10
9	Molecular and Immunologic Characterization of a Highly Cross-Reactive Two EF-Hand Calcium-Binding Alder Pollen Allergen, Aln g 4: Structural Basis for Calcium-Modulated IgE Recognition. <b>1998</b> , 161, 7031-7039	12
8	Immunosuppressive Activities of Recombinant Glycosylation -Inhibiting Factor Mutants. <b>1999</b> , 162, 195-202	7
7	An Extensive Region of an MHC Class I ☑ Domain Loop Influences Interaction with the Assembly Complex. <b>1999</b> , 163, 4427-4433	18
6	Human Transaldolase and Cross-Reactive Viral Epitopes Identified by Autoantibodies of Multiple Sclerosis Patients. <b>1999</b> , 163, 4027-4032	4
5	Bi-allelic variants in NAE1 cause intellectual disability, ischiopubic hypoplasia, stress-mediated lymphopenia and neurodegeneration. <b>2023</b> , 110, 146-160	О
4	Aldose Reductase from Pig Lens. <b>1995</b> , 30, 589s-603s	2

3 Industrial applications of thermophilic/hyperthermophilic enzymes. **2023**, 105-284 o

Bi-allelic SNAPC4 variants dysregulate global alternative splicing and lead to neuroregression and progressive spastic paraparesis. **2023**, 110, 663-680

A second case of glutaminase hyperactivity: Expanding the phenotype with epilepsy.

О